

## 1. INTRODUCTION

Electro-osmotic pumping (EOP) is a variant of conventional electrodialysis (ED) that should be suitable for concentration/desalination of saline waters<sup>(1)</sup>. In EOP, brine is not circulated through the brine compartments, but is evolved in a closed cell. Brine enters the cell as electro-osmotic and osmotic water and leaves the cell by electro-osmotic pumping. This leads to very high concentration factors (high brine concentration) and thus high recovery of product water and small volume of brine to be disposed of. The relatively simple design of an EOP-ED stack, the possibility that an EOP-ED stack may be cheaper than conventional ED and the small brine volume produced, are the major advantages of EOP-ED<sup>(1)</sup>.

Electro-osmotic pumping of sodium chloride solutions has been described by Garza<sup>(1)</sup>; Garza and Kedem<sup>(2)</sup>; Kedem *et al.*<sup>(3)</sup>; Kedem and Cohen<sup>(4)</sup> and Kedem and Bar-On<sup>(5)</sup>. Water and salt fluxes were studied through ion-exchange membranes as a function of current density and feed concentration and mathematical models were developed to describe the experimental data<sup>(1)</sup>. Kedem has reported that current efficiency determined in EOP experiments was close to the value expected from transport number determinations when sodium chloride solutions were electrodialyzed<sup>(5)</sup>. Kedem has also reported that apparent transport numbers gave a lower estimate of current efficiency in ED<sup>(2)</sup>. However, only results for sodium chloride solutions and one commercially available ion-exchange membrane, viz. *Selemin* AMV and CMV were reported. It would be very useful if membrane performance for concentration/desalination applications could be accurately predicted from transport numbers obtained from simple potential measurements. Information in this regard for ion-exchange membranes to be used for saline, acidic and basic effluent treatment, is limited.

A sealed-cell ED (SCED - membranes are sealed together at the edges) laboratory stack (EOP-ED stack) was also developed for evaluation of desalination/concentration of sodium chloride solutions<sup>(3, 4, 5)</sup>. However, only one membrane type that is presently not commercially available, viz., polysulphone based membranes, have been used in the SCED studies. Only desalination/concentration of sodium chloride solutions has been reported in the studies. Saline, acidic and alkaline effluents frequently occur in industry. These effluents have the potential to be treated with EOP-ED for water and chemical recovery and effluent volume reduction. No information, however, could be found in the literature regarding EOP characteristics (brine volume, current efficiency, electro-osmotic coefficients, etc.) of membranes suitable for EOP-ED of acidic and alkaline solutions. In addition, little information is available in the literature regarding EOP characteristics of membrane types to be used for EOP-ED of saline solutions. Consequently, information regarding EOP characteristics of commercially

available ion-exchange membranes suitable for saline, acidic and basic solution treatment is insufficient and information in this regard will be necessary to select membranes suitable for EOP-ED of saline, acidic and basic effluents. In addition, no information exists regarding the performance of an EOP-ED stack for industrial effluent treatment. Information on the theory of EOP-ED and ED is scattered throughout the literature<sup>(1 - 5, 6 - 19)</sup> and is not well documented in any single publication.

Much information, on the other hand, is available in the literature regarding electro-osmosis in general and factors affecting water transport through ion-exchange membranes<sup>(5, 20 - 32)</sup>. Much information is also available in the literature regarding concentration/desalination of saline solutions and saline industrial effluents with conventional ED<sup>(6, 7, 33 - 37)</sup> and electro dialysis reversal (EDR)<sup>(8)</sup>. Conventional ED and EDR, however, are established processes for brackish water desalination and to a lesser extent for wastewater treatment. These processes are applied with success, especially for brackish water treatment for potable use<sup>(6, 8, 38, 39)</sup>. Conventional ED and EDR, however, have the potential to be applied more for industrial effluent treatment.

The objectives of this study were therefore to:

- Consider and document the relevant EOP-ED theory properly;
- Study the EOP-ED characteristics (transport numbers, brine concentration, current density, current efficiency, electro-osmotic coefficients, etc.) of commercially available ion-exchange and other membranes in a single cell pair with the aim to identify membranes suitable for saline, acidic and alkaline effluent treatment;
- Determine whether membrane performance can be predicted effectively from simple transport number determinations and existing models;
- Study EOP-ED of saline solutions in a conventional ED stack;
- Study EOP-ED of saline solutions and industrial effluents in a SCED stack.

## 2. LITERATURE SURVEY

### 2.1 Electro-osmotic Pumping of Salt Solutions with Homogeneous Ion-Exchange Membranes

Garza<sup>(1)</sup> and Garza and Kedem<sup>(2)</sup> have described electro-osmotic pumping of salt solutions with homogeneous membranes in a single cell pair. Brine concentrations, volume flows and current efficiencies were determined at different current densities (0 - 60 mA/cm<sup>2</sup>) for three different sodium chloride feed water concentrations (0,01; 0,1 and 0,5 mol/l). *Selemion* AMV and CMV and polyethylene-based membranes, however, were the only membranes used.

It was found that model calculations described the system in an appropriate way. The results predicted important results such as:

- a) approaching of a limiting (plateau) value of the maximum brine concentration ( $c_b^{\max}$ ) as the current density is increased;
- b) dependence of  $c_b^{\max}$  on the electro-osmotic coefficient (EOC) of the membranes;
- c) approaching of a limiting value (plateau) of current efficiency ( $\epsilon_p$ ) at high current density (below its limiting value);
- d) approaching of a constant slope for curves of volume flow (J) through the membranes versus effective current density ( $I_{\text{eff}}$ ).

It was experimentally found <sup>(1, 2)</sup> that graphs of brine concentration ( $c_b$ ) versus current density levelled off at high values of current and that  $c_b$  approached a maximum plateau,  $c_b^{\max}$ , which depended only on the electro-osmotic coefficients ( $\beta$ ) of the membrane pair ( $c_b^{\max} = \frac{1}{2} F\beta$ ). The smaller the ratio between the osmotic and electro-osmotic water flows, the smaller the current necessary to reach this plateau.

Graphs of volume flow versus effective current density became straight lines at high values of the current. The electro-osmotic and osmotic coefficients could be determined from the slope and the intercept of the lines, respectively. The results have agreed quite well with values obtained from a standard method<sup>(1)</sup> which is very time consuming.

The average value of the apparent transport number for the different membrane pairs

( $\bar{\Delta t}$ 's) was determined from the membrane potential for a concentration difference similar to that obtained in the EOP experiments at high current densities<sup>(2)</sup>. It was found to give a good (lower) estimate of the actual Coulomb efficiency of the process at a salt concentration of 0,1 mol/l. However, no results at higher or lower concentrations were reported. *Selemon* AMV and CMV ion-exchange membranes were the only commercially available membranes used.

The maximum brine concentration,  $c_b^{\max}$ , was predicted from the following two relationships<sup>(2)</sup>:

$$\text{a) } c_b^{\max} = \frac{1}{2\beta F} \quad \text{and} \quad (2.1)$$

$$\text{b) } c_b^{\max} = c_b (1 + J_{\text{osm}}/J_{\text{elosm}}) \quad (2.2)$$

(Note:  $J = J_{\text{osm}} + J_{\text{elosm}}$ ).

Good correlations between the two methods were obtained with the membranes and the salt solutions used.

The EOP results have shown that with appropriate membranes and control of polarization, EOP may be used as a good alternative to conventional ED for desalination/concentration of saline solutions. Laboratory scale EOP experiments may also be conducted as an alternative and convenient way of determining osmotic and electro-osmotic coefficients.

Experimental results were obtained for non-porous membranes. Current efficiencies were in the range of 60 - 85%. It was suggested by Garza<sup>(1)</sup> that a current efficiency of 90% could be obtained with a porous ion-exchange membrane. However, no other results were reported.

Most of the energy consumption in the EOP system will take place in the dialysate compartments<sup>(1)</sup>. Therefore, to reduce it and to suppress concentration polarization, it would be advisable to combine the membranes with open dialysate compartments containing ion-conducting spacers.

It was suggested by Garza<sup>(1)</sup> that EOP would have the following advantages in relation to conventional ED when used for desalination:

- a) the capital cost of the equipment would be decreased due to the simpler

- construction of the unit-cell stack compared to the conventional plate-and-frame stack;
- b) the membrane utilization factor in the membrane bags could be about 95% compared to about 70 to 75% for membranes in conventional ED stacks;
  - c) higher current densities would be possible in unit-cell stacks because of the higher linear flow velocities that could be obtained. These higher current densities would result in higher production rates;
  - d) there would be a decrease in brine volume, and as a consequence, less brine disposal problems.

The only disadvantages could be the fact that more electrical energy per unit of product water would be experienced in the unit-cell stack because higher current densities were used. However, the increased cost for electrical energy would be more than off-set by the decrease in the cost of membrane replacement and amortization of the capital investment, according to Garza<sup>(1)</sup>.

No information could be found in the literature regarding EOP characteristics (brine concentration, current efficiency, electro-osmotic coefficient, etc.) of membranes for acid and alkaline solution treatment in a single cell pair similar to that described for saline solutions.

## 2.2 **Electro-Osmotic Pumping of Saline Solutions in a Unit-Cell Stack**

The so-called unit-cell stack was described by Nishiwaki<sup>(6)</sup> for the production of concentrated brine from seawater by ED. It consisted of envelope bags formed of cation- and anion-exchange membranes sealed at the edges and provided with an outlet, alternated with feed channels. The direction of volume flow through the stack was such to cause ionic flow into the membrane bags. The only water entering the bags was the electro-osmotic water drawn along with the ions plus the osmotic flow caused by the higher pressure of the brine compared to the feed. This variant of ED is called electro-osmotic pumping (EOP) and is used for production of concentrated brine from seawater for salt production.

A simple sealed-cell ED stack (SCED) was described by Kedem *et al.*<sup>(3)</sup> in 1978. This cell consisted of thermally sealed polyethylene based membranes (21 bags, 5 x 9 cm). The membranes were not very selective at high salt concentration. It was found that smooth continuous operation was obtained with stable voltage and pH in the

concentration range from 0,01 to 0,04 mol/l and current densities from 5 to 20 mA/cm<sup>2</sup>.

Kedem and Cohen<sup>(4)</sup> have described the performance of a laboratory SCED unit for desalination/concentration of sodium chloride solutions. Heterogeneous ion-exchange membranes were used. The selectivity of these membranes, however, were lower than that of commercially available membranes. Nevertheless, it was demonstrated that various sodium chloride feed concentrations could be desalinated effectively. The results are shown in Table 2.1.

**Table 2.1: Desalination of sodium chloride solutions at various cell pair voltages.**

$c_{\text{feed}}$	$c_{\text{product}}$	Output	Energy Consumption	$c_{\text{brine}}$	Recovery	$V_{\text{cp}}$	$d_{\text{eff}}$
mg/l	mg/l	$\frac{\text{m}^3}{\text{m}^2\text{day}}$	$\frac{\text{kWh}}{\text{m}^3}$	mg/l	%	Volt	mm
2 670	810	3,25	1,55	82 780	98	1	1,13
1 910	320	1,86	1,33	60 610	97,3	1	1,13
1 570	570	2 60	0,56	45 800	97,8	0,72	1,07
1 910	540	1,62	0,54	46 040	97	0,5	0,82

$c_f$  : feed concentration  
 $c_p$  : product concentration  
 $c_b$  : brine concentration  
 $V_{\text{cp}}$  : cell pair voltage  
 $d_{\text{eff}}$  : effective thickness of dialysate compartment (polarization factor).

Product water yield (output), electrical energy consumption, brine concentration,  $c_b$ , water recovery, cell pair voltage,  $V_{\text{cp}}$ , and the polarization factor ( $d_{\text{eff}}$ ) are also shown in Table 2.1.

Kedem and Bar-on<sup>(5)</sup> have reported results on the desalination of sodium chloride solutions with a SCED stack using heterogeneous ion-exchange membranes. The results are shown in Table 2.2.

**Table 2.2: Desalination of sodium chloride solutions at a linear flow velocity of 14,4 cm/s.**

$V_{cp}$	$c_f$ mg/ℓ	$c_p$ mg/ℓ	Energy consumption kWhr/m <sup>3</sup>	Output m <sup>3</sup> /day	$n_c$ %	$c_b$ mg/ℓ	$d_{eff}$ mm
0,9	2 200	100	1,01	1,41	77,0	68 390	1,24
	1 500	500	0,51	3,68	76,5		1,10
	1 000	300	0,35	3,62	79,5		0,85
0,7	2 100	100	0,80	1,16	78	59 620	0,97
	1 500	500	0,39	3,06	78,5		0,83
	1 000	300	0,27	3,05	77		0,80
0,5	2 500	500	0,53	1,22	80	60 200	0,88
	1 500	500	0,27	1,95	80		0,71
	1 000	300	0,19	2,62	80		0,60

$V_{cp}$  : cell pair voltage  
 $c_f$  : feed concentration  
 $c_p$  : product concentration  
 $n_c$  : current efficiency  
 $c_b$  : brine concentration  
 $d_{eff}$  : effective thickness of dialysate compartment (polarization factor).

The current efficiency ( $n_c$ ) is shown for varying cell pair voltages and feed water concentrations. It was mentioned by Kedem and Bar-on<sup>(5)</sup> that the permselectivity of the ion-exchange membranes that were used decreased substantially at high salt concentration. This, however, is not reflected in the data on the current efficiency that was obtained in the SCED stack (Table 2.2). It appears therefore, according to Kedem and Bar-on, that electro-osmosis contributes to salt transfer and helps to maintain current efficiency.

At constant cell pair voltage ( $V_{cp}$ ), polarization is nearly constant and plots of cell pair resistance ( $R_{cp}$ ) versus specific resistance of the dialysate ( $\rho$ ) give straight lines in a rather wide concentration range<sup>(5)</sup>. As shown in Figure 2.1, this is not true for the whole range covered. Polarization decreases slightly with increasing current. For the estimated effective thickness of the dialysate compartment,  $d_{eff}$ , this is approximated by straight lines for parts of this range.

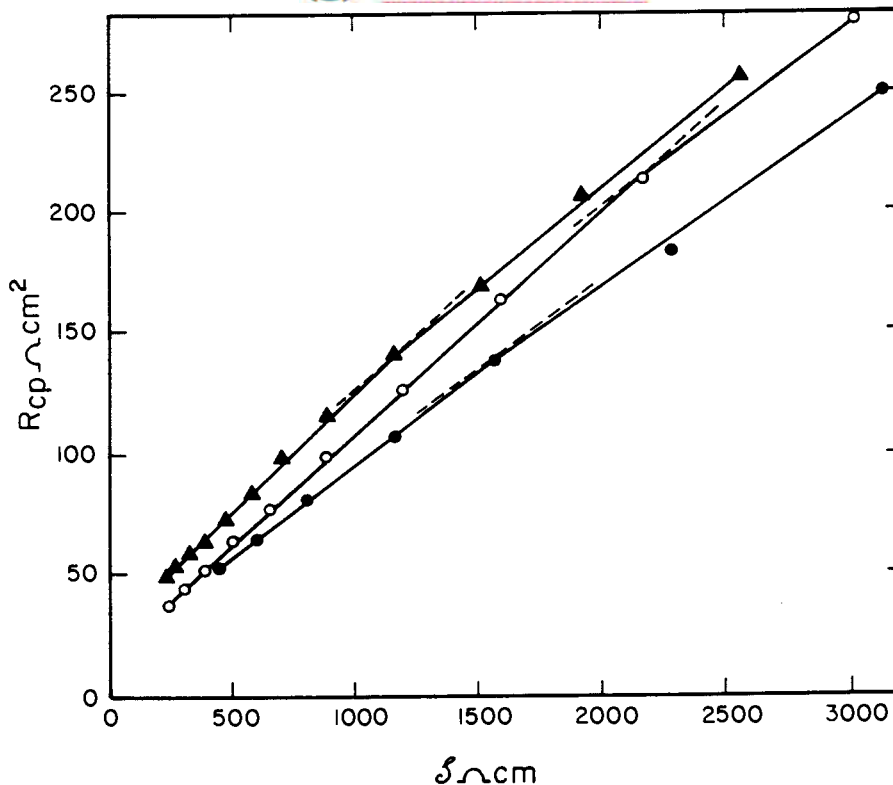


**Figure 2.1:** Apparent resistance per cell pair as a function of the specific resistance of the dialysate solution.  $V_{cp} = 0,7$  V.

Membrane potentials and ohmic resistance for a pair of membranes are shown in Table 2.3. Membrane potentials were measured with calomel electrodes between stirred cells. Column 4 shows the potentials for ideal permselectivity (absolute values). Membrane resistance ( $\Omega$ C) was measured in 0,5 and 0,1 mol/l sodium chloride solutions.

**Table 2.3:** Membrane potential and ohmic resistance of a heterogeneous cation-exchange membrane (c) and a similar anion-exchange membrane (a)

Solutions	Membrane Potential				Solution Concentration	Membrane Resistance	
	$\Delta\psi_m^c$	$\Delta\psi_m^a$	$\Delta\psi_m^0$	$\frac{\Delta\psi_m^c +  \Delta\psi_m^a }{2\Delta\psi_m^0}$		C	A
NaCl mol/l	mV	mV	mV	%	mol/l	$\Omega\text{cm}^2$	$\Omega\text{cm}^2$
0,02/0,04	15,6	14,9	16,7	91	0,5	9,5	9,8
0,1/0,2	14,8	14,4	16,3	89	0,1	37,1	26,6
0,5/1,0	13,2	11,9	16,8	75			
1,0/2,0	12,4	11,1	18,2	64			
0,02/1,0	80,0	72,6	93,0	82			

$\Delta\psi_m^c$  : membrane potential of cationic membrane  
 $\Delta\psi_m^a$  : membrane potential of anionic membrane  
 $\Delta\psi_m^0$  : membrane potential for ideal permselectivity.



## 2.3 Electro-Osmotic and Osmotic Flows

Electro-osmosis of different salt, acid and alkaline solutions have been studied extensively through a wide variety of membranes<sup>(5, 20 - 27, 28 -32, 40, 41)</sup>.

Brydges and Lorimer<sup>(20)</sup> showed that when current density is varied, water transport number can:

- a) increase at low current density because osmotic water flow has been superimposed on water transport by the electric field;
- b) decrease at higher current density because of accumulation of salt in the membrane;
- c) decrease more at current densities near or above the limiting value because of an increased contribution of hydrogen and hydroxide ions to transport. These phenomena arise from a combination of diffusion (film) at both the membrane-solution interface and from the dependence of counter-ions and water transport numbers on external salt concentration.

Kruissink<sup>(21)</sup> has showed that with *Nafion* 170 membranes under practical conditions (concentrated alkali ( $\geq 10$  mol/l) and 5 mol/l sodium chloride), that electro-osmotic water transport caused the maximum current efficiency to increase from 0,45 (electro-osmotic water transport number zero) to about 0,75 to 0,80 (at electro-osmotic water transport number of 1).

Hidalgo-Alvarez *et al.*<sup>(22)</sup> have found that at low electric current, the electro-osmotic coefficient undergoes a sharp elevation. This effect was very similar to that found by Lakshminarayanaiah<sup>(40)</sup>. At high electric current the electro-osmotic coefficient tends toward a constant value. This value depends on the concentration of the solution. When the concentration increases, the electro-osmotic permeability decreases.

Ceynowa<sup>(23)</sup> has indicated that the water transport number depends on many factors, such as experimental conditions (current density, stirring, difference in the concentration which occurs in the course of electrolysis on both sides of a membrane) as well as membrane parameters such as cross-linking, water content, ion-exchange capacity. Consequently, the resulting water transport number may sometimes be questionable and its properties complex.

The decrease of the water transport number with an increase in concentration of the external solution is usually given as the main non-controversial property<sup>(23)</sup>. However, Tombalakian *et al.*<sup>(24)</sup> found constant values of the water transport number for the homogeneous sulphonic acid membranes of high cross-linking and low water content in hydrochloric acid solution. Demarty *et al.*<sup>(41)</sup> stated the same for the heterogeneous *Ionac* MC 3470 XL membrane in hydrochloric acid solutions. Similarly Oda and Yawataya<sup>(27)</sup> reported that in some membranes in the presence of hydrochloric acid solution the water transport number remained constant at about 1,0 and the hydrogen ion transfer number only drops from 1,0 to 0,99. They also suggested that membranes deswell with increasing electrolyte concentration.

Ceynowa<sup>(23)</sup> found that the water and ion transport numbers at low sulphuric acid concentrations were in a wide range (5 - 70 mA/cm<sup>2</sup>) independent of current density in the case of the heterogeneous MRF-26 ion-exchange membrane. However, at high concentration (2,26 mol/kg water) the increase in water transport number with current density was remarkable. It was also found that the water transport number in the MRF membrane decreased with increasing concentration (0,5 to 2,0 mol/kg water). With Nafion-120 membrane the water transport number remained almost constant with increasing feed concentration.

Rueda *et al.*<sup>(25)</sup> stated that the decrease of water transport number with increase in external salt concentration could be attributed to the decrease of the selectivity of the membrane. At very dilute solutions, the current is carried by the cations because the anions are almost completely excluded from the cationic cellulose acetate membrane. As the external solution concentration increases, the permselectivity of the membrane decreases. Anions are now present in the membrane and cations and anions participate in the transport of current across the membrane in opposite directions. Obviously, water transport will be reduced. An increase of external salt concentration leads to an increase of charge concentration in the neighbourhood of the matrix and consequently a decreasing of the electro-osmotic permeability.

Electro-osmotic permeability of several cellulose acetate membranes have been determined using solutions of alkali-chlorides<sup>(25)</sup>. The electro-osmotic permeability has been studied as a function of the external electrolyte concentration (0,001 to 0,1 mol/l) and of current density applied. The results showed that the electro-osmotic permeability depended on the thickness of the membranes and the nature of the cations. The electro-osmotic permeability has been found to be strongly dependent

on the external salt concentration. However, the electro-osmotic permeability was not significantly affected by current density.

Tasaka *et al.*<sup>(66)</sup> have also studied electro-osmosis in charged membranes. At low electrolytic concentrations the direction of electro-osmosis is the same as that of counter-ion flow, because most of the movable ions in the membrane are counter-ions. With increasing external salt concentration the concentration of co-ions in the membrane increases, and then electro-osmosis decreases. In many instances electro-osmosis tends towards zero at the limit of high electrolyte concentrations.

Oda and Yawataya<sup>(27)</sup> have found that the electro-osmotic coefficient of hydrochloric acid through a cation-exchange membrane remains almost constant over the concentration range from 0,5 to 4,0 mol/l. In hydrochloric acid solutions the electro-osmotic water transference is merely about one mole water per Faraday through a membrane.

Narebska *et al.*<sup>(28)</sup> have investigated the isothermal transport of ions and water across the perfluorinated Nafion 120 membrane in contact with sodium chloride solutions at a concentration of 0,05 up to 4 mol/l based on irreversible thermodynamics of transport. It was found that the specific conductivity of the membrane increased at low external electrolyte concentration. The apparent transport number of the cation decreased significantly at higher external electrolyte concentration. The electro-osmotic coefficient also decreased significantly at higher external electrolytic concentration. The osmotic volume flux, and salt diffusion flux increased with increasing electrolyte concentration while the hydrodynamic volume flow decreased with increasing electrolytic concentration. The membrane also deswelled significantly with increasing electrolyte concentration.

Narebska and Koter<sup>(29)</sup> have studied the conductivity of ion-exchange membranes on the grounds of irreversible thermodynamics of transport. They have found that convection conductivity covers 50 to 55% of the total membrane conductivity and even more at increased temperature. This means that the flowing water doubles the ability of the membrane to transport the ionic current. This confirms the substantial role that water plays in the transport behaviour of a membrane.

Narebska *et al.*,<sup>(30)</sup> have performed a detailed analysis of membrane phenomena in the system Nafion 120/NaOH<sub>aq</sub>. They have determined the phenomenological resistance -

( $r_{i,k}$ ) and friction coefficient ( $f_{i,k}$ ). They have found that the resistance imposed by the membrane on the permeating  $\text{OH}^-$  ions is much lower than that for  $\text{Cl}^-$  ions. The three factors contributing to this effect - i.e. the frictions imposed by the cation ( $f_{21}$ ), water ( $f_{2w}$ ) and the polymer matrix ( $f_{2m}$ ) - influence the flow of  $\text{OH}^-$  and  $\text{Cl}^-$  to a different degree. Chloride ions are hindered mainly by water, especially at increasing sorption. The flow of  $\text{OH}^-$  ions in diluted solution is hindered by the matrix and, at a higher concentration, by the cation and then by water.

Considering these results, it is apparent that the easy flow of  $\text{NaOH}$  results not only from the high mobility of  $\text{OH}^-$  ions, but also from the low osmotic flux (2 to 3 times less than in  $\text{NaCl}$  solutions) opposing the stream of electrolyte and the very low friction of the  $\text{OH}^-$  ions with water.

The water transport number decreased from 10 mol/Faraday to 2 mol/Faraday over the concentration range of 0,05 to 4 mol/l. The apparent transport number ( $\Delta t^c$ ) also decreased significantly with increasing caustic soda concentration.

The transport of aqueous  $\text{NaCl}$  solutions across the perfluorinated Nafion 120 membrane have been studied on the basis of irreversible thermodynamics by Narebska *et al.*<sup>(31)</sup>. The straight resistance coefficients  $r_{ij}$ , partial frictions  $f_{ik}$  and diffusion indexes have been determined.

Since the Donnan equilibrium and TMS theory were published, it is a well known and documented fact that co-ions are rejected from a charged polymer by the high potential of the polymer network. It was found by Narebska *et al.*, that friction of this co-ion with the charged polymer was not the main force which resisted the flow of negative ions in the negatively charged polymer network. Except at 289 K and  $m_{\text{ext}} = 0,5$ , the anion-polymer frictional force ( $2m$ ) was below the friction with water ( $2w$ ) and it decreases with increasing electrolyte concentration and temperature. As a result, at high temperature and  $m_{\text{ext}}$ , the resistance against flowing anions is imposed by water; the lower the amount of water in the membrane, the higher this resistance.

Koter and Narebska<sup>(32)</sup> have investigated the mobilities of  $\text{Na}^+$ ,  $\text{Cl}^-$  and  $\text{OH}^-$  ions and water in Nafion 120 membranes. They have found that the interactions of  $\text{Na}^+$  and  $\text{Cl}^-$  ions running in opposite directions are negligible in the whole concentration range (0,05 to 4 mol/l) studied. However, hydroxide ions impede cations, particularly at higher external concentrations (high sorption). This fact can be attributed to the higher

partial friction between  $\text{Na}^+$  and  $\text{OH}^-$  ions caused by the phenomenon called "local hydrolysis".

The mobility of hydroxide ions exceeds that of chloride ions even more in the membrane than in the free solution. The mobility of hydroxide ions is much more sensitive to concentration than that of chloride ions. The mobility of the hydroxide ions declines much more rapidly than the mobility of the chloride ions. This reflects the dehydration of the membrane with increasing sorption of an electrolyte.

Kedem and Bar-on<sup>(5)</sup> have mentioned that the current efficiency ( $n_c$ ) for a single membrane pair was sometimes equal to and even higher than the apparent transport number of the membrane pair ( $\bar{t}$ ) measured with calomel electrodes. According to them, this is due to the substantial influence of electro-osmotic and osmotic flow into the brine cells during ED which increase the current efficiency. Both osmotic and electro-osmotic water flow enters the brine cell through both membranes. It increases the flows of counter-ions leaving the brine. The total effect of volume flow into a brine cell is increased salt flow. There will also be a slight influence of osmotic flow on the potential measurements. This will decrease the potential measurement and therefore the apparent transport number<sup>(5)</sup>.

#### 2.4 Structural Properties of Membrane Ionomers

Mauritz and Hopfinger<sup>(42)</sup> have described structural properties of ion-exchange membranes. Common functionalities of ion-exchange membranes are:  $-\text{SO}_3^-$ ;  $-\text{COO}^-$ ;  $-\text{NH}_3^+$ ;  $=\text{NH}_2^+$ . These hydrophilic groups are responsible for the swelling of the hydrophobic network of ion-exchange membranes on exposure to water. Swelling of ion-exchange membranes may be inhibited by the presence of crystalline domains within the membrane matrix.

The approach to equilibrium for an initially dry ion-exchange membrane (in a given counter-ion salt form and containing no co-ions) that is subsequently immersed in pure water, can be visualized in the following way: Although the interaction between the organic polymer backbone is endothermic and may influence the rate of swelling, the strongly exothermic tendency of the counter-ions and ionogenic side chains to hydrate results in having the initially arrived water molecules strongly bound in ionic solvation shells resulting in little or no volume expansion of the network. In the truly dry state, the counter-ions are strongly bound by electrostatic forces in contact ion pairs. Further

uptake of water beyond that which is barely required for maximum occupancy of all the hydration shells results in moving the association - dissociation equilibrium between bound and unbound counter-ions toward increased counter-ion mobility. The driving force for swelling is the tendency for the water to dilute the polymer network. Stated in precise thermodynamic formalism, the difference between the water activity in the interior ( $\bar{a}_w < 1$ ) and exterior ( $a_w = 1$ ) of the membrane gives rise to a membrane internal osmotic pressure,  $\Pi$ , that results in a deformation of the polymer chain network:

$$\Pi v_w = RT \ln \bar{a}_w \quad (2.4.1)$$

This equation is a statement of the free energy balance across the membrane - water interface at equilibrium and that  $v_w$  the partial molar volume of the internal water component may, in reality, not be the same as for the bulk water, nor be of a uniform value throughout the polymer because of local structuring effects.

As the water uptake proceeds, the increased side-chain counter-ion dissociation allows for more complete ionic hydration. The deformation of the polymer chain network upon further incorporation of water molecules also proceeds by a shift in the distribution of rotational isomers to higher energy conformations and changes in other intra-molecular, as well as inter-molecular interactions. Consequently, the increased overall energy state, for a given membrane water content of  $n$  moles, per equivalent of resin, is manifested by polymer chain retractive forces that resist expansion of the network. Accordingly, the configurational entropy decreases as less conformations become available within the matrix. Eventually, an equilibrium water content,  $n_o$ , is reached at which the osmotic swelling pressure is balanced by the cohesive energy density.

A qualitative set of rules that describe the equilibrium water swelling of polymeric ion-exchangers are as follows according to Mauritz and Hopfinger:

- a) Increasing the cross-link density reduces the swelling by decreasing the average inter-chain separation;
- b) Swelling will greatly depend on the pK of the ionogenic groups as well as their number per unit volume. For example, the equilibrium water uptake for strong acid resins exceeds that of resins containing the less hydrophilic weak acid groups;

- c) The nature of the counter-ion can influence swelling in a number of ways. Firstly, water uptake naturally increases with increasing hydrative capacity of the counter-ion. In general, for alkali counter-ion forms, the following progression is noted:  $\text{Li}^+ > \text{Na}^+ > \text{K}^+ > \text{Rb}^+ > \text{Cs}^+$ . Increased valence reduces swelling by: (i) reducing the number of counter-ions in the resin through the electroneutrality requirement; (ii) forming ionic cross-links; and (iii) reducing the hydrative capacities by the formation of triplet associations such as:  $-\text{SO}_3^- \cdots \text{Ca}^{2+} \cdots \text{SO}_3^-$ ;
- d) The internal resin osmotic pressure is enhanced as the association - dissociation equilibrium between bound and unbound counter-ions shifts to greater dissociation by allowing for more complete hydration shell formation.

Narebska and Wodzki<sup>(43)</sup> have investigated water and electrolyte sorption (sulphuric acid) in perfluorosulphonic and polyethylene-poly (styrene sulphonic acid) membranes of different cross-linking in the temperature range of 293 to 333 K and a concentration of external electrolyte up to 5,7 mol/kg  $\text{H}_2\text{O}$ . As the hydration of the membranes is an exothermic process, a decrease of swelling with increasing temperature could be predicted. Also due to the nature of sulphuric acid one could expect dehydration of the membranes with an increasing concentration of acid. It was found that an increase of both variables, i.e. temperature and concentration, caused deswelling of the membranes in a higher degree when the cross-linking is lower. Only for the membranes with a low degree of cross-linking (2 and 5% DVB) equilibrated with diluted solutions of sulphuric acid, a small increase of swelling is visible at a temperature range of 293 to 303 K.

Narebska *et al.*,<sup>(44)</sup> have studied swelling and sorption equilibria for Nafion membranes in concentrated solutions of sodium chloride (0 to 6 mol/kg  $\text{H}_2\text{O}$ ), and sodium hydroxide (0 to 18 mol/kg  $\text{H}_2\text{O}$ ), at 293 to 363 K. It was found that significant deswelling of the membranes took place with increasing electrolyte concentration. Increasing temperature (above 333 K), also caused a loss of water. Narebska *et al.*, have stated that deswelling of a membrane depends on the kind of membrane, temperature and the nature of the external electrolyte.

## 2.5 Measurement of Transport Number

The efficiency with which a membrane transport selectively any particular ionic species may be inferred by measuring the transport number of the species in the membrane. Two methods are normally used to determine membrane transport number. They are:

- the emf method<sup>(45)</sup> and;
- the Hittorf's method<sup>(45)</sup>. In these methods different concentrations of electrolyte exist on either side of the membrane, even though in the Hittorf's method one might start initially with the same concentration. Therefore, the transport number values derived by these methods cannot be directly related to a definite concentration of the external solution.

Membrane potentials measured using concentrations  $c'$  and  $c''$  on either side of the membrane may be used in the following equation to derive an average transport number:

$$E/E_{\max} = 2\bar{t}_+ - 1; \quad \bar{t}_+ = (E/E_{\max}) + 0,5 \quad (2.5.1)$$

If Ag-AgCl electrodes immersed in two chloride solutions are used,  $\bar{t}_+$  is derived from<sup>(45)</sup>:

$$E = 2\bar{t}_{+(app)} \frac{RT}{F} \ln \frac{a'}{a''} \quad (2.5.2)$$

The derived transport number value has been called the apparent transport number because in this type of measurement water transport has not been taken into account. This apparent value will be close to the true value when very dilute solutions are used.

In the Hittorf's method a known quantity of electricity is passed through the membrane cell containing two chambers filled with the same electrolyte separated by a membrane. Cations migrate to the cathode and anions migrate to the anode. The concentration change brought about in the two chambers, which is not more than about 10%, is estimated by the usual analytical methods. The transport number is calculated from  $t_i = FJ/l$ .

The determination of meaningful transport numbers for any membrane-electrolyte system calls for careful control of a number of factors. The important factors for the



control of the concentration of the donating or receiving side are<sup>(45)</sup>:

- a) external concentration;
- b) current density; and
- c) difference in concentration on either side of the membrane.

The effect of current density on the values of  $\bar{t}_i$  has been demonstrated by Kressman and Tye<sup>(46)</sup> using multi-compartment cells and by Lakshminarayanan and Subrahmanyam<sup>(47)</sup> using simple cells. When external concentrations are small ( $< 0,1$  mol/l) an increase of current density decreases  $\bar{t}_i$  values. This is attributed to polarization effects at the membrane-solution interface facing the anode.

The amount of polarization decreases as the concentration is increased. When the external concentration is  $0,1$  mol/l,  $\bar{t}_i$  exhibits a maximum at a certain current density below which the  $\bar{t}_i$  values decrease as the current density is decreased and above which also  $\bar{t}_i$  values decreased as the current density is increased. The decrease as the current density is lowered is attributed to back diffusion of the electrolyte<sup>(47)</sup>.

When external concentrations  $> 0,1$  mol/l are used, polarization effects are negligible but back diffusion becomes dominant. As the quality of back flux due to diffusion is determined by the concentration differences allowed to build-up during electro dialysis, it should be made as small as possible to derive meaningful values for  $\bar{t}_i$ .

## 2.6 Transport Properties of Anion Exchange membranes in contact with Hydrochloric Acid Solutions. Membranes for Acid recovery by Electrodialysis

Boudet-Dumy *et al.*<sup>(48)</sup> have recently investigated chloride ion fluxes through *Selemion* AAV and ARA Morgane membranes specially designed for the recovery of acids by ED. In addition, measurement of the electrical conductance of the membranes and of the amount of sorbed electrolyte (HCl), at equilibrium, have been carried out. The analysis of the results suggested a low dissociation degree of acid present in the membrane. The lower dissociation of sorbed acid is a factor which decreases the proton leakage of the anion-exchange membrane. It was also shown that the flux of chloride ions from the anode to the cathode steadily increased as the amount of sorbed electrolyte increased. This result means that chloride ions are associated with the movement of positively charged species. This fact may be due to the formation of an aggregate form such as  $(H_4OCl)^+$  resulting from the solvation of a proton by a water

molecule and an HCl molecule - ion association inside the membrane overcoming the state of a neutral HCl molecule. This result confirms the role of ion association in the membrane.

## 2.7 Electrodialysis Applications

Electrodialysis applications and potential applications<sup>(6 - 8, 33 - 39, 49 - 62)</sup> are widely discussed in the literature. Electrodialysis is a membrane based separation technique that is appealing because of its capability to deionize one stream while concentrating the electrolytes in another stream. Thus, ED produces a purified stream that can either be discharged or reused, and a concentrated electrolyte stream that can be disposed of or processed for reclamation of the dissolved salt. Some applications of ED include desalination of brackish waters<sup>(56)</sup>, desalting of whey and stabilization of wine<sup>(57)</sup>, purification of protein solutions<sup>(58)</sup>, recovery of metals from plating rinse waters<sup>(38)</sup>, recovery of acids<sup>(59)</sup>, recovery of heavy metals from mining mill process<sup>(60)</sup>, and the treatment of cooling-tower blowdown for water recovery and effluent volume reduction<sup>(61)</sup>.

When concentration polarization is absent in ED, there are two main causes of the decrease in current efficiency<sup>(62)</sup>: Co-ion intrusion and counter-ion backdiffusion. Co-ion intrusion is the passage of co-ions through an ion-exchange membrane from the concentrate to the diluate, and is due to the electrical potential and concentration gradients across the membrane. Counter-ion backdiffusion is the backward passage of counter-ions through an ion-exchange membrane from the concentrate to the diluate due to a high concentration gradient across the membrane. The effects of counter-ion backdiffusion can be decreased by increasing stack voltage, that is, increasing the electrical potential driving force. However, such an increase in stack voltage is limited by the limiting current density and high energy costs. Co-ion intrusion can be reduced by using ion-exchange membranes that exclude co-ions to a greater degree.

Kononov *et al.*<sup>(33)</sup> have described the removal of hydrochloric acid from waste waters containing organic products. The possibility was demonstrated of concentrating hydrochloric acid by ED. The model effluent contained 4,4 g/l hydrochloric acid, 58 g/l sofolene-3 and 20 g/l chlorohydrin. At a current density of 10 mA/cm<sup>2</sup> a brine was obtained containing 51 g/l acid with a current efficiency of 35%. The low current efficiency is explained by diffusion of acid from the brine into the dialysate and the decrease in the selectivity of the membranes in contact with concentrated hydrochloric

acid solution (50 g/l).

Korngold<sup>(34)</sup> has described the recovery of sulphuric acid from rinsing waters used in a pickling process. Sulphuric acid was concentrated from 9 100 mg/l to 34 300 mg/l while the diluate contained 3 700 mg/l sulphuric acid. Approximately 70% of the sulphuric acid in the rinsing water could be recovered by ED treatment.

Urano *et al.*<sup>(37)</sup> have described concentration/desalination of model hydrochloric and sulphuric acid solutions in a laboratory scale conventional electro-dialyzer. Newly developed Selemion AAV anion-exchange membrane were used. The transport number for hydrogen ions of this membrane is much smaller than that of conventional anion-exchange membranes with the result that the acid could be efficiently concentrated. However, no acid feed and brine concentrations were given.

The concentration of carbonate solutions by ED was reported by Laskorin *et al.*<sup>(35)</sup>. The feed solution had the following composition: sodium carbonate (4 to 7 g/l); sodium bicarbonate (4 - 7 g/l) and sodium sulphate (2 to 3 g/l). The total salt content of the solution did not exceed 15 g/l. The first series of experiments was carried out with liquid circulation in both the diluting and concentrating compartments. A linear liquid velocity and a current density of 5 to 6 cm/s and 20 mA/cm<sup>2</sup> was used, respectively. The duration of the desalting cycle was 1,5 to 2,0 hour. A fresh portion of feed was introduced after each desalting cycle. The portion of concentrate remained unchanged for 10 cycles. MKK cation- and MAK anion selective membranes were used. The brine concentration was increased from 22,9 g/l at the end of the first cycle to 87, 8 g/l at the end of the 10th cycle at a current efficiency of 81%. The diluate concentration at the end of the cycles varied between 0,16 and 0,47 g/l.

A second series of experiments was conducted without circulation of liquid through the brine compartments. The solvent entered the brine compartments as a result of electro-osmotic transport through the membranes. The brine salt content reached a value of 182,8 g/l after 3 cycles. The current efficiency varied between 70 and 75% and the electrical energy consumption was approximately 2,7 kWh/kg salt. A higher brine concentration was obtained without circulation of brine through the brine compartments.

Smagnin and Chukkin<sup>(36)</sup> have described concentration of caustic soda and sodium

chloride with ED. Caustic soda and sodium chloride concentrations of 0,07 and 1,07 mol/l, respectively, were chosen as the feed solutions. No circulation of brine was used in a conventional ED stack. The change of brine concentration in relation to the current density was determined. MA-40 and MK-40 ion-exchange membranes were used. Maximum brine concentrations of 346 g/l caustic soda and 365 g/l sodium chloride were obtained at current densities of 249 and 117 mA/cm<sup>2</sup>, respectively.

### 3. THEORY

#### 3.1 Theories of Membrane Transport

##### 3.1.1 Nernst-Planck and Pseudo-Thermodynamic Treatments

Theories of membrane transport and the application of non-equilibrium thermodynamics to transport processes have been described by Meares *et al.*<sup>(9)</sup>.

Many of the earlier treatments of membrane transport use the Nernst-Planck equations to describe the relationships between the flows of the permeating species and the forces acting on the system<sup>(10, 63)</sup> according to Meares *et al.* According to these equations the flux  $J_i$  of species  $i$  at any point is equal to the product of the local concentration  $c_i$  of  $i$ , the absolute mobility  $u_i$  of  $i$ , and the force acting on  $i$ . This force has been identified with the negative of the local gradient of the electrochemical potential  $\mu_i$  of  $i$ . Thus, at a distance  $x$  from a reference plane at right angles to the direction of unidimensional flow through a membrane

$$J_i = -c_i u_i d\mu_i/dx \quad (3.1.1.1)$$

The electrochemical potential of  $i$  can be divided into its constituent parts giving in place of equation eq. (3.1.1.1)

$$J_i = -c_i u_i (RT d \ln c_i/dx + RT d \ln \gamma_i/dx + \bar{V}_i dp/dx + z_i F d\psi/dx) \quad (3.1.1.2)$$

where  $\gamma_i$ ,  $\bar{V}_i$ ,  $z_i$ ,  $p$ , and  $\psi$  represent the activity coefficient, the partial molar volume, the valence charge on  $i$ , the hydrostatic pressure, and the electrical potential, respectively.  $R$  is the gas constant,  $T$  the absolute temperature, and  $F$  the Faraday. It is apparent from eq. (3.1.1.2) that the Nernst-Planck equations make use of the Nernst-Einstein relation between the absolute mobility  $u_i$  and the diffusion coefficient  $D_i$  of species  $i$ . This is

$$D_i = u_i RT \quad (3.1.1.3)$$

On replacing the electrochemical mobility in eq. (3.1.1.2) by the diffusion coefficient, the more usual form of the Nernst-Planck flux equation is obtained according to Meares *et al.*

$$J_i = -D_i \left( \frac{dc_i}{dx} + c_i \frac{d \ln \gamma_i}{dx} + \frac{c_i \bar{V}_i}{RT} \frac{dp}{dx} + \frac{c_i z_i F}{RT} \frac{d\psi}{dx} \right) \quad (3.1.1.4)$$

On the basis of the Nernst-Planck equations, the flow of species *i* is regarded as unaffected by the presence of any other permeating species except in so far as the other species either influences the force acting on *i* by, for example, affecting the values of  $\gamma_i$  or  $\psi$ , or alters the state of the membrane and hence alters the value of  $D_i$ .

To obtain relationships between the flows of the permeating species and the observable macroscopic differences in concentration, electrical potential, and hydrostatic pressure between the solutions on the two sides of the membrane, it is necessary to integrate the Nernst-Planck equation (eq. 3.1.1.4) for each mobile component across the membrane and the membrane/solution boundaries. In order to carry out this integration an additional assumption has to be made. The differences between the various treatments derived from the Nernst-Planck equations lie in the different assumptions used. For example, in the theory of Goldman<sup>(63)</sup>, which is widely applied to biological membranes, it is assumed that the gradient of electrical potential  $d\psi/dx$  is constant throughout the membrane. It is usually assumed also that thermodynamic equilibrium holds across the membrane/solution interfaces and that the system is in a steady state so that the flows  $J_i$  are constant throughout the membrane. Generally these integrations do not lead to linear relationships between the flows and the macroscopic differences of electrochemical potential between the two bathing solutions.

The main disadvantage of the Nernst-Planck approach according to Meares<sup>(9)</sup> is that it fails to allow for interactions between the flows of different permeating species. Such interactions are most obvious when a substantial flow of solvent, usually water, occurs at the same time as a flow of solute. For example, during the passage of an electric current across a cation-exchange membrane, the permeating cations and anions both impart momentum to the water molecules with which they collide. Since the number of cations is greater than the number of anions, the momentum imparted to the water by the cations is normally greater than the momentum imparted by the anions and an electro-osmotic flow of water is set up in the direction of the cation current. The

resultant bulk flow of the water has the effect of reducing the resistance to the flow of cations and increasing the resistance to the flow of anions. This flow of water occurs under the difference of electrical potential and in the absence of a concentration gradient of water. The appropriate Nernst-Planck equation would predict no flow of water under these conditions according to Meares *et al.* Furthermore the flows of cations and anions differ from those which would be predicted from the respective Nernst-Planck equations on account of the effect of the water flow on the resistances to ionic flow.

This effect of solvent flow on the flows of solute molecules or ions can be allowed for by adding a correction term to the Nernst-Planck equations<sup>(9)</sup>. Thus, it can be written

$$J_i = -c_i u_i \, d\mu/dx + c_i v \quad (3.1.1.5)$$

where  $v$  is the velocity of the local centre of mass of all the species<sup>(11)</sup>. The term  $c_i v$  is often called the convective contribution to the flow of  $i$  and some authors have preferred to define  $v$  as the velocity of the local centre of volume.

The addition of this convection term to the Nernst-Planck equation for the flow of a solute is probably a sufficient correction in most cases involving only the transport of solvent and nonelectrolyte solutes across a membrane in which the solvent is driven by osmotic or hydrostatic pressure according to Meares *et al.* The situation is much more complex when electrolyte solutes are considered according to Meares *et al.* Even at low concentrations the flows of cations and anions may interact strongly with each other. Interactions between the different ion flows may be of similar size to their interactions with the solvent flow. Under these circumstances the convection-corrected Nernst-Planck equations may still not give a good description of the experimental situation regarding the ion flows.

The theoretical difficulties arising from interacting flows can be formally overcome by the use of theories of transport based on nonequilibrium thermodynamics. Such theories are described in the next section.

### 3.1.2 Treatments based on Nonequilibrium Thermodynamics

Since the original papers of Staverman<sup>(12)</sup> and Kirkwood<sup>(64)</sup>, many papers have appeared on the application of nonequilibrium thermodynamics to transport across synthetic and biological membranes. In particular, major contributions have been

made by Katchalsky, Kedem, and co-workers. In view of the appearance of extensive texts<sup>(13, 14)</sup>, this account is intended only as a brief summary of the general principles.

### 3.1.2.1 The Phenomenological Equations

The theory of nonequilibrium thermodynamics allows that, in a system where a number of flows are occurring and a number of forces are operating, each flow may depend upon every force. Also, if the system is not too far from equilibrium, the relationships between the flows and forces are linear. Therefore, the flow  $J_i$  may be written as follows

$$J_i = \sum_{\text{all } k} L_{ik} X_k \quad (3.1.1.6)$$

where the  $X_k$  are the various forces acting on the system and the  $L_{ik}$  are the phenomenological coefficients which do not depend on the sizes of the fluxes or forces. The flow  $J_i$  may be a flow of a chemical species, a volume flow, a flow of electric current, or a flow of heat. The forces  $X_k$  may be expressed in the form of local gradients or macroscopic differences across the membrane of the chemical potentials, electric potential, hydrostatic pressure, or temperature. If a discontinuous formulation is used so that the macroscopic differences in these quantities across the membrane are chosen as the forces, then the  $L_{ik}$  coefficients in eq. (3.1.1.6) are average values over the membrane interposed between a particular pair of solutions.

Equation (3.1.1.6) imply, for example, that the flow of a chemical species  $i$  is dependent not only on its conjugate force  $X_i$ , i.e., the difference or negative gradient of its own chemical or electrochemical potentials but also on the gradients or differences of the electrochemical potentials of the other permeating species. Hence eq. (3.1.1.6) imply that a difference of electrical potential may cause a flow of an uncharged species, a fact which, as previously indicated, the Nernst-Planck equations do not recognize according to Meares *et al.* In general, eq. (3.1.1.6) allow that any type of vectorial force can, under suitable conditions, give rise to any type of vectorial flow.

In a system where  $n$  flows are occurring and  $n$  forces are operating, a total of  $n^2$  phenomenological coefficients  $L_{ik}$  are required to describe fully the transport properties of the system. This must be compared with the  $n$  mobilities used in the Nernst-Planck description of the system. A corresponding number  $n^2$  experimental transport measurements would have to be made to permit the evaluation of all the  $L_{ik}$  coefficients.



Fortunately a simplification can be made with the help of Onsager's reciprocal relationship<sup>(13)</sup>. This states that under certain conditions

$$L_{ik} = L_{ki} \quad (3.1.1.7)$$

The conditions required for eq. (3.1.1.7) to be valid are that the flows be linearly related to the forces and that the flows and forces be chosen such that

$$T\sigma = \sum_i J_i X_i \quad (3.1.1.8)$$

where  $\sigma$  is the local rate of production of entropy in the system when the  $X_i$  are the local potential gradients. The quantity  $T\sigma$  is often represented by the symbol  $\Phi$  and called the dissipation function because it represents the rate at which free energy is dissipated by the irreversible processes. In fact there is no completely general proof of eq. (3.1.1.7) but its validity has been shown for a large number of situations<sup>(14)</sup>.

With the help of the reciprocal relationship the number of separate  $L_{ik}$  coefficients required to describe a system of  $n$  flows and  $n$  forces is reduced from  $n^2$  to  $\frac{1}{2}n(n + 1)$ .

This nonequilibrium thermodynamic theory holds only close to thermodynamic equilibrium. The size of the departure from equilibrium for which the linear relationship between flow and force, eq. (3.1.1.6), and the reciprocal relationship, eq. (3.1.1.7), are valid, depends upon the type of flow considered. Strictly, the range of validity must be tested experimentally for each type of flow process. In the case of molecular flow processes, electronic conduction, and heat conduction the linear and reciprocal relationships have been found to be valid for flows of the order of magnitude commonly encountered in membranes<sup>(65)</sup>. In describing the progress of chemical reactions the relationships are valid only very close to equilibrium. Systems in which chemical reactions are taking place will be excluded from this discussion.

### 3.1.2.2 The Choice of Flows and Forces

In an isothermal membrane system the most obvious choice of flows is the set of flows of the permeating species--solvent, nonelectrolyte solutes, and ions. The conjugate forces are then the differences or local gradients of the electrochemical potentials of these species. To accord with eq. (3.1.1.8), in which  $T\sigma$  must be positive, increasing potentials in the direction of positive fluxes constitute negative forces. A set of

phenomenological equations corresponding to eq. (3.1.1.6) can be written relating the flows to the forces. The values of the  $L_{ik}$  coefficients appearing in these equations depend on the interactions occurring in the membrane, i.e., on the chemical nature of the permeating species and of the membrane, on the detailed microstructure of the membrane, and on the local concentrations of the permeating species.

In principle it should be possible to obtain values for the  $\frac{1}{2}n(n + 1)$   $L_{ik}$  coefficients by carrying out a suitable set of  $\frac{1}{2}n(n + 1)$  independent experiments. For example, if all the forces except one,  $X_a$ , were held at zero and the flows  $J_i, J_j$ , etc. of all the  $n$  species were measured, then the values of the coefficients  $L_{ia}, L_{ja}$  etc. could be obtained directly. Similar experiments would give the values for the remaining  $L_{ik}$  coefficients. Other sets of experiments may be used, and one may combine experiments where some of the forces are kept at zero, experiments where some of the flows are kept at zero, and experiments where some forces and some flows are kept at zero<sup>(14)</sup>.

Although the set of flows and conjugate forces outlined above may seem to be convenient for the molecular interpretation of the interactions occurring in a membrane system, the equations written in terms of these flows and forces are not convenient for the design of experiments for the evaluation of the  $L_{ik}$  coefficients. For example, the forces which are usually controlled experimentally are not differences of electrochemical potential, but differences of concentration, electrical potential, and hydrostatic pressure. Also, it may be more convenient to measure the total volume of the flows across a membrane rather than the flow of solvent, or to measure the electric current and one ionic flow rather than two ionic flows. For these reasons, sets of practical flows and forces are often chosen to describe membrane transport<sup>(14)</sup>. These practical sets of flows and their conjugate forces must satisfy the relationship of eq. (3.1.1.8), which gives the dissipation function.

A system involving the transport of water and a nonelectrolyte solute across a membrane can be described by giving the flows of water  $J_w$  and of solute  $J_s$ . The conjugate forces are then the differences, or the local gradients, of the chemical potentials of water  $\mu_w$  and solute  $\mu_s$ . The transport properties of this system are described by the following equations:

$$J_w = L_w \Delta \mu_w + L_{ws} \Delta \mu_s \quad (3.1.1.9)$$

$$J_s = L_{sw} \Delta \mu_w + L_s \Delta \mu_s$$

where according to the reciprocal relationship  $L_{sw} = L_{ws}$  and the dissipation function of the system is given by the expression

$$\Phi = J_w \Delta \mu_w + J_s \Delta \mu_s \quad (3.1.1.10)$$

When considering ideal external solutions the forces  $\Delta \mu_w$  and  $\Delta \mu_s$  are often expanded into separate terms giving the contributions of the concentration differences and pressure difference to the total driving forces. Thus

$$\Delta \mu_w = (RT/c_w) \Delta \bar{c}_w \Delta c_w + V_w \Delta p$$

Here  $V_w$  is an average partial molar volume of water and  $\bar{c}_w$  is an average concentration of water. When  $\Delta \mu_w$  and  $\Delta \mu_s$  in eq. (3.1.1.10) are expanded in this way and the resulting concentration and pressure terms are grouped separately the expression for the dissipation function becomes<sup>(50)</sup>

$$\Phi = J_v \Delta p + J_D RT \Delta c_s \quad (3.1.1.11)$$

where  $J_v$  the total volume flow is equal to  $(\bar{V}_w J_w + \bar{V}_s J_s)$  and  $J_D$  is equal to  $(J_s/\bar{c}_s - J_w/\bar{c}_w)$ .  $J_D$  is sometimes called the exchange flow and represents the apparent mean velocity of the solute relative to the water. According to eq. (3.1.1.11) the system can be described in terms of  $J_v$  and  $J_D$  as flows and  $\Delta p$  and  $RT \Delta c_s$  (or  $\Delta \pi_s$ ) as their conjugate forces. Thus

$$J_v = L_p \Delta p + L_{pD} \Delta \pi_s \quad (3.1.1.12)$$

$$J_D = L_{Dp} \Delta p + L_D \Delta \pi_s$$

where  $L_{Dp}$  equals  $L_{pD}$  and  $\Delta \pi_s$  is the difference in osmotic pressure between the solutions. Experimentally it is easier to control the values of the forces appearing in eq. (3.1.1.12) than those appearing in eq. (3.1.1.9).

Similarly a system involving flows of water and a salt dissociated into a cationic species and an anionic species can be described in terms of the flows  $J_w$ ,  $J_1$ , and  $J_2$  of these molecular species or by the set comprising the total volume flow, the electric current, and the defined flow of salt, i.e.,  $J_v$ ,  $I$  and  $J_s$ <sup>(14)</sup>. In the former case the conjugate forces are the differences of the electrochemical potentials of the species across the membrane, in the latter case the conjugate forces are the pressure difference minus the osmotic pressure difference, the electrical potential difference, and the difference of the pressure-independent part of the chemical potential of the salt. Care must be taken in the precise definition of these forces, particularly of the electrical potential difference<sup>(67)</sup>.

Since the choice of flows and forces is to some extent open as long as the flows and forces satisfy eq. (3.1.1.8) a set can be chosen primarily for ease of theoretical interpretation of  $L_{ik}$  coefficients or for ease of experimental evaluation of the  $L_{ik}$  coefficients. Furthermore, given values of the  $L_{ik}$  coefficients relevant to one set of flows and forces, it is a straightforward operation to calculate the values of  $L_{ik}$  coefficients relevant to another set of flows and forces<sup>(67)</sup>.

It is of course possible and often convenient to describe the transport properties of a system in terms of flows and forces which are not conjugate and which do not obey eq. (3.1.1.8). The system where the membrane is permeated by a flow of water and a flow of a solute can be described in terms of the flow of water  $J_w$ , the flow of solute  $J_s$ , the pressure difference  $\Delta p$ , and the difference in concentration of the solute  $RT\Delta c_s$  or  $\Delta\pi_s$ . These flows and forces are interrelated by the equations

$$J_v = L_p \Delta p - \sigma L_p \Delta \pi_s \quad (3.1.1.13)$$

$$J_s = \bar{c}_s (1 - \sigma) J_v + \omega \Delta \pi_s$$

Here  $L_p$  has the same significance as in eq. (3.1.1.12).  $\sigma$  is called the reflection coefficient of the solute and is equal to  $\Delta p / \Delta \pi_s$  at zero  $J_v$ ,  $\omega$  is the solute permeability  $J_s / \Delta \pi_s$  at zero  $J_v$ , and  $\bar{c}_s$  is the average concentration of the solute in the two solutions<sup>(67)</sup>.

In practice eq. (3.1.1.13) may be easier to use than eq. (3.1.1.12) because the flows generally measured are  $J_v$  and  $J_s$  rather than  $J_w$  and  $J_D$ . However, eq. (3.1.1.13) are not

a proper set of phenomenological equations in the sense of eq. (3.1.1.6). Neither are  $\sigma$  and  $\omega$  phenomenological coefficients in the sense used so far. They are related to the  $L_{ik}$  coefficients of eq. (3.1.1.12) by the relationships<sup>(66)</sup>.

$$\sigma = -L_{pD}/L_p \text{ and } \omega = \bar{c}_s(L_p L_D - L_{pD}^2)/L_p$$

### 3.1.2.3 Uses and Limitations of the Theory

The theory of nonequilibrium thermodynamics has been applied to membranes in a number of papers where the aim has been to obtain general relationships between observable macroscopic flows and forces. Topics investigated in this way have included: isotopic tracer flows and flux ratios<sup>(68, 69)</sup>, electrokinetic phenomena<sup>(70)</sup>, the transport properties of complex membranes<sup>(14)</sup>, and the coupling of transport processes with chemical reactions, so-called active transport<sup>(13)</sup>. However, the main concern of these investigations has been the transport of non-electrolyte solutes and ions across charged and uncharged membranes<sup>(12, 13, 46)</sup>.

The  $L_{ik}$  coefficients obtained from experimental measurements of transport phenomena under one set of conditions can either be used to predict values of flows and forces under other sets of conditions or they can be analyzed for the purpose of interpreting, at a molecular level, the various interactions which occur between the permeating molecules and ions and the membrane material. This second use of the  $L_{ik}$  coefficients is especially interesting but it is by no means simple.

An inspection of any of the sets of phenomenological equations [(3.1.1.6), (3.1.1.9), (3.1.1.12), and (3.1.1.13)] shows that nowhere is any direct reference made to the membrane or its properties. The  $L_{ik}$  coefficients relate the flows of the permeating species to the gross thermodynamic forces acting on these species and, in general, no particular coefficient represents only the interaction of a permeating species with the membrane. Instead the properties of the membrane material affect the values of each of the  $L_{ik}$  coefficients to a greater or lesser extent.

The physical interpretation of measurements of transport properties is made more straightforward by inverting the matrix of the phenomenological equations [eq. (3.1.1.6)] to give the set of eqs. (3.1.1.14)

$$X_i = \sum_{\text{all } k} R_{ik} J_k \quad (3.1.1.14)$$

These represent the forces as linear functions of the flows. The  $R_{ik}$  and  $L_{ik}$  coefficients of eq's. (3.1.1.14) and (3.1.1.6) are related by the expression

$$R_{ik} = A_{ik} / |L| \quad (3.1.1.15)$$

where  $A_{ik}$  is the minor of  $L_{ik}$  and  $|L|$  is the determinant of the  $L_{ik}$  coefficients. If the reciprocal relation is valid for the  $L_{ik}$  coefficients, it is valid also for the  $R_{ik}$  coefficients. Whereas the  $L_{ik}$  coefficients have the dimensions of conductance (i.e., flow per unit force), the  $R_{ik}$  coefficients have the dimensions of resistance (i.e., force per unit flow) and are frequently called resistance coefficients.

The  $R_{ik}$  coefficients are easier to interpret at the molecular level than the  $L_{ik}$  coefficients. A non-zero  $R_{ik}$  ( $i \neq k$ ) implies a direct interaction between  $i$  and  $k$ , that is, the molecular flow of  $k$  directly causes a force to act on species  $i$ . On the other hand, a non-zero  $L_{ik}$  ( $i \neq k$ ) does not necessarily imply a direct molecular interaction between species  $i$  and  $k$ , it means that the force acting on  $k$  affects the flow of  $i$ , perhaps directly or indirectly.

In effect eq. (3.1.1.14) means that, in the steady state, the gross thermodynamic force  $X_i$  acting on species  $i$  is balanced by the forces  $R_{ik}J_k$  summed over all species  $k$ , including  $i$ . The term  $R_{ii}J_i$  is the drag force per mole which would act on  $i$  when moving at a rate  $J_i/c_i$  through a medium where there was no net flow of any other species. Thus the  $R_{ii}$  coefficients are still complex quantities including contributions from the interactions between  $i$  and all other species present, including the membrane. However, each  $R_{ik}$  ( $i \neq k$ ) coefficient represents only the single interaction between the flows of  $i$  and  $k$ . The  $R_{ii}$  coefficients, like the  $L_{ii}$ , must always be positive but  $R_{ik}$  ( $i \neq k$ ) and the  $L_{ik}$  coefficients may be positive, negative, or zero.

### 3.1.3 The Frictional Model of Membrane Transport

The frictional model of membrane transport has been described by Meares *et al.*<sup>(9)</sup>. The idea of describing steady-state transport processes in a membrane as balances between the gross thermodynamic forces acting on the system and frictional interactions between the components of the system is one of long standing. More recently, the term molecular friction coefficient has been applied to the coefficient which relates the frictional force between two components to the difference between their

velocities. This approach has been used to describe transport processes across membranes by several authors. The precise treatment that will be considered here is the frictional model as proposed by Spiegler<sup>(71)</sup>.

The fundamental statement of the frictional model is that when the velocity of a permeating species has reached a constant value, the gross thermodynamic force  $X_i$  acting on one mole of that species must be balanced by the interactive forces,  $F_{ik}$ , acting between one mole of the same species and the other species present. Mathematically this is expressed by

$$X_i = - \sum_{k \neq i} F_{ik} \quad (3.1.3.1)$$

Furthermore, these interactions are assumed to be frictional in character so that each force  $F_{ik}$  is equal to a friction coefficient  $f_{ik}$  multiplied by the difference between the velocities  $v_i$  and  $v_k$  of the two species. Thus

$$F_{ik} = -f_{ik}(v_i - v_k) \quad (3.1.3.2)$$

and

$$X_i = \sum_{k \neq i} f_{ik}(v_i - v_k) \quad (3.1.3.3)$$

It should be noted that  $f_{ik}$  is the force acting on one mole of  $i$  owing to its interaction with the amount of  $k$  normally in the environment of  $i$  and under unit difference between the mean velocities of  $i$  and  $k$ . In general the concentrations of  $i$  and  $k$  are not equal and consequently the coefficients  $f_{ik}$  and  $f_{ki}$  are not equal. When the balance of forces is taken over unit volume of the system it is readily seen that

$$c_i f_{ik} = c_k f_{ki} \quad (3.1.3.4)$$

The quantity  $f_{ik}/c_k$  or  $f_{ki}/c_i$  represents the force acting between one mole of  $i$  and one mole of  $k$  at unit velocity difference. Its value obviously depends on the chemical types of the two species.

Besides containing a term such as  $f_{ik}(v_i - v_k)$  for the interactions between  $i$  and each of the other permeating species, the right-hand side of eq. (3.1.3.3) also includes a term

$f_{im}(v_i - v_m)$  which allows for the interaction between  $i$  and the membrane. Usually the membrane is taken as the velocity reference so that  $v_m$  is zero.

With the help of the relationship

$$J_i = c_i v_i \quad (3.1.3.5)$$

eq. (3.1.3.3) can be rearranged to

$$X_i = (J_i/c_i) \frac{\sum_{K \neq i} f_{ik}}{K \neq i} - \frac{\sum_{K \neq i} (J_K f_{ik}/c_K)}{K \neq i} \quad (3.1.3.6)$$

Equation (3.1.3.6) has the same form as eq. (3.1.1.14) which relate the forces to the flows via the  $R_{ik}$  coefficients. Each  $R_{ik}$  coefficient can be equated to the corresponding  $\sum f_{ik}/c_i$ . This illustrates the complex nature of the  $R_{ik}$  coefficient. Each  $R_{ik}$  ( $i=k$ ) coefficient is equivalent to the corresponding  $-f_{ik}/c_k$ .

In a system with  $n$  flows,  $(n - 1)$  friction coefficients are required to describe the interactions of any one permeating species with the other permeating species. One further coefficient is required to describe its interaction with the membrane. A total of  $n^2$  friction coefficients is thus required to describe the transport properties of the system but with the use of eq. (3.1.3.4) this number is reduced to  $\frac{1}{2}n(n + 1)$ , i.e., the same as the minimum number of independent  $L_{ik}$  or  $R_{ik}$  coefficients. Hence the minimum number of experimental measurements required to characterize the system fully is the same whether it is described in terms of the  $L_{ik}$  coefficients, the  $R_{ik}$  coefficients, or the  $f_{ik}$  coefficients. The most convenient set of experimental parameters to be measured may depend on which set of coefficients is chosen to represent the properties of the system.

The choice of coefficients can be made mainly on the basis of experimental convenience because, having obtained values of one set of coefficients, it is no problem to obtain values for the other sets from these. The relationships between the  $R_{ik}$  and  $L_{ik}$  coefficients, and between these and the friction coefficients have already been given briefly above and are discussed in more detail elsewhere<sup>(9)</sup>. Direct relationships between the friction coefficients and experimentally measurable quantities have also been discussed in several papers<sup>(9)</sup>. The method of obtaining one such relationship is mentioned here as an illustration of Spiegler's treatment.



In a system consisting of a membrane, water, one species of univalent cation and one species of univalent anion, the electrical conductivity  $k$  is given by the expression

$$k = F(J'_1 - J'_2) \quad (3.1.3.7)$$

where  $J'_1$  and  $J'_2$  are the flows of univalent cations and anions per unit area, respectively, under an electrical potential gradient of  $1 \text{ V cm}^{-1}$ . Under these conditions the forces acting on the cations, anions and water are  $F$ ,  $-F$ , and  $0 \text{ J cm}^{-1} \text{ mole}^{-1}$ , respectively. On substituting these forces into the set of eqs. (3.1.3.6) describing the system, the equations can be solved for the flows  $J'_1$  and  $J'_2$  in terms of the friction coefficients and the concentrations of the ions and water. These expressions for  $J'_1$  and  $J'_2$  can then be substituted into eq. (3.1.3.7) to give an expression for  $k$  in terms of the friction coefficients operating in the system and the concentrations of the permeating species.

It is possible to obtain expressions for other transport parameters, such as the electro-osmotic permeability, transport numbers of the ions, and the self-diffusion coefficients of the permeating species in terms of the friction coefficients in a somewhat similar manner. A set of such expressions can then be solved to give the individual friction coefficients in terms of the transport parameters and the concentrations.

The procedure outlined above becomes rather tedious as the expressions giving the individual transport parameters in terms of the friction coefficients may be very complicated. Under certain circumstances a simpler procedure can be used to obtain values for the friction coefficients<sup>(9)</sup>.

The main advantage claimed for the use of the frictional model to describe transport processes in membranes, is that each friction coefficient represents the interaction between a particular pair of flows. They are not complex combinations of several interactions as are the  $L_{ik}$  and  $R_{ij}$  coefficients. The model also permits a direct evaluation of the interactions between the various permeating species and the membrane, interactions which are hidden in treatments which use only the  $L_{ik}$  and  $R_{ik}$  coefficients.

It may be possible under favourable conditions to neglect some of the frictional interactions on the basis of previous knowledge of the properties of the membrane and permeants. A smaller number of experimental measurements is then necessary to describe the system. For example Spiegler<sup>(71)</sup> suggested that, in a system where a

cation-exchange membrane is in equilibrium with a dilute electrolyte solution, the friction coefficient  $f_{12}$  (where 1 represents cations and 2 represents anions) can be set equal to zero because of the low concentration of diffusible anions.

Simplifications such as that described above should be made only with great care. It is possible that even though  $f_{ik}$  may be negligibly small  $f_{ki}$  may be quite large because the ratio  $c_k/c_i$  [c.f. eq. (3.1.3.4)] may be large. In such a case the full number of experimental measurements must still be made.

The quantitative application of the frictional model to biological membrane systems is restricted by the difficulty of measuring or estimating values for the average or local concentrations of the permeating species in the membrane. These values are required for the calculation of the friction coefficients from the measured experimental parameters. Thus, although values for sets of  $L_{ik}$  coefficients (particularly  $L_p$ ,  $\sigma$ , and  $\omega$ ) have been obtained for some biological systems, it has been possible to interpret these in terms of the friction coefficients in only a qualitative manner<sup>(9)</sup>. With homogeneous synthetic resin membranes the situation seems to be simpler. Some limited measurements of friction coefficients for such systems have been reported<sup>(9)</sup>.

## 3.2 Conductance and Transport Number

### 3.2.1 Conductance and Transport Number and their Relation to Flows and Forces in Electrodialysis

The author has derived the following relationships for conductance and transport number and their relation to flows and forces in electrodialysis

Consider a system consisting of two aqueous solutions containing only one permeable electrolyte separated by a membrane<sup>(14)</sup>. Different concentrations, pressures, and electrical potentials are allowed on both sides of the membrane. Envisage further the operation of two forces with two conjugated flows which may pass from one side of the membrane to the other. The simplest choice of flows and forces would be the flow of cation  $J_1$ , driven by the difference in electrochemical potential  $\Delta\widehat{\mu}_1$ , and the flow of anion  $J_2$ , driven by the corresponding force  $\Delta\widehat{\mu}_2$ . The following simple phenomenological equations can then be set-up<sup>(13)</sup>. (see eq. 3.1.1.6)

$$J_1 = L_1 \Delta \hat{\mu}_1 \quad (3.2.1)$$

$$J_2 = L_2 \Delta \hat{\mu}_2 \quad (3.2.2)$$

where  $L_1$  and  $L_2$  are the phenomenological coefficients which characterize the system.

The chemical potential of the electrolyte,  $\Delta \mu_s$ , is equal to the electrochemical potentials of the cation and the anion<sup>(14)</sup>.

$$\Delta \mu_s = \Delta \hat{\mu}_1 + \Delta \hat{\mu}_2 \quad (3.2.3)$$

The electrical current,  $I$ , through a membrane is related to the ionic flows by the relationship<sup>(13)</sup>.

$$I = (z_1 J_1 + z_2 J_2) F \quad (3.2.4)$$

where  $z_1$  = valence of cation;  $z_2$  = valence of anion;  $F$  = Faraday's constant.

When  $I = 0$ , then  $J_1 = J_2$

The electromotive force,  $E$ , acting on the system can be determined by introducing a pair of electrodes reversible to one of the ions, say ion 2, and measuring the potential difference. The value of  $E$  is related thermodynamically to the difference in electrochemical potential of ion 2<sup>(14)</sup>:

$$E = \frac{\Delta \hat{\mu}_2}{z_2 F} \quad (3.2.5)$$

for NaCl,  $z_2 = -1$

$$\text{and } E = \frac{\Delta \hat{\mu}_2}{-F} \quad (3.2.6)$$

$$\text{or } EF = -\Delta \hat{\mu}_2 \quad (3.2.7)$$

Membrane conductance is usually carried out under isothermal, isobaric conditions with constant salt concentrations across the membrane.

$$\text{when } \Delta\mu_s = 0, \text{ then } \Delta\tilde{\mu}_1 = -\Delta\tilde{\mu}_2 \quad (3.2.8)$$

The electric current,  $I$ , through the membrane is:

$$I = F(J_1 - J_2) \quad (3.2.9)$$

Substituting eq. (3.2.1) and (3.2.2) into eq. (3.2.9), gives

$$I = F(L_1\Delta\tilde{\mu}_1 - L_2\Delta\tilde{\mu}_2) \quad (3.2.10)$$

$$\text{But, } \Delta\tilde{\mu}_1 = -\Delta\tilde{\mu}_2 \quad (\text{see eq. 3.2.8})$$

$$\therefore I = F(-L_1\Delta\tilde{\mu}_2 - L_2\Delta\tilde{\mu}_2) \quad (3.2.11)$$

$$= -F\Delta\tilde{\mu}_2(L_1 + L_2) \quad (3.2.12)$$

$$\text{But } EF = -\Delta\tilde{\mu}_2 \quad (\text{see eq. 3.2.7})$$

$$\therefore I = F^2E(L_1 + L_2)$$

$$\therefore \left[ \frac{I}{E} \right]_{\Delta\mu_s = 0, J_v = 0} = F^2(L_1 + L_2) = \text{Conductance} \quad (3.2.13)$$

when  $I = 0$ , then

$$J_1 - J_2 = 0 \quad (3.2.14)$$

Substituting eqs. (3.2.1) and (3.2.2) into eq. (3.2.14) gives

$$L_1\Delta\tilde{\mu}_1 - L_2\Delta\tilde{\mu}_2 = 0 \quad (3.2.15)$$

$$\text{But } \Delta\tilde{\mu}_1 = \Delta\mu_s - \Delta\tilde{\mu}_2 \quad (\text{see eq. 3.2.3})$$

$$L_1 (\Delta \mu_s - \Delta \tilde{\mu}_2) - L_2 \Delta \tilde{\mu}_2 = 0 \quad (3.2.16)$$

$$\text{and } \Delta \tilde{\mu}_2 = \frac{L_1}{L_1 + L_2} \Delta \mu_s \quad (3.2.17)$$

$$\text{or } -EF = \frac{L_1}{L_1 + L_2} \Delta \mu_s \quad (3.2.18)$$

$$\therefore \left[ \frac{EF}{\Delta \mu_s} \right]_{I=0, J_v=0} = - \frac{L_1}{L_1 + L_2} \quad (3.2.19)$$

$$\text{Consider } \left[ \frac{J_1/I}{\Delta \mu_s} \right]_{\Delta \mu_s=0} = \frac{L_1 \Delta \tilde{\mu}_1}{F^2 E (L_1 + L_2)} \quad (3.2.20)$$

But  $\Delta \tilde{\mu}_1 = -\Delta \tilde{\mu}_2$  and  $EF = -\Delta \tilde{\mu}_2$

$$\therefore \left( \frac{J_1/I}{\Delta \mu_s} \right)_{\Delta \mu_s=0} = \frac{L_1 (-\Delta \tilde{\mu}_2)}{-\Delta \tilde{\mu}_2 (L_1 + L_2) \cdot F} \quad (3.2.21)$$

$$= \frac{1}{F} \cdot \frac{L_1}{L_1 + L_2} \quad (3.2.22)$$

$$\therefore \left[ \frac{JF/I}{\Delta \mu_s} \right]_{\Delta \mu_s=0; J_v=0} = \frac{L_1}{L_1 + L_2} \quad (3.2.23)$$

$$= \Delta t \text{ (transport number)} \quad (3.2.23)$$

$$= - \left( \frac{EF}{\Delta \mu_s} \right)_{I=0; J_v=0} \quad (3.2.24)$$

Note: The membrane potential  $\Delta \Psi$  is related to the electromotive force measured between reversible electrodes by the expression<sup>(13)</sup>:

$$\Delta \Psi = E - \frac{\Delta \tilde{\mu}_2}{z_2 F}$$

### 3.3 Ion Coupling from Conventional Transport Coefficients

#### 3.3.1 Ion Association and the Coupling of Flows

Kedem<sup>(15)</sup> has described ion association and coupling of flows, charged hydrophobic membranes and the association model, transport properties and transport coefficients in the absence of volume flows and transport coefficients in the absence of a pressure gradient.

Anions and cations will exist in part as neutral ion pairs or molecules when the dielectric constant of the membrane is low. Three mobile species can be identified in the membrane phase according to Kedem: free anion, free cation and ion pair (only a univalent electrolyte will be considered). The dissipation function for ion flows, in this case, can be expressed either in terms of the two stoichiometric ion flows,  $J_1$  and  $J_2$ , or in terms of three species: free ion,  $J_1^*$  and  $J_2^*$ , and neutral molecule,  $J_s$ . Assuming dissociation equilibrium, the thermodynamic potential of the molecule is equal to that of the sum of the ions:

$$X_s = X_1 + X_2 \quad (3.3.1)$$

The relation between  $J_1$  and  $J_1^*$  is:

$$J_1 = J_1^* + J_s \quad (3.3.2)$$

$$J_2 = J_2^* + J_s$$

and thus the two species dissipation function

$$\phi = J_1 X_1 + J_2 X_2$$

is equal to the three flow expression

$$\phi = J_1^* X_1 + J_2^* X_2 + J_s X_s = (J_1 - J_s) X_1 + (J_2 - J_s) X_2 + (X_1 + X_2) J_s$$

Assuming that no frictional interactions exist between the free ions and the neutral molecule and that volume flow is either negligible or absent, a linear relationship between flows and forces can be described by the following set of equations:

$$X_1 = R_{11}^* J_1^*; \quad X_2 = R_{22}^* J_2^*; \quad X_s = R_s J_s \quad (3.3.3)$$

Equations (3.3.1), (3.3.2) and (3.3.3) give:

$$R_{11}^*(J_1 - J_s) + R_{22}^*(J_2 - J_s) = R_s J_s \quad (3.3.4a)$$

from which  $J_s$  is expressed in terms of individual resistance coefficients of the three mobile species and the flow of the free ions,

$$J_s = \frac{R_{11}^* J_1^* + R_{22}^* J_2^*}{\Sigma R} \quad (3.3.4b)$$

where  $\Sigma R = R_s + R_{11}^* + R_{22}^*$ .

From the relations one obtains the phenomenological equations which describe the total stoichiometric ionic flows and forces by means of the individual resistance coefficients of the free and associated mobile species:

$$X_1 = R_{11}^* \left( 1 - \frac{R_{11}^*}{\Sigma R} \right) J_1 - \frac{R_{11}^* R_{22}^*}{\Sigma R} J_2 \quad (3.3.5)$$

$$X_2 = - \frac{R_{11}^* R_{22}^*}{\Sigma R} J_1 + R_{22}^* \left( 1 - \frac{R_{22}^*}{\Sigma R} \right) J_2$$

The corresponding resistance coefficients are:

$$R_{11} = R_{11}^* \frac{R_{22}^* + R_s}{R_{11}^* + R_{22}^* + R_s}$$

$$R_{22} = R_{22}^* \frac{R_{11}^* + R_s}{R_{11}^* + R_{22}^* + R_s} \quad (3.3.6)$$

$$R_{12} = - \frac{R_{11}^* R_{22}^*}{R_{11}^* + R_{22}^* + R_s}$$

The relative importance of the ion-coupling, according to Kedem, is best expressed in terms of the degree of coupling,  $q^2 = R_{12}^2 / R_{11} R_{22}$ , where  $q^2 = 1$  means that the coupling between the flows is complete, and  $q^2 = 0$  indicates absence of coupling<sup>(72)</sup>.

For the case of ion association, this coefficient is given by:

$$q^2 = \frac{R_{11}^* R_{22}^*}{(R_s + R_{11}^*)(R_s + R_{22}^*)} \quad (3.3.7)$$

If  $R_s \gg R_{11}^*$  and  $R_s \gg R_{22}^*$  then  $R_{11} \approx R_{11}^*$ ,  $R_{22} \approx R_{22}^*$  and  $q^2 \rightarrow 0$ ; i.e. there is no significant coupling. If, on the other hand,  $R_s$  is much smaller than the  $R_i^*$  terms, coupling can be practically complete.

The physical significance of these limits becomes clear if we introduce concentration and friction coefficients for the R's,  $R_{ii} = f_i / c_i$ .

To discuss the orders of magnitude, let us take all  $f_i$ 's approximately equal; then

$$q^2 \approx \frac{c_s^2}{(c_s + c_1^*)(c_s + c_2^*)} \quad (3.3.8)$$

Negligible coupling, i.e.  $q^2 \rightarrow 0$ , is found when the concentration of the free ion are much larger than the concentrations of associated molecules; on the other hand, strong association leads to a high degree of coupling, that is  $q^2 \rightarrow 1$ . In other words, the degree of coupling and degree of association are closely related.

Consider first a matrix, which does not carry fixed charges, i.e.  $c_1^* = c_2^* = c^*$ . The expression for the coupling coefficient will be given by



$$q^2 \cong \frac{c_s^2}{(c_s + c^*)^2} \quad (3.3.9)$$

For slight association expected in high dielectric media,  $c_s \ll c^*$  and:

$$q^2 \cong \frac{c_s^2}{2c_s c^* + c^{*2}} = \frac{(c_s/c^*)^2}{1 + 2 c_s/c^*} \rightarrow 0 \quad (3.3.10)$$

No coupling will thus be observed.

In these media  $q^2$  also remains small in the presence of fixed charges, i.e.

$$c_1^* \neq c_2^*$$

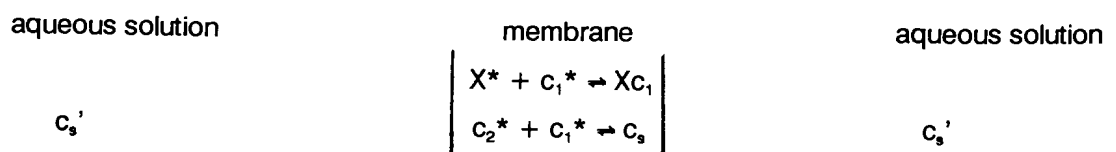
For slight dissociation, as is to be expected in hydrophobic membranes,  $c_s \gg c^*$ , and:

$$q^2 \cong \frac{1}{(1 + c^*/c_s)^2} \rightarrow 1 \quad (3.3.11)$$

The presence of fixed charges in hydrophobic membranes complicates the analysis of coupling effects, according to Kedem and requires a detailed consideration of a model.

### 3.3.2 Charged Hydrophobic Membranes - The Association Model

Consider a polymeric membrane matrix with chemically bound ionizable groups at a total concentration of  $X_t$ , and low water content<sup>(73)</sup>. Several ion-exchange and dissociation equilibria are established when immersing such a membrane in an aqueous salt solution with a concentration  $c_s'$ .



Assuming ideality in the aqueous solutions, dissolution equilibria of the free counter-ion  $c_1^*$  and free co-ion  $c_2^*$  between the membrane and the aqueous solution are obtained

by equating the electrochemical potentials in the two phases:

$$\begin{aligned}\tilde{\mu}_1' &= \mu_1^{\circ'} + RT \ln c_1' + z_1 F \psi' = \mu_1^{\circ} + RT \ln c_1^* + z_1 F \psi = \tilde{\mu}_1 \\ \tilde{\mu}_2' &= \mu_2^{\circ'} + RT \ln c_2' + z_2 F \psi' = \mu_2^{\circ} + RT \ln c_2^* + z_2 F \psi = \tilde{\mu}_2.\end{aligned}\quad (3.3.12)$$

Adding the respective terms and applying the condition for ion pair formation reaction in the membrane:  $\mu_s = \tilde{\mu}_1 + \tilde{\mu}_2$ , we obtain after rearrangement:

$$c_s = k c_s'^2 \quad (3.3.13)$$

where  $c_s'$  is the concentration of the fully dissociated salt in water;  $c_s$  is the concentration of the undissociated salt in the membrane phase;  $c_1^*$ ,  $c_2^*$  are the concentrations of free ions in the membrane; and  $k = \exp [(\mu_s^{\circ} - \mu_1^{\circ'} - \mu_2^{\circ'})/RT]$ .

Ion pair formation between the small ions is expressed by:

$$\frac{c_1^* c_2^*}{c_s} = K_d^s \quad c_s = c_2^t - c_2^* \quad (3.3.14)$$

where  $c_2^t$ ,  $c_s$  indicate the concentration of the total and the undissociated salt in the membrane phase. Ion pair formation at the fixed ionic sites is given by:

$$\frac{c_1^* X^*}{(X_t - X^*)} = K_d^f \quad (3.3.15)$$

where  $X_t$  is the total concentration of fixed groups and  $X^*$  is its free fraction. Introducing electroneutrality for the dissociated species,  $c_1^* = c_2^* + X^*$ , into the above expressions and rearranging the equations for the modified Donnan equilibrium for non-aqueous membranes, we obtain a polynomial of 3rd degree with respect to  $c_2^*$ :

$$K_d^f c_2^{*3} + (K_d^f X_t + \alpha) c_2^{*2} - K_d^f \alpha c_2^* - \alpha^2 = 0 \quad (3.3.16)$$

$$\text{where } \alpha = K_d^s k c_s'^2$$

The adsorption isotherm of the co-ions,  $c_2^t$ , is given from the above relations by

$$c_2^t = c_2^* + c_s = c_2^* + \alpha/K_d^s \quad (3.3.17)$$

For analysis of the coupling coefficient, explicit expressions for the concentrations of the co-ion or counter-ion are obtained from eqs. (3.3.14) and (3.3.15) and the

electroneutrality condition:

for free co-ions:

$$c_2^* = \frac{K_d^s}{K_d^f} \left[ \frac{c_2^t - c_2^*}{X_t - X^*} \right] X^* \quad (3.3.18)$$

for free counter-ions:

$$c_1^* = \left( \frac{K_d^s}{K_d^f} \left[ \frac{c_2^t - c_2^*}{X_t - X^*} \right] + 1 \right) X^* \quad (3.3.19)$$

for small dissociation:

$$c_2^* \ll c_2^t \cong c_s \text{ and } X^* \ll X_t$$

At these conditions, free co-ion concentration becomes

$$c_2^* \cong m c_2^t a \quad (3.3.20)$$

where

$$m = K_d^s/K_d^f \text{ and } a = X^*/X_t \ll 1$$

Free counter-ion concentration is given by

$$c_1^* \cong m c_2^t a + X^* = a(m c_2^t + X_t) \quad (3.3.21)$$

Coupling coefficient is thus given by

$$q^2 = \frac{1}{(1 + c_1^*/c_s) (1 + c_2^*/c_s)} \cong \frac{1}{(1 + c_1^*/c_2^t) (1 + c_2^*/c_2^t)} \cong \frac{1}{1 + c_1^*/c_2^t} \quad (3.3.22)$$

High coupling  $q^2 \rightarrow 1$  is obtained when  $c_1^*/c_2^t \ll 1$ ;

$$\frac{c_1^*}{c_2^t} = a \frac{(m c_2^t + X_t)}{c_2^t} = a(m + X_t/c_2^t) \quad (3.3.23)$$

According to Kedem, high coupling will be observed in non-charged hydrophobic membranes with small salt dissociation constants; in charged hydrophobic membranes a high degree of coupling will be observed only in the case of large salt invasion.

### 3.3.3 Transport Properties and Transport Coefficients in the Absence of Volume Flow

Phenomenological equations for two stoichiometric ionic flows in the absence of volume flow is given by:

$$X_1 = R_{11}J_1 + R_{12}J_2 \quad (3.3.24)$$

$$X_2 = R_{21}J_1 + R_{22}J_2$$

with  $R_{12} = R_{21}$

Electric current, electric potential and concentration are measured in practice and the conventional transport coefficients are defined accordingly. The relation between the driving forces and the  $R_{ij}$ 's are obtained from the constraints imposed for each measurement. The expression for driving force for ion transport, i.e. the difference in the electrochemical potential for equal concentrations on both sides of the membrane, is given by:

$$X_i = \Delta \tilde{\mu}_i = -z_i F E \quad (3.3.25)$$

So that

$$X_1 + X_2 = 0 \quad (3.3.26)$$

#### 3.3.3.1 Electric conductance

Membrane conductance,  $\kappa$ , is:

$$\kappa = \left( \frac{I}{E} \right)_{\Delta\mu = 0; J_v = 0} \quad (\text{see eq. 3.2.13})$$

where the electric current,  $I$ , is given by

$$I = F(z_1 J_1 + z_2 J_2) \quad (\text{see eq. 3.2.4})$$

The current  $I$  can be expressed in terms of resistance coefficients and two driving forces by substituting eq. (3.3.24) into eq. (3.3.26).

$$\therefore J_2 = - \frac{R_{11} + R_{12}}{R_{22} + R_{12}} J_1 \quad (3.3.27)$$

Introducing  $J_2$  from eq. (3.3.27) into eq. (3.3.24), and rearranging, gives:-

$$X_1 = R_{11} J_1 - \frac{R_{12}(R_{11} + R_{12})J_1}{R_{22} + R_{12}} = \frac{R_{11}R_{22} - R_{12}^2}{R_{22} + R_{12}} J_1 \quad (3.3.28)$$

From eqs. (3.2.4), (3.3.27) and (3.3.28), the current is

$$I = (J_1 - J_2) = \frac{R_{11} + R_{22} + 2R_{12}}{R_{11}R_{22} - R_{12}^2} X_1 \quad (3.3.29)$$

and the conductance,  $\kappa$ , is

$$\frac{\kappa}{F^2} = \left( \frac{I}{E} \right) \frac{1}{F^2} = \frac{J_1 - J_2}{X_1} = \frac{R_{11} + R_{22} + 2R_{12}}{R_{11}R_{22} - R_{12}^2} \quad (3.3.30)$$

### 3.3.3.2 Transport numbers

Transport numbers  $t_{1,2}$  are defined as the fraction of the electric current carried by each of the ions, without concentration gradients. In practice, membrane potentials are measured assuming Onsager's symmetry.

The transport numbers in terms of the  $R_{ij}$ 's are:

$$t_1 = \frac{J_1}{J_1 - J_2} = \frac{R_{22} + R_{12}}{R_{11} + R_{22} + 2R_{12}} \quad (3.3.31)$$

$$t_2 = 1 - t_1 = \frac{R_{11} + R_{12}}{R_{11} + R_{22} + 2R_{12}} \quad (3.3.32)$$

The product of  $t_1$  and  $t_2$  is

$$t_1 t_2 = \frac{(R_{11} + R_{12})(R_{22} + R_{12})}{(R_{11} + R_{22} + 2R_{12})^2} \quad (3.3.33)$$

### 3.3.3.3 Salt permeability

Salt permeability or salt "leak",  $\omega_s$ , is measured in the absence of electric current, so that

$$J_1 = J_2 = J_s \quad (3.3.34)$$

The driving force for salt flow is the gradient of its thermodynamic potential:

$$X_s = X_1 + X_2 \quad (3.3.35)$$

Adding the respective terms from eq. (3.3.24) gives:

$$X_s = (R_{11} + R_{22} + 2R_{12}) J_s \quad (3.3.36)$$

and

$$\frac{J_s}{X_s} = \omega_s c_s^{\text{av}} = \frac{1}{R_{11} + R_{22} + 2R_{12}} \quad (3.3.37)$$

where  $c_s^{\text{av}}$  is mean salt concentration on the two membrane sides.

### 3.3.3.4 Correlation between $\kappa_1, t_{1,2}$ and $\omega_s$

In aqueous charged ion-exchange membranes where the total amount of co-ions is very small compared to that of the counter-ions, the electro-neutral salt leak will become a very small fraction of total membrane conductance. Comparing the expression for the leak-conductance (LC) ratio obtained from eqs. (3.3.30) and (3.3.37), the following equation is obtained:

$$\frac{\omega_s c_s^{av}}{\kappa/F^2} = \frac{R_{11} R_{22} - R_{12}^2}{(R_{11} + R_{22} + 2R_{12})^2} \quad (3.3.38)$$

This and the expression for the product of the transport numbers, eq. (3.3.33), shows that

$$\frac{\omega_s c_s^{av}}{\kappa/F^2} = t_1 t_2 - \frac{R_{12}}{R_{11} + R_{22} + 2R_{12}} = t_1 t_2 - R_{12} \omega_s c_s^{av} \quad (3.3.39)$$

In the case of zero volume flow and no coupling between the co- and counter-ions  $R_{12} = 0$ ; a plot of the permeability ratio vs. the product of the two transport numbers should give a straight line with slope of 1, intersecting the origin:

$$\frac{\omega_s c_s^{av}}{\kappa/F^2} = t_1 t_2 \quad (3.3.40)$$

In general,  $R_{12} \neq 0$  should lead to a substantial deviation from this curve which will depend on the type and the extent of coupling.

Mutual drag reflects positive coupling between ion flows by any type of mechanism and is represented by a negative value of  $R_{12}$ . In this case the relation between the LC ratio and the product of the two transport numbers will be characterized by an inequality.

$$\frac{\omega_s c_s^{av}}{\kappa/F^2} > t_1 t_2 \quad (3.3.41)$$

An estimate of  $R_{12}$  is readily obtained from measured values of salt leak, membrane conductance and transport numbers as is shown in eq. (3.3.42).

$$- R_{12} = \frac{1}{\kappa/F^2} - \frac{t_1 t_2}{\omega_s c_s^{av}} \quad (3.3.42)$$

### 3.3.4 Transport Coefficients in the Absence of a Pressure Gradient

In practice, membrane conductance is usually measured in open cells with atmospheric pressure on both sides of the membrane and with equal salt concentrations. Under these conditions, volume flow is in general not zero. Thus in charged membranes, electro-osmotic volume flow is to be expected.

The electric conductance  $(I/E)_{\Delta p = 0} \equiv \kappa'$  is related to  $\kappa$  by<sup>(14)</sup>

$$\kappa' \equiv \frac{\kappa}{1 + P_E \beta} \quad (3.3.43)$$

where  $\kappa$  and  $P_E$  are the electric conductance and the electro-osmotic pressure respectively, measured under conditions of zero volume flow and salt gradient, and  $\beta$  is the electro-osmotic permeability, measured at zero pressure and salt gradient.

For a homogeneous charged membrane has  $\beta$  and  $P_E$  opposite signs<sup>(14)</sup>, and

$$\beta = - \frac{P_E L_p}{\kappa} \quad (3.3.44)$$

$L_p$  and  $\kappa$  are straight coefficients and therefore always positive. This implies that  $\kappa' > \kappa$ , i.e. electro-osmosis enhances membrane conductivity as a consequence of water-ion frictional drag; its direction is that of counter-ion flow. Similarly salt permeability is usually measured at zero pressure and osmotic flow is allowed to take place. In this case, however, volume flow is opposed to the direction of salt diffusion and therefore,

$$\frac{J_s}{X_j/c_s} \equiv \omega_s'' < \omega_s \quad (3.3.44)$$

where (\*) is used for measurement at  $\Delta p = 0$ . From eqs. (3.3.30), (3.3.43) and (3.3.44), the interaction between water flow and ion flows leads to the inequality.



$$\left( \frac{J_s}{X_s/c_s} \sqrt{\frac{J_1 - J_2}{X_1}} \right)_{\Delta p = 0} < \left( \frac{J_s}{X_s/c_s} \sqrt{\frac{J_1 - J_2}{X_1}} \right)_{J_v = 0} \quad (3.3.45)$$

Therefore, salt diffusion in the presence of volume flow is less than salt diffusion in the absence of volume flow. The membrane potential at  $\Delta p = 0$  in practice would also differ from that measured in the absence of water flow. In general, existence of volume flow would result in the flattening of the concentration difference between the two membrane-solution interfaces. In charged ion-exchange membranes, this will mostly affect the counter-ions, and therefore the observed membrane potential would be lowered by water flow, even with ideal stirring which would give in effect no unstirred layers. In real measurement, the existence of unstirred layers would make this effect even larger. Maximum values of  $t_1 t_2 = 0,25$  is obtained in completely non-permselective membranes, i.e.  $t_1 = t_2 = 0,5$ ; in highly permselective membranes this product will approach zero. Volume flow will thus result in a smaller membrane potential of which will shift the measured data towards larger  $t_1 t_2$  values.

In general, ion-water coupling, causes the experimental data to be shifted in the opposite direction to that affected by ion-ion coupling, according to Kedem.

Correlations (3.3.42) and (3.3.45) show that from customary measurements of conductance and membrane potential plus salt permeation, one gets a sharp distinction between ion-water coupling as found in usual ion-exchange membranes on the one hand, and ion-ion coupling as expected in hydrophobic membranes on the other hand. Zero coupling in the absence of volume flow was given by eq. (3.3.40).

### 3.4 Transport Processes Occurring During Electrodialysis

A number of transport processes occur simultaneously during ED, and these are illustrated in Figure 3.4.1<sup>(7)</sup>.

Counter-ion transport constitutes the major electrical movement in the process; the counter-ions transport with them by electro-osmosis a certain quantity of water. Co-ion transport is comparatively small and is dependent upon the quality of the ion-selective membrane and upon the brine concentration. Water is also transported electro-osmotically with the co-ions. Diffusion of electrolyte occurs from the brine to the dialysate compartment because in the ED process the brine stream is usually more concentrated than the dialysate stream. Water transport is also associated with

electrolyte diffusion. Water transport due to osmosis takes place from the low concentration dialysate compartment into the higher concentration brine compartment.

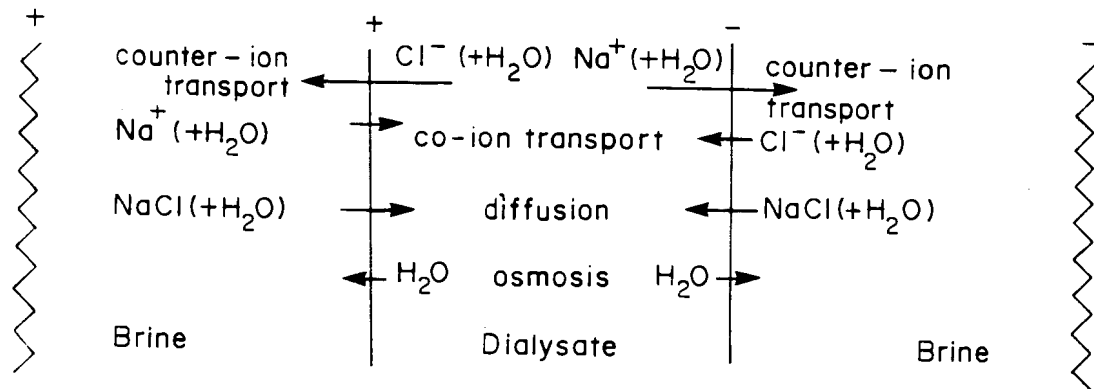


**Figure 3.4.1: Illustration of transport processes which can occur simultaneously during the electro dialysis process.**

The efficiency of demineralization of the liquid in the dialysate compartment may be considerably reduced by the counter effects of co-ion transport, diffusion, water transport associated with counter-ion movement and osmosis. The effect of these unwanted transfer processes can, however, be reduced by the correct selection of membranes and by the selection of the optimum operational procedure for a particular application<sup>(7)</sup>. Osmosis and electro-osmosis are effects which limit the usefulness of ED as a method of concentrating electrolyte solutions.

### 3.5 Current Efficiency and Transport Phenomena in Systems with Charged Membranes

The interaction between the current efficiency of electro dialytic separation with ion-exchange membranes and all the fluxes depressing selectivity, i.e., electric transport of co-ions, electro-osmotic flow of water, diffusion and osmosis have been described and experimentally examined by Koter and Narebska<sup>(17)</sup>. They have presented a simple definition of the current efficiency (CE) for a single ion-exchange membrane system. It allows for the estimation of CE from a determination of concentration changes in

cathode and anode solutions. With the proposed definition, CE can be expressed as a simple function of different kinds of transport taking place in the system. This fact makes it possible to examine the effects of these transports on current efficiency, that is to calculate the losses of CE due to:

- a) electric transport of co-ions;
- b) electro-osmotic flow of water;
- c) diffusion of a salt; and
- d) osmotic transport of water.

Thus, the full characteristics of a single ion-exchange membrane (cation- or anion-exchange) for a separation process like ED can be obtained. The mathematical solution has been examined for computing the current efficiency and its losses for the system  $\text{NaCl}_{\text{aq}}/\text{Nafion 120 membrane}$  and  $\text{NaOH}_{\text{aq}}/\text{Nafion 120 membrane}$  based on the experimental results published earlier<sup>(17)</sup>.

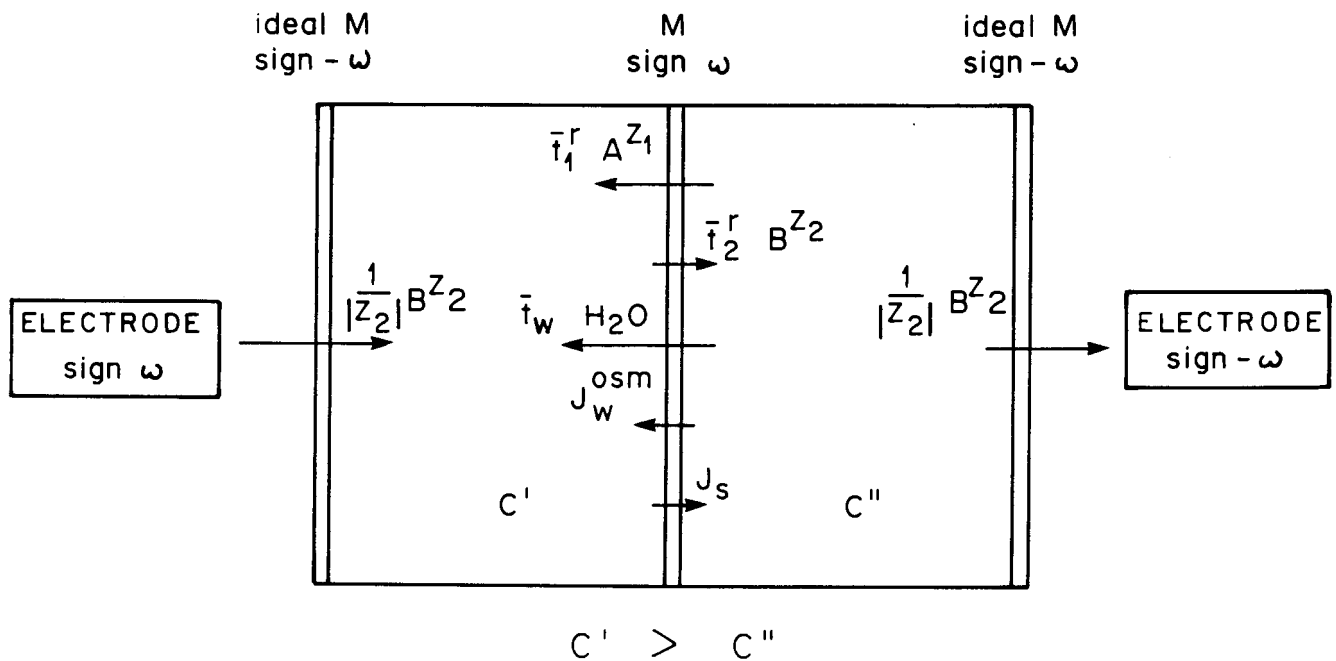
### 3.5.1 Current Efficiency of a Membrane System - A Definition

Consider the one membrane system as shown in Figure 3.5.1. The ion-exchange membrane (M) separates two solutions of an  $\text{Av}_1\text{Bv}_2$  electrolyte differing in concentrations. For the cation-exchange membrane (sign  $W = -1$ ) the cathode is on the more concentrated side whereas for the anion-exchange membrane ( $W = +1$ ) it is on the diluted side. The electrodes and electrode reactions do not belong to the system. They are separated from the system by ideal membranes of reverse sign to the investigated membrane.

At  $t = 0$ , the concentration difference across the membrane is  $\Delta c^0 = c^{0'} - c^{0''}$ . After passing an electric current through the membrane for time  $t$ , the concentration difference changes to  $\Delta c^t$ . The ratio of  $(\Delta c^t - \Delta c^0)$  for the real membrane to  $(\Delta c^t - \Delta c^0)$  for the ideal membrane system ( $t_2, t_w, J_s, J_w^{\text{os}} = 0$ ) is a measure of the current efficiency:

$$\text{CE} = \frac{(\Delta c^t - \Delta c^0)}{(\Delta c^t - \Delta c^0)_{\text{ideal}}} \quad (3.5.1)$$

Rearrangement of this formula<sup>(17)</sup> leads to the following equation relating the current efficiency to the total counter-ions ( $J_1$ ) and water ( $J_w$ ) fluxes (see Appendix B).



A – counter-ion  
B – co-ion

**Figure 3.5.1: Standard system for defining the current efficiency of an ion-exchange membrane in the isobaric condition ( $\Delta p = 0$ ). The transport processes caused by the passage of 1 Faraday of electric charge ( $\bar{t}_1$  and  $\bar{t}_2$  are the electric transport of counter-ions and co-ions, respectively;  $\bar{t}_w$  is the electro-osmotic transport of water) and by the concentration difference ( $J_s$  - diffusion of a salt,  $J_w^{osm}$  = osmotic flux of water) are shown.**

$$CE = \omega z_1 v_1 (J_1/v_1 - 0,018\bar{m}J_w)/I \quad (3.5.2)$$

Consider that the counter-ions are driven by the constant electric field and the chemical potential gradient, and that the same holds for water, eq. (3.5.2) can be rearranged to:

$$CE = z_1 v_1 (\bar{t}_1^r/v_1 - 0,018\bar{m}\bar{t}_w - \omega(J_s - 0,018\bar{m}J_w^{osm})F/I \quad (3.5.3)$$

where

- $\bar{t}_1^r$  = reduced transport number of counter-ions (eq. A2, Appendix B)
- $\bar{t}_w$  = transport number of water
- $\bar{m}$  = mean molality (eq. B17, Appendix B)
- $J_s, J_w^{osm}$  = diffusion and osmotic fluxes
- $I$  = electric current
- $\omega$  = -1 for cation-exchange membrane
- = +1 for anion-exchange membrane

The formula indicating the fluxes that decrease current efficiency, is as follows:

	Electrical transport of co-ions	Electro-osmotic transport of water	Diffusion of salt	Osmotic flux of water
CE = 1 -	$\bar{i}_2 - z_1$	$z_1 v_1 0,018 \tilde{m} \bar{i}_w -$	$z_1 v_1 \omega (J_s -$	$0,018 \tilde{m} J_w^{os}) F/l$

(3.5.3a)

With the help of the transport equations of irreversible thermodynamics and the Gibbs - Duhem equation, the diffusion and osmotic fluxes,  $J$ , and  $J_w^{os}$ , can be expressed as a function of the difference of the chemical potential of a solute,  $\Delta \mu_s$ <sup>(9)</sup>.

$$J_s - 0,018 \tilde{m} J_w^{os} = \left[ \left( \frac{J_s}{\Delta \mu_s} \right) - 0,018 \tilde{m} \left( \frac{J_w^{os}}{\Delta \mu_s} \right) \right] \Delta \mu_s$$

$$= f(L_{ik}, \tilde{m}) \Delta \mu_s \quad (3.5.4)$$

Here  $f(L_{ik}, \tilde{m})$  represents a combination of the phenomenological conductance coefficients  $L_{ik}$  and the mean molality,  $\tilde{m}$ , of a solute. Equation (3.5.3) and (3.5.4) clearly show that losses of selectivity due to osmotic and diffusion fluxes are dependent on the ratio of the chemical potential difference of solute and the current  $\Delta \mu_s/l$ .

### 3.5.2 Determination of Current Efficiency in a System with Electrode Reactions

Substituting the concentration changes for the system with ideal membrane,  $(\Delta c^t - \Delta c^o)_{ideal}$  (eq. B15, Appendix B), and the equation

$$\Delta c^t - \Delta c^o = \omega (\Delta c_o^t - \Delta c_c^t) \quad (3.5.5)$$

Into eq. (3.5.1), eq (3.5.6) is obtained:

$$CE = \frac{z_1 v_1 V^o F (\Delta c_c^t - \Delta c_a^t)}{2(1 - v_s c^o) I \Delta t} \quad (3.5.6)$$

where  $\Delta c_a^t, \Delta c_c^t$  = concentration changes of anolyte and catholyte after time  $\Delta t$   
 $c^o$  = mean concentration of anolyte and catholyte at time  $t = 0$ ,  
 $c^o = (c_a^o + c_k^o)/2$ .

Equation (3.5.6) can only be applied to the standard system (Fig. 3.5.1) without any other effect but transport, i.e., without the electrode reactions. Actually, the experimentally determined variations of the concentrations of the cathodic and anodic solutions are produced by both the transport phenomena and the electrode reaction.

For computing the current efficiency related to the transport phenomena only, the concentration/volume effects of the electrode reactions should be accounted for. The use of electrodes makes it necessary to correct the numerator of eq. (3.5.6), i.e., the difference  $\Delta c_c - \Delta c_a$ . In the general form the formula for the membrane current efficiency determined in the practical system can be written as:

$$CE = \frac{z_1 v_1}{2(1 - \bar{v}_s \bar{c}^o)} \left[ \frac{FV^o}{I} \left( \frac{\Delta c_c^t}{\Delta t} - \frac{\Delta c_a^t}{\Delta t} \right)_{\text{pract}} + \text{correction} \right] \quad (3.5.7)$$

Some electrodes and the formulas for corrections are given by Koter and Narebska<sup>(17)</sup>.

### 3.5.3 Relation Between Current Efficiency and Efficiency of Energy Conversion

Regarding the general formula for efficiency of energy conversion given by Kedem and Caplan<sup>(72)</sup>, the efficiency of energy conversion,  $\eta_E$ , for the system studied here, takes the form

$$\eta_E = \omega \frac{J_1^w}{I} \frac{\Delta \mu_s}{\Delta E} \quad (3.5.8)$$

where  $J_1^w = J_1/v_1 - 0,018 \bar{m} J_w$  (3.5.9)  
 $\Delta E =$  is the difference of electrical potential measured with electrodes reversible to co-ions.

$$\Delta E = \Delta \tilde{\mu}_2 / z_2 F \quad (3.5.10)$$

By comparing eq. (3.5.8) for  $J_1^w$  and eq. (3.5.3) for the current efficiency, it can be seen that  $\eta_E$  can be written as the product of current efficiency and the force-to-force ratio  $\Delta \mu_s / \Delta E$ :

$$\eta_E = \omega \frac{1}{z_1 v_1} CE \frac{\Delta \mu_s}{\Delta E} \quad (3.5.11)$$

### 3.5.4 The Losses of Current Efficiency

To determine losses of current efficiency due to different kinds of transport (eq. 3.5.3a), four experiments can be performed. Results are here presented for the systems  $\text{NaCl}_{\text{aq}}/\text{Nafion 120}$  and  $\text{NaOH}_{\text{aq}}/\text{Nafion 120}$ . All the experimental results used for computing CE have been published elsewhere<sup>(17)</sup>.

Figures 3.5.2(a) and 3.5.2(b) present the effects of the conjugated fluxes on efficiency of electric transport of counter-ions across the cation-exchange membrane (Nafion 120) for two different values of concentration ratio;  $m'/m''$  and current density,  $i$ :  $m'/m'' = 5$ ,  $i = 100 \text{ A/m}^2$ , and  $m'/m'' = 10$ ,  $i = 500 \text{ A/m}^2$ .

On both figures the current efficiency corresponds to the abscissa (see eq. 3.5.3a)

$$CE = 1 - \Sigma \text{ losses}$$

and is dependent on the mean concentration  $\bar{m}$  (eq. B17, Appendix A). The effects which diminish current efficiency are<sup>(17)</sup>:

- Electric transport of co-ions, i.e., imperfect membrane permselectivity ( $\bar{t}_2$ )
- Diffusion of solute ( $J_s$ )
- Electro-osmotic flow ( $\bar{t}_w$ )
- Osmotic water fluxes ( $J_w^{os}$ )

The following conclusions can be drawn from the figures<sup>(17)</sup>:

The imperfect selectivity ( $\bar{t}_2$ ), assumed to be one of the most important characteristics of a membrane, produces up to 8% (NaCl) and 35% (NaOH) of the CE losses at  $\bar{m} = 2$ . Similar to  $\bar{t}_2$ , the effect of electro-osmotic flow of water ( $\bar{t}_w$ ) increases with  $m$ . It plays a significant role in the system with NaCl where it diminishes CE up to 30%.

Depending on the working conditions, i.e., on the concentration ratio  $m'/m''$  and current density, the decrease of CE due to osmotic and diffusion flows can be larger than that caused by electric transport of co-ions and water. This effect is especially

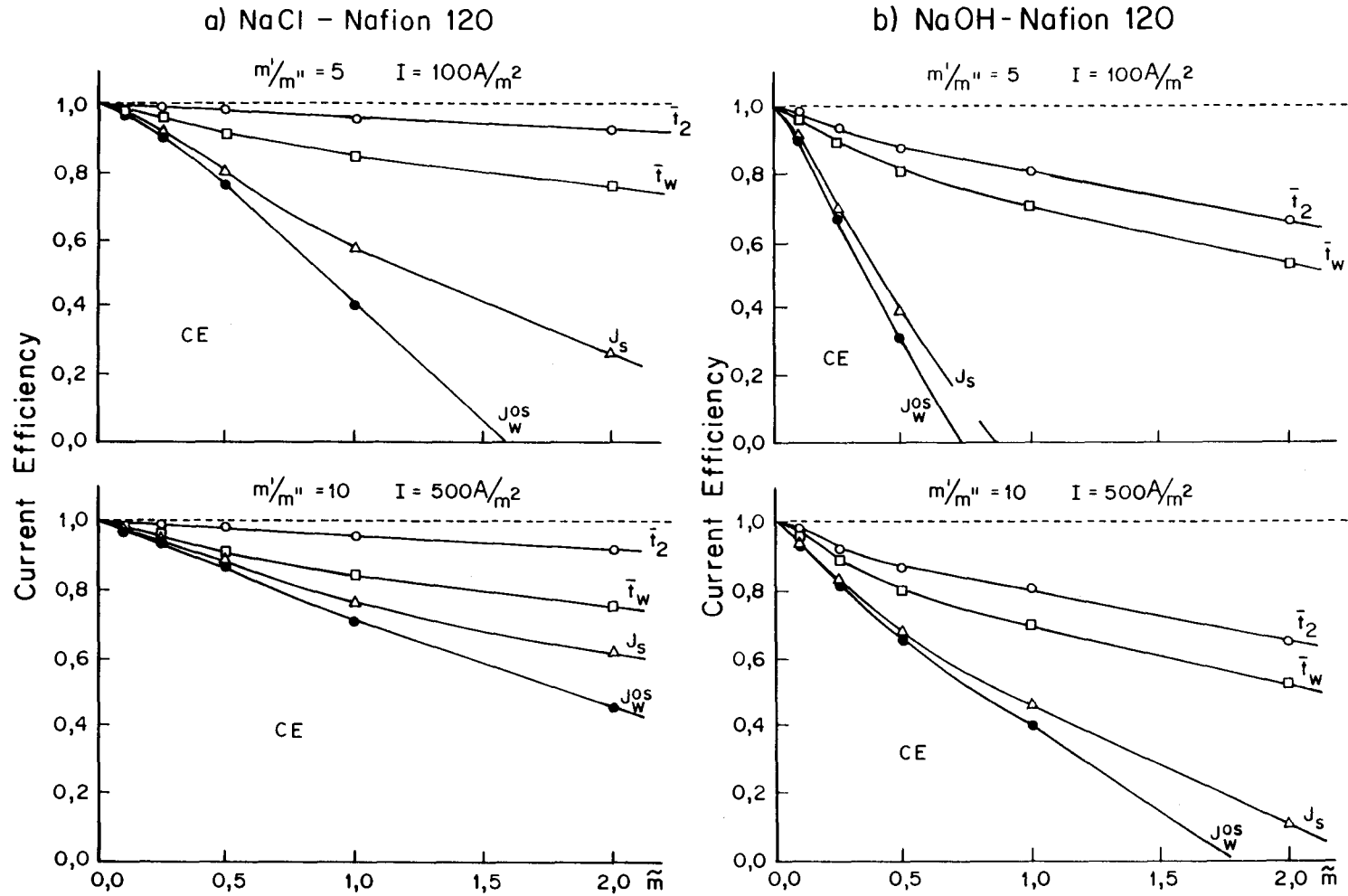


Figure 3.5.2: Losses of current efficiency due to imperfect selectivity of a membrane ( $\bar{i}_2$ ), diffusion of a solute ( $J_s$ ) and electro-osmotic flow ( $\bar{i}_w$ ) and osmotic ( $J_w^{os}$ ) fluxes.  $T = 298\text{K}$ .



seen at higher mean concentrations where the current efficiency can even be reduced to zero.

### 3.6 Efficiency of Energy Conversion in Electrodialysis

Efficiency of energy conversion in separation processes with Nafion 120 membranes from phenomenological transport coefficients has been described by Narebska and Koter<sup>(18)</sup>.

In systems devised for desalination/concentration processes with ion-exchange membranes separating single electrolyte solutions of different concentrations, electrical energy is used to drive a solute against its concentration gradient. In these processes, the electrical energy is converted into free energy of mixing and in that way it is stored in the system. The efficiency of energy conversion ( $\eta$ ) depends both on the degree of coupling between the driving process and the driven flow ( $q$ ), as well as the operating conditions.

Kedem and Caplan<sup>(72)</sup> have defined  $\eta$  and  $q$  in terms of irreversible thermodynamics and outlined the methods available to access both parameters for thermocouples, fuel cells, osmotic batteries and desalination stacks by treating the system as a two-flow process. Later, Caplan<sup>(74)</sup> published some data on the overall degree of coupling  $q$  and  $\eta_{\max}$  for hyperfiltration, concentration cells and ED, taking for the calculations the experimental results for a few points in dilute solutions.

Narebska and Koter<sup>(18)</sup> have presented results for the degree of coupling and efficiency of energy conversion calculated for the system composed of a perfluorinated Nafion 120 membrane and sodium chloride solutions of different concentrations. Their aim have been to conduct a detailed analysis of input-output relations by treating the system and the transport involved as a three-flow process and describing quantitatively the transport of water which consumes energy unprofitably.

The system consisted of a cation exchange membrane and aqueous solutions of 1 : 1 electrolyte of different concentrations in the adjacent compartments. Sodium are driven by the applied electrical potential difference opposite the concentration difference of NaCl.

### 3.6.1 Mathematical Formulation

#### 3.6.1.1 The degree of coupling and the efficiency of energy conversion in the two-flow system (basic definitions)

The efficiency of energy conversion  $\eta$  is based in the dissipation function  $\phi$  which for the two-flow system takes the general form:

$$\phi = J_1 X_1 + J_2 X_2 \geq 0 \quad (3.6.1)$$

According to Kedem and Caplan<sup>(72)</sup>, with one flow producing entropy ( $J_2 X_2$ ), which is always positive and the other flow consuming entropy, being negative ( $J_1 X_1$ ), the efficiency of energy conversion can be expressed as:

$$\eta = - \frac{J_1 X_1}{J_2 X_2} \quad (3.6.2)$$

Denoting the force ratio as  $X_1/X_2$  and the ratio of the straight conductance coefficients  $L_{ij}$  appearing in the flow equations

$$J_1 = L_{11} X_1 + L_{12} X_2 \quad (3.6.3)$$

$$J_2 = L_{21} X_1 + L_{22} X_2$$

as  $Z^2 = L_{11}/L_{22}$ , the efficiency function can be calculated with the equation:

$$\eta = - \frac{q + Zx}{q + 1/Zx} \quad (3.6.4)$$

$q$  is the degree of coupling of the flows satisfying the relation  $|q| \leq 1$ .

The conversion of energy of process 2 to process 1 is only possible when the two flows are coupled, therefore, the degree of coupling can be defined as:

$$q^2 = 1 - \frac{(J_2)_{J_1=0}}{(J_2)_{X_1=0}} = 1 - \frac{(J_1)_{J_2=0}}{(J_1)_{X_2=0}} = \frac{L_{12}^2}{L_{11} L_{22}} \quad (3.6.5)$$

For electrodialysis, the dissipation function can be written in the form:

$$\phi = J_1 \Delta \mu_s + IE \quad (3.6.6)$$

where  $J_1$  is the flux of counterions,  $\Delta \mu_s$  the difference of chemical potential of an electrolyte,  $I$  the electric current and  $E$  the potential difference between the solutions on opposite sides of the membrane measured with electrodes reversible to the anions.

Kedem and Caplan have presented the general solution for the degree of coupling in ED. They admitted, however, that in their solution the contribution of water flow was neglected. This means that they have treated the process as a two-flow system.

### 3.6.1.2 Three-flow System

In any real system with a single electrolyte and the ion-exchange membrane separating solutions of different concentrations, the flow of water is another process which participates in the entropy production. Consequently, the equation describing the dissipation function should contain the third component,  $J_w \Delta \mu_w$ :

$$\phi = J_1 \Delta \mu_s + J_w \Delta \mu_w + IE \geq 0 \quad (3.6.7)$$

Thus, the efficiency of energy conversion for multiple-flow system can be defined as<sup>(74)</sup>:

$$\eta = - \frac{\sum_{i=1}^{n-1} J_i X_i}{J_n X_n} \quad (3.6.8)$$

In eq. (3.6.8)  $J_n X_n$  represents the driving process and  $J_i X_i$  represents the driven flow.

As for ED  $J_n X_n = IE$  and  $\sum_i^{n-1} J_i X_i = J_1 \Delta \mu_s + J_w \Delta \mu_w$ , one gets:

$$\eta = \left( - \frac{J_1 \Delta \mu_s}{IE} \right) + \left( - \frac{J_w \Delta \mu_w}{IE} \right) = \eta_{IE} + \eta_{wE} \quad (3.6.9)$$

The first term of eq. (3.6.9) is the same as before, i.e. it expresses the storage of energy in producing a concentration difference in the permeant. The second term corresponds to the transport of water which acts opposite to the separation of the components. It causes a waste of energy by decreasing the concentration difference.

To find the degrees of coupling in both processes, the equations for transport of ions ( $J_1$ ), water ( $J_w$ ) and current ( $I$ ) should be used in a general formula:

$$J_1 = L_{11}\Delta\mu_s + L_{1w}\Delta\mu_w + L_{1E}E$$

$$J_w = L_{1w}\Delta\mu_s + L_{ww}\Delta\mu_w + L_{wE}E \quad (3.6.10)$$

$$I = L_{1E}\Delta\mu_s + L_{wE}\Delta\mu_w + L_E E$$

### 3.6.1.3 Degrees of coupling for the three-flow system

Defining the degree of coupling according to Kedem and Caplan, three coefficients for the three-flow system are obtained which denote sodium ion-current coupling ( $q_{1E}$ ), water-current coupling ( $q_{wE}$ ) and sodium ion-water coupling ( $q_{1w}$ ).

$$q_{ik}^2 = 1 - \left[ \frac{(J_i)_{J_k=0}}{(J_i)_{X_k=0}} \right]_{X_j=0} = \frac{L_{ik}^2}{L_{ii}L_{kk}} \quad i,k = 1,w,E, \quad i \neq k \quad (3.6.11)$$

All the degrees of coupling were calculated according to eq. (3.6.11) using conductance coefficients  $L_{ik}$ , of eq. (3.6.10).

For the more practical discussion of the input-output relation, such as finding the maximum output or the driven region for ED, the overall degree of coupling  $q_E$  is also helpful. This can be derived from the general formula

$$\bar{q}^2 = 1 - \frac{(J_n)_{J_{i \neq n} = 0}}{(J_n)_{X_{i \neq n} = 0}} \quad (3.6.12)$$

For the system with three forces operating ( $\Delta C$ ,  $\Delta p$ ,  $E$ , eq. (3.6.10),  $\bar{q}_E$  takes the form:

$$\bar{q}_E^2 = 1 - \frac{(I)_{J_1, J_w = 0}}{(I)_{\Delta\mu_s, \Delta\mu_w = 0}} = \frac{q_{1E}^2 + q_{wE}^2 - 2q_{1E}q_{wE}q_{1w}}{1 - q_{1w}^2} \quad (3.6.13)$$

At  $\Delta p = 0$ , which corresponds to operating conditions in ED, and applying the Gibbs-Duhem equation  $c_s d\mu_s + c_w d\mu_w = 0$ , the flow equations can be written in the form:

$$J_1 - \frac{c_s}{c_w} J_w = J_1^w = L'_{11} \Delta \mu_s + L'_{TE} E \quad (3.6.14)$$

$$I = L'_{TE} \Delta \mu_s + L_E E$$

where

$$L'_{11} = L_{11} - 2 \frac{c_s}{c_w} L_{1w} + \frac{c_s^2}{c_w^2} L_{ww} \quad (3.6.15)$$

$$L'_{TE} = L_{TE} - \frac{c_s}{c_w} L_{wE}$$

For these equations the formula for the overall degree of coupling takes the form:

$$q_E^2 = 1 - \frac{(I)_{J_1^w = 0}}{(I)_{\Delta \mu_s = 0}} = \frac{L_{TE}^2}{L'_{11} L_E} \quad (3.6.16)$$

#### 3.6.1.4 Efficiency of Energy Conversion

Introducing eq. (3.6.10) into eq. (3.6.9) and assuming that  $\Delta p = 0$ , it is possible to derive the equations for both components of  $\eta$  (eq. 3.6.9), i.e.  $\eta_{IE}$  and  $\eta_{wE}$

$$\eta_{IE} = - \frac{\left[ Z_{TE} - \frac{c_s}{c_w} Z_{wE} q_{1w} \right] X + q_{IE}}{q_{IE} - \frac{c_s}{c_w} Z_{w1} q_{wE} + \frac{1}{Z_{wE} X}} \quad (3.6.17)$$

$$\eta_{wE} = \frac{c_s}{c_w} \frac{\left[ Z_{TE} q_{1w} - \frac{c_s}{c_w} Z_{wE} \right] X + q_{wE}}{Z_{1w} q_{1w} - \frac{c_s}{c_w} q_{wE} + \frac{1}{Z_{wE}} X} \quad (3.6.18)$$

The meaning of  $q_{ik}$  is as before eq. (3.6.11),  $x = \Delta \mu_s / E$  and  $Z_{ik} = \sqrt{L_{ij} / L_{kk}}$  where  $i, k = 1, \omega, E, i \neq k$ . These equations are appropriate for calculating  $\eta$  for ED.

### 3.6.2 The Two-Flow and Overall Degrees of Coupling

Model calculations have shown the following<sup>(18)</sup>:

Tight coupling, ranging up to 0.98, was found between the ion and current flows ( $q_{IE}$ ) for solutions up to 0,5 mol/l. (Fig 3.6.1).

The sodium transport number  $\bar{t}_1$  was in the range 1,0 to 0,98 over this concentration range. The sodium transport number ( $\bar{t}_1$ ) and  $q_{IE}$  decreased at higher concentrations.

The coupling of water-current flows ( $q_{wE}$ ) was close to 0,5 at approximately 0,1 to 0,5 mol/l (Fig. 3.6.1). In that region  $q_{wE} \approx q_{1w}$  implying that  $q_{wE}$  represents the coupling of water to ion flow; known as electro-osmosis. In more concentrated solutions  $q_{wE}$  and  $q_{1w}$  diverge. Water-ion coupling becomes higher and water-current coupling becomes lower. At higher concentrations ( $> 0,5$  mol/l) the amount of "free" water in the membrane, the transport number of water  $\bar{t}_w$  and the osmotic flow, decrease. Effects originating in the deswelling of the membrane at high external concentration may result in the observed decrease of the electro-osmotic flow and the increased coupling between ions and the amount of water crossing the membrane. The overall coupling coefficient  $q_E$  slightly exceeds  $q_{IE}$  and changes with external concentration similar to  $q_{IE}$ .

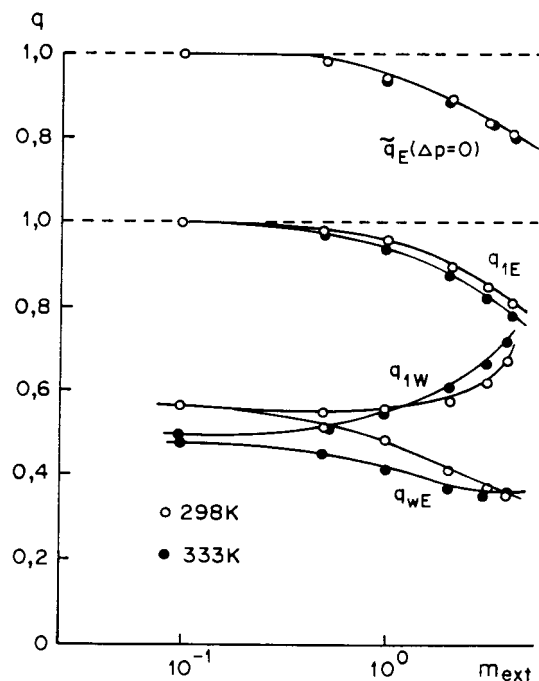


**Figure 3.6.1:** The concentration dependence of the degrees of coupling: sodium ions-current ( $q_{IE}$ ), sodium ions-water ( $q_{1w}$ ), water-current ( $q_{wE}$ ), and the overall degree of coupling ( $\bar{q}_E$ ) for the system  $\text{NaCl}_{aq}$ /Nafion 120 membrane.

### 3.6.3 Total Efficiency of Energy Conversion and its Components

The component efficiencies of energy conversion are not only of different meaning but of different sign (Fig. 3.6.2). The positive term  $\eta_{IE}$  indicates the fraction of the free energy of mixing produced by the driving process IE and stored in the system by the uphill transport of ions  $J_1 \Delta \mu_s$ , against their spontaneous flow. The negative term  $\eta_{wE}$  means that the transport of water proceeds in the direction of the conjugated force  $\Delta \mu_w$  (downhill). The energy input increases the rate of flow. Thus, this term causes the entropy of the system to increase and the energy supplied to the system to be wasted.

Both  $\eta_{IE}$  and  $\eta_{wE}$  change with the ratio  $\Delta \mu_s/FE$  and with the concentration of electrolyte. The maximum in the  $\eta_{IE}$  curve means that for any concentration range of NaCl solutions there is an optimal concentration difference for which the efficiency of energy conversion is at a maximum. There is no such maximum in the  $\eta_{wE}$  curve. The waste of energy due to water flow becomes much higher as the electrolyte becomes more concentrated and the concentration difference between the NaCl solutions in the adjacent compartments is higher.

The sum of  $\eta_{IE}$  and  $\eta_{wE}$  gives the total efficiency as  $\eta$ . The total efficiency,  $\eta$ , decreases with increasing concentration. The degree of coupling,  $\bar{q}_E$ , also decreases with increasing concentration.

Computations of  $q$  (coupling) and  $\eta$  (efficiency) employing the derived equations and phenomenological conductance coefficients determined for the system Nafion 120 membrane/sodium chloride solutions led to the following conclusions<sup>(18)</sup>:

- Coupling of the current to the flow of sodium ions ( $q_{IE}$ ), of importance for the efficiency of energy conversion, is close to unity when the membrane is in contact with dilute solutions and is going down with increasing external concentration.
- Coupling of the current to the flow of water ( $q_{wE}$ ), which is achieved by water-cation coupling ( $q_{lw}$ ), reaches a value as high as half that of  $q_{IE}$ , pointing to the unavoidable loss of energy during ED.

- The total efficiency of energy conversion ( $\eta$ ) depends both on the concentration of separated electrolytes and on the ratio of thermodynamic forces ( $\Delta\mu_s/FE$ ) acting in the system. The maximum of efficiency depends on the force ratio and decreases with increasing external concentration.
- The total efficiency of energy conversion is a complex quantity composed of a positive component ( $\eta_{IE}$ ) related to the transport of cations and a negative one ( $\eta_{WE}$ ) related to the transport of water; both components change with the external concentration to a different degree. The measure of the loss of energy ( $\eta_{WE}$ ) may reach a value of as much as 70% of  $\eta_{max}$  in the more concentrated solutions.

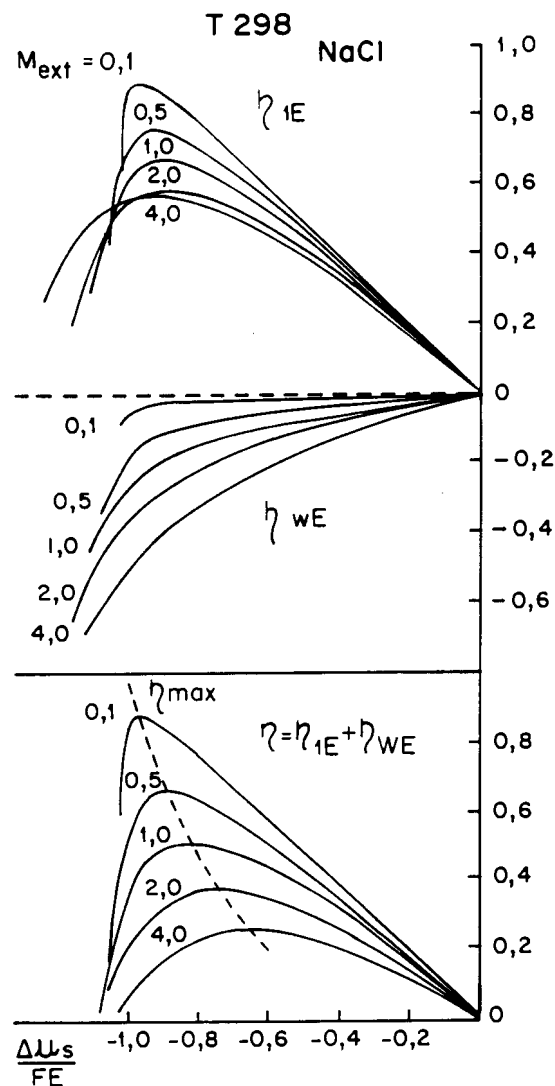


**Figure 3.6.2:** The efficiency of energy conversion  $\eta$  and the component efficiencies  $\eta_{IE}$ ,  $\eta_{WE}$  and force ratio  $\Delta\mu_s/FE$ , at different concentrations NaCl in the external solution ( $T = 333\text{ K}$ ).



### 3.7 Conversion of Osmotic into Mechanical Energy in Systems with Charged Membranes

Narebska *et al.*,<sup>(19)</sup> have described the problem of conversion of osmotic energy into mechanical energy within the framework of irreversible thermodynamics. Using the numerical results for the conductance coefficients for the system Nafion 120 membrane/single salt and alkali solutions, the couplings between the volume and the osmotic fluxes,  $q$ , and the efficiency of osmotic into mechanical energy conversion,  $\eta$ , have been computed.

The standard application of membrane systems is for separation of suspensions and molecular mixtures, gaseous or liquid, into components on an expense of supplied energy. Mechanical, thermal or electric energy can be used. More than twenty membrane separation techniques are known. In each of these systems, however, the difference in concentration of components on both sides of a membrane presents the effective source of osmotic energy, generating the spontaneous osmotic flux affecting the separation. For example, in ED, the osmotic flow of water dilutes the brine, thus lowering the energetic efficiency of desalination. In reverse osmosis, the osmotic pressure is a powerful force to overcome. Osmotic energy is thereby a native energy of a membrane system affecting both the income of energy and the separation process itself.

Conversion of osmotic energy into electric energy was postulated and theoretically described by Kedem and Caplan<sup>(72)</sup>. Systems converting osmotic energy into mechanical energy called "osmotic pumps" were proposed by Lee *et al.*,<sup>(75)</sup>. The energetic efficiency of the process, however, still seems to be a problem.

The work by Narebska *et al.*,<sup>(19)</sup> has been aimed at a theoretical analysis of osmotic into mechanical energy conversion, using irreversible thermodynamics as the underlying theory.

#### 3.7.1 Theoretical

The system consists of an ion-exchange membrane separating electrolyte solutions of different molalities. Assuming ideal membrane permselectivity (totally impermeable to a solute) and the zero current condition, the only flow in the system should be the osmotic flow of water which is driven to the more concentrated side. However, for real

polymer membranes and particularly when they are in contact with concentrated solutions, diffusion of a solute across the membrane should be admitted as an additional phenomenon. The solute permeates the membrane towards the dilute solution side, that is, opposite to the osmotic flow.

In terms of irreversible thermodynamics the two flows

- the osmotic flow of water  $J_w$  and
- the diffusional flow of the solute  $J_s$  are described by the following equations:

$$J_s = L_s \Delta \mu_s + L_{sw} \Delta \mu_w \quad (3.7.1a)$$

$$J_w = L_{ws} \Delta \mu_s + L_w \Delta \mu_w \quad (3.7.1b)$$

$\Delta \mu_s$ ,  $\Delta \mu_w$  are the differences of chemical potential of a solute and water, respectively.  $L_{ik}$  denotes the phenomenological conductance coefficients.

It is convenient to transform eq. (3.7.1a) and (3.7.1b) into another set of equations.

$$J_w' = L_w' \Delta \mu_w^c + L_{wp}' \Delta p \quad (3.7.2a)$$

$$J_v = L_{pv}' \Delta \mu_w^c + L_p' \Delta p \quad (3.7.2b)$$

Here  $J_w'$  denotes the flow of water against the flow of a solute conjugated to the concentration part of the chemical potential difference of water,  $\Delta \mu_w^c$ :

$$J_w' = J_w - \bar{c}_w / \bar{c}_s * J_s \quad (3.7.3)$$

$$\Delta \mu_w^c = RT \ln (a_w' / a_w'') \quad (3.7.4)$$

$J_v$  of equation (3.7.2b) denotes the total volume flow conjugated to the difference of pressure in the compartments on the opposite sides of the membrane,  $\Delta p$ .

$$J_v = \bar{v}_s J_s + \bar{v}_w J_w \quad (3.7.5)$$

The relation between the fluxes and forces of equations (3.7.1a and 3.7.1b) and of equations (3.7.2a and 3.7.2b) can be expressed in a matrix form

$$\begin{pmatrix} J_w' \\ J_v' \end{pmatrix} = A * \begin{pmatrix} J_s \\ J_w \end{pmatrix}, \quad \begin{pmatrix} \Delta \mu_w^c \\ \Delta p \end{pmatrix} = A^{-1T} * \begin{pmatrix} \Delta \mu_s \\ \Delta \mu_w \end{pmatrix} \quad (3.7.6 \text{ and } 3.7.7)$$

$$L' = A * L * A^T \quad (3.7.8)$$

where

$$A = \begin{pmatrix} -\bar{c}_w/\bar{c}_s & 1 \\ \bar{v}_s & \bar{v}_w \end{pmatrix}, \quad L = \begin{pmatrix} L_s & L_{sw} \\ L_{ws} & L_w \end{pmatrix}$$

With the flows of equations (3.7.2a and 3.7.2b) the dissipation function  $\Phi$  consists of two components:

$$\Phi = \begin{matrix} J_w' \Delta \mu_w^c & + & J_v \Delta p \\ \text{osmotic} & & \text{mechanical} \\ \text{energy} & & \text{energy} \\ \text{component} & & \text{component} \end{matrix} \quad (3.7.9)$$

The efficiency of energy conversion,  $\eta$ , as defined by Kedem and Caplan<sup>(72)</sup>, can be written as follows:

$$\eta = - \frac{J_v \Delta p}{J_w' \Delta \mu_w^c} \quad (3.7.10)$$

$$0 < \eta < 1$$

For the system discussed here,  $\eta$ , means the output of mechanical energy produced by the input of unit osmotic energy. To acquire computational verification of various systems this equation should be transformed by substituting equations (3.7.2a and 3.7.2b) into equation (3.7.10) to give

$$\eta = - \frac{q + z * \Delta p / \Delta \mu_w^c}{q + 1 / (Z * \Delta p / \Delta \mu_w^c)} \quad (3.7.10 \text{ a})$$

Here

$$q = L'_{wp} / (L'_w L'_p)^{0.5}$$

$$Z = (L'_p/L'_w)^{0,5}$$

q is called a coupling coefficient. For energy conversion the size of q is fundamental. The value of q may vary between -1 and +1. A high value of q indicates tight coupling between the two processes involved in energy conversion. For the system discussed here, these are the spontaneous osmotic flow of water and the volume flow producing energy.

### 3.7.2 Transport Experiments and Computations

The perfluorinated cation-exchange membrane Nafion 120 (Du Pont de Nemours, USA), was used for measuring the membrane transport process as well as performing experiments with an osmotic unit. The measured membrane transport properties were the membrane electric conductivity, concentration potential, osmotic, electro-osmotic, diffusion and hydrodynamic flows. From these data the set of coefficients of equation (3.7.2), that is  $L'_w$ ,  $L'_p$ ,  $L'_{wp}$  was calculated and then the coupling coefficient q (eq (3.7.11)) and the efficiency of energy conversion,  $\eta$  (eq. 3.7.10(1)) were found.

The theory was experimentally verified in a simple osmotic unit<sup>(19)</sup>.

### 3.7.3 Osmotic and Diffusion Fluxes in Membrane Systems

For a given membrane, the flow of water and the diffusion of a solute, flowing in the opposite direction, depend strongly on the nature of the electrolyte. For the electrolytes used and the Nafion 120 membrane, the osmotic flow is low with sodium hydroxide solution, higher with sodium chloride and the highest with sulphuric acid solutions (Table 3.7.1). For the same system the diffusion fluxes change in the opposite direction.  $J_s$  of NaOH is about 25% of the osmotic flow;  $J_s$  of NaCl 4%; and  $J_s$  of  $H_2SO_4$  is zero within the range of concentrations used.

**Table 3.7.1: Osmotic and diffusion fluxes per unit of the chemical potential difference of a solute for systems with Nafion 120 membrane.  $m = 1$ ,  $T = 25^\circ C$ .**

Flows	NaOH	NaCl	$H_2SO_4$
	(* $10^{-10} \text{ mol}^2/\text{m}^3 \text{ Ns}$ )		
Osmotic flow of water ( $-J_w/\Delta\mu_s$ )	4,7	8,0	17,7
Diffusion of solute ( $-J_s/\Delta\mu_s$ )	1,1	0,33	- 0,16

### 3.7.4 Osmotic Energy Conversion

The coupling coefficient,  $q$ , and the efficiency of energy conversion,  $\eta$ , have been calculated with equations (3.7.10a) and (3.7.11). The couplings between the spontaneous osmotic flow ( $J_w$ ) driven by the difference of solvent activity ( $\Delta\mu_w$ ) and the volume flow ( $J_v$ ) producing the pressure ( $\Delta p$ ) are shown as a function of the mean molalities of solutions bathing the membrane (Fig. 3.7.2). The coupling coefficient,  $q$ , is high for the system with sulphuric acid, ranging from 0,6 to 0,95 in 1 molar solution. For the other two electrolytes  $q$  does not exceed 0,4 (NaCl) or is even as low as 0,1 (NaOH). These results show the necessity of using membranes rejecting a solute almost perfectly. Even little diffusion as in the case of sodium chloride can disturb the coupling drastically.

This effect is even more pronounced as can be seen from the energy conversion,  $\eta$  (Fig. 3.7.3). Again, the  $\eta$  coefficient is the highest for the system with  $H_2SO_4$  reaching 0,4. For this system the maximum of  $\eta$  is observed for the ratio of produced pressure to the osmotic one  $\Delta p/\Delta\pi = 0,8$  (for ideal system it is one). In the case of the easily diffusing NaOH the energy conversion becomes negligible and decreased to 0,01 and the ratio  $\Delta p/\Delta\pi$  for  $\eta_{max}$  is as low as 0,15.

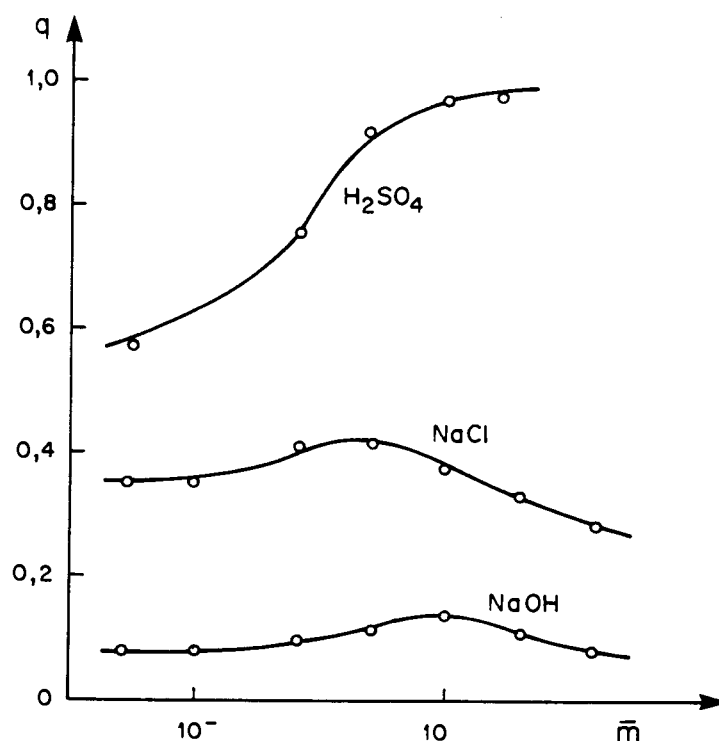


**Figure 3.7.2:** The concentration of coupling coefficient (eq. (3.7.11)) for various electrolyte solutions and Nafion 120 membrane; 298 K.

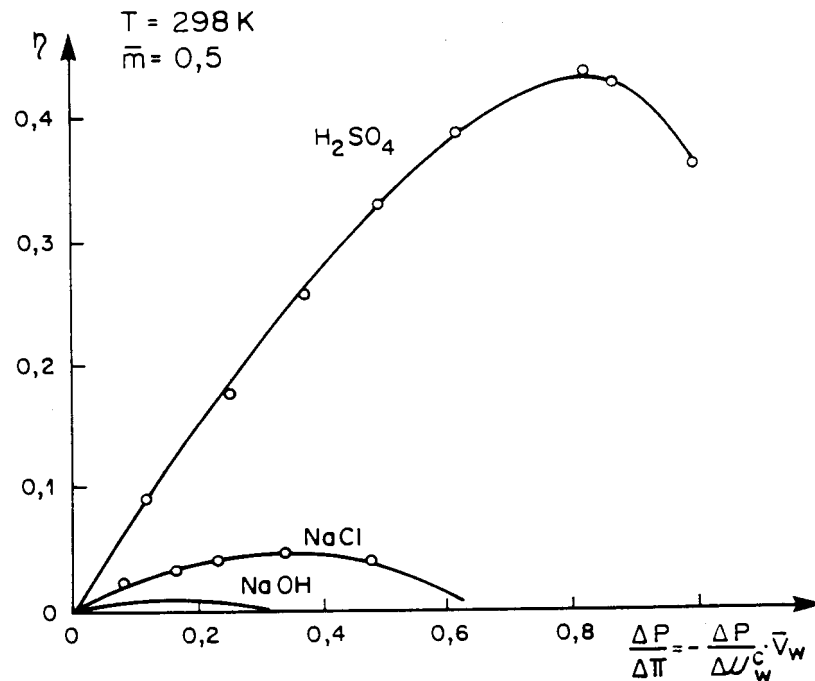


**Figure 3.7.3:** The dependence of the efficiency of osmotic into mechanical energy conversion (eq. 3.7.10) on the ratio  $\Delta P/\Delta\Pi$ ; 298 K.

In order to examine the system further, the rate of fluxes for other electrolytes were measured (Table 3.7.2). These results confirm that only the solutes perfectly rejected by a membrane, like sulphuric acid, appears to be efficient in an osmotic pump. Only in the case of a membrane highly permselective to the given electrolyte, the free energy of mixing, which usually goes unexploited, can be put to effective use.

The following conclusions can be drawn<sup>(19)</sup>:

- A high degree of osmotic to mechanical energy conversion ranging from 0,4 to 0,5 can only be achieved in a system with a membrane, which rejects the solute almost entirely, that is with  $\sigma \rightarrow 1$ .
- A salt flux reaching even 4% of the osmotic flux of water (Table 3.7.1, NaCl) results in a vast decrease of the efficiency of energy conversion ( $\eta < 0,1$ ).
- While in contact with an electrolyte which permeates Nafion 120 membrane more easily (like NaOH), the system cannot convert the osmotic energy to any remarkable degree ( $\eta < 0,01$ ).

**Table 3.7.2: Experimental volume fluxes in the systems with Nafion 120 membrane**

ELECTROLYTE	$J_v$	$J_v/\Delta\pi$
	(* $10^{-8}$ m/s)	(* $10^{-8}$ m/s atm)
NaCl	10,8	0,236
Na <sub>2</sub> SO <sub>4</sub>	4,59	0,145
HCl	36,7	0,70
H <sub>2</sub> SO <sub>4</sub>	42,0	1,76
H <sub>3</sub> PO <sub>4</sub>	6,72	0,60

### 3.8 Donnan Exclusion

If a resin is allowed to equilibrate in an electrolyte solution rather than in pure water, the water uptake is comparatively less due to the lowered external water activity,  $a_w(< 1)$ . Specifically, the osmotic swelling pressure becomes<sup>(11)</sup>

$$\Pi = -(RT/v_w) \ln (\bar{a}_w/a_w) < -(RT/v_w) \ln \bar{a}_w \quad (3.8.1)$$

In addition to the water fraction, the dissolved ions will distribute themselves across the membrane-solution interface according to a condition of free energy balance. Qualitatively, the driving force for electrolyte uptake is the initial solute chemical potential gradient across the interface. Considering this solely, the equilibrium concentrations within and exterior to the membrane would be equal were it not for the presence of the ionizable side-chains that through the constant of electro-neutrality, resist the co-ion uptake. A simple theory that explains the overall features of electrolyte uptake by ion-exchangers was outlined by Donnan<sup>(76)</sup>.

Assuming complete ionization, equivalent interdiffusion, electro-neutrality, and the equality of single-ion activities and concentrations, the theoretical result for the free energy balance across the interface between a 1 : 1 electrolyte solution of concentration  $C$  (mol per litre) and cation-exchange membrane, in which the ionogenic side-chain density is  $R$ , is

$$\bar{C}(\bar{C} + R) = C^2 \quad (3.8.2)$$

where  $\bar{C}$  is the internal equilibrium electrolyte concentration and the membrane was originally in the salt form. Immediately, it is seen that  $\bar{C} < C$  and that co-ion exclusion is enhanced by increasing  $R$ . As  $C$  becomes very large, the Donnan exclusion

mechanism becomes increasingly less effective.

### 3.9 Relationship Between True and Apparent Transport Numbers

The relationship between true and apparent transport numbers has been described by Laskshminarayanaiah<sup>(45)</sup>.

The emf of a cell of the type shown in Figure 3.9.1 is given by the following equation which cannot be integrated without knowledge of how  $\bar{t}_i$  and  $\bar{t}_w$  vary with external electrolyte concentration.

$$E = - (2 RT/F) \int_1^2 (\bar{t}_i - 10^{-3} m_{\pm} M \bar{t}_w) d \ln a_{\pm} \quad (3.9.1)$$

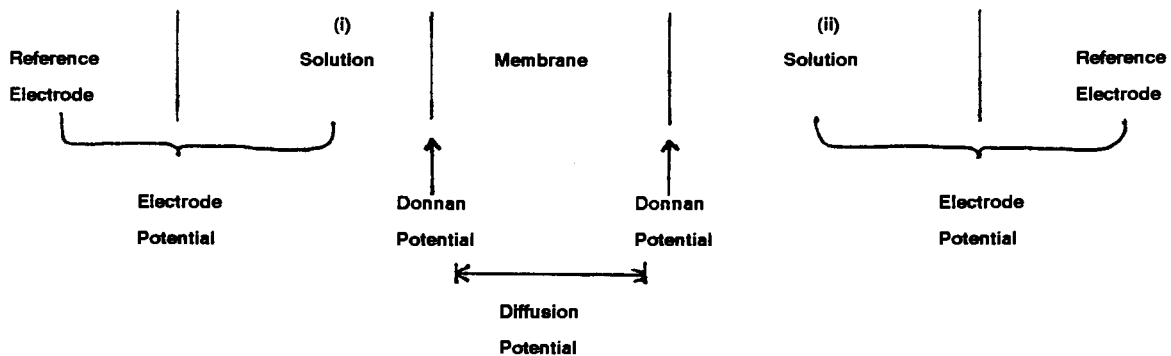


**Figure 3.9.1: Electric potentials across an ionic membrane separating different salt solutions.**

$\bar{t}_i$  and  $\bar{t}_w$  must be found by separate experiments and their values must be unambiguous without being influenced by factors such as current density and back diffusion. Even then, what relation these experimental values bear to  $\bar{t}_i$  and  $\bar{t}_w$  of eq. (3.9.1) is not clearly known.

However, an approximate approach can be made by integrating eq. (3.9.1) within narrow limits  $a_{\pm}'$  and  $a_{\pm}''$ . On integration, eq. (3.9.1) takes the form:

$$E = - \frac{2RT}{F} (\bar{t}_i - 10^{-3} m_{\pm} M \bar{t}_w) \ln \frac{a_{\pm}'}{a_{\pm}''} \quad (3.9.2)$$



The emf of a cell of the type shown in Figure 3.9.1 can be calculated from the modified Nernst equation.

$$E = 2\bar{t}_{+(app)} \frac{RT}{F} \ln \frac{a'}{a''} \quad (3.9.3)$$

which can be equated to eq. (3.9.3) to give<sup>(77)</sup>:

$$\bar{t}_+ = t_{+(app)} + 0,018m_{\pm} \bar{t}_w \quad (3.9.4)$$

Hale and McCouley tested eq. (3.9.4) using different heterogeneous membranes and found good agreement between true  $\bar{t}_+$  measured directly and  $\bar{t}_+$  calculated using eq. (3.9.4). Their measurements although confined to a number of different membranes, were made with one set of electrolyte solutions only (0,667 and 1,333 mol/l NaCl). Lakshminarayanaiah<sup>(78)</sup> checked eq. (3.9.4) over a wide concentration range. He found that the  $\bar{t}_+$  values calculated from eq. (3.9.4) were higher than the measured values particularly in high electrolyte concentrations. This discrepancy existing in the case of strong solutions is difficult to reconcile in view of the fact that Lakshminarayanaiah and Subrahmanyas<sup>(47)</sup> showed that eq. (3.9.1) is able to generate values for E (however from measured values of  $t_+$  and  $t_w$ ) agreeing with observed values. A more recent evaluation by Lakshminarayanaiah<sup>(79)</sup> has shown that eq. (3.9.4) is able to give values for  $\bar{t}_+$  agreeing with those measured directly.

The relationship of  $\bar{t}_{+(app)}$  obtained from emf measurements to  $\bar{t}_+$  measured directly, unlike eq. (3.9.4), has been approached from a different standpoint by Oda and Yawataya<sup>(80)</sup>. The apparent transport number ( $\bar{t}_{+(app)}$ ) calculated from emf data was related to the concentration of the external solution by an "interpolation technique". This consists in measuring E using two solutions,  $c'$  and  $c''$ , in the cell shown in Figure 3.9.1. In the first measurement of membrane potential, solution (") is so chosen that  $c''$  is less than  $c'$  and in the second measurement  $c'$  is held constant and  $c''$  is so chosen that it is now greater than  $c'$ . Each of the two values of  $\bar{t}_{+(app)}$  calculated from the two measurements is now referred to that particular concentration of  $c'$  used in the experiment and plotted. The value of  $\bar{t}_{+(app)}$  pertaining to  $c'$  which is kept constant in the two experiments is obtained by interpolation. Usually,  $\bar{t}_{+(app)}$  is related to the mean external electrolyte concentration, i.e.  $(c' + c'')/2$ .

True values of  $\bar{t}_+$  and  $\bar{t}_w$  were determined by Oda and Yawataya from the same experiment by the mass method which consisted in estimating the mass changes in

both the salt and the water in the cathode chamber following the passage of a known quantity of current through the system, electrolyte solution (c)  $\rightleftharpoons$  membrane  $\rightleftharpoons$  electrolyte solution (c). The relationship between  $\bar{t}_+$  and  $\bar{t}_{+(app)}$  was derived in the following manner<sup>(80)</sup>.

A selective membrane of fixed charge density  $\bar{X}$  (equivalent per unit volume of swollen membrane) in equilibrium with an external electrolyte solution contains  $\bar{X}(1 - \bar{s})$  equivalents of counter-ions and  $\bar{X}\bar{s}$  equivalents of co-ions where  $\bar{s}$  is the equivalent of co-ions per equivalent of fixed group present in the membrane. This arises from the Donnan absorption of the electrolyte by the membrane.

When an electric field is applied, ions and water move. In a membrane in which interactions between different membrane components, viz., counter-ion, co-ion, water and membrane, matrix, are absent, one may assume that the fixed water in the membrane is negligible and that all mobile water moves with the same velocity and in the same direction as the counter-ion. As a result, counter-ions move faster and co-ions move slower than they would otherwise if water stood still. Consequently, the mobilities ( $u$ 's) of the counter-ion and co-ion may be written as:

$$\bar{u}'_+ = \bar{u}_+ + \bar{u}_w \quad (3.9.5)$$

$$\bar{u}'_- = \bar{u}_- - \bar{u}_w \quad (3.9.6)$$

where +, -, and w stand for cation, anion and water, respectively.  $\bar{u}'_+$  and  $\bar{u}'_-$  are the increased and decreased mobilities due to the transport of water.

Due to water transport, the specific conductance of the membrane is increased. If  $k'$  is the membrane specific conductance, then

$$\bar{k}' = F[\bar{X}(1 + \bar{s})\bar{u}'_+ + \bar{X}\bar{s}\bar{u}'_-] \quad (3.9.7)$$

On substituting from eqs. (3.9.5) and (3.9.6), eq. (3.9.7) becomes

$$\bar{k}' = F\bar{X}[(1 + \bar{s})\bar{u}_+ + \bar{s}\bar{u}_- + \bar{u}_w] \quad (3.9.8)$$

If water transport is absent, the membrane conductance  $k$  is given by

$$\bar{k}' = Fx[(1 + \bar{s})\bar{u}_+ + \bar{s}\bar{u}_-] \quad (3.9.9)$$

It follows from eqs. (3.9.8) and (3.9.9) that the increase in conductance due to water transport is given by

$$\bar{k}' - \bar{k} = F\bar{X}\bar{u}_w \quad (3.9.10)$$

Transport numbers by definition are given by

$$t_+ = \frac{(1 + \bar{s})\bar{u}'_+}{(1 + \bar{s})\bar{u}_+ + \bar{s}\bar{u}'_-} \quad (3.9.11)$$

$$t_{+(app)} = \frac{(1 + \bar{s})\bar{u}_+}{(1 + \bar{s})\bar{u}_+ + \bar{s}\bar{u}'_-} \quad (3.9.12)$$

Substituting from eqs. (3.9.5) - (3.9.10) into eqs. (3.9.11) and (3.9.12) and remembering that  $\bar{t}_{+(app)} + \bar{t}_{-(app)} = 1$ , it can be shown that<sup>(80)</sup>:

$$\bar{t}_+ - \bar{t}_{+(app)} = (\bar{t}_{-(app)} + \bar{s})[(\bar{k}' - \bar{k})/\bar{k}'] \quad (3.9.13)$$

Substituting from eq. (3.9.10), eq. (3.9.13) becomes

$$\bar{t}_+ - \bar{t}_{+(app)} = [\bar{t}_{-(app)} + \bar{s}][F\bar{X}\bar{u}_w/\bar{k}'] \quad (3.9.14)$$

When a potential of E volts acts along length  $\lambda$  cm of a membrane capillary, the water in the pore moves with a mobility,  $u_w$  cm/s (i.e.,  $E/\ell$  is unity). The volume (millilitres) of water flowing per second through a membrane subject to unit potential gradient is given by  $\beta_E$  and is equal to  $(u_w A)$  where A is the pore area. But  $\beta$ , the volume of water flowing per Coulomb is given by:

$$\beta = V/i \quad (3.9.15)$$

where V is millilitres of water flowing per second and i is the current in amperes. But  $i = k_p A$  per unit potential gradient and  $k_p$  is the specific conductance of the pore liquid of an infinitely swollen membrane ( $k_p$  is really a modified membrane conductance). Consequently, it follows that

$$\beta_E = \bar{u}_w A = \bar{k}_i A \beta \quad (3.9.16)$$

Equation (3.9.16) differs from the original equation of Oda and Yawataya which is dimensionally incorrect<sup>(45)</sup>.

Substitution of eq. (3.9.16) into eq. (3.9.14) gives

$$\bar{t}_+ = t_{+(app)} + (\bar{t}_{-(app)} + \bar{s}) F \bar{X}_1 \bar{k}_i \beta / k' \quad (3.9.17)$$

But  $k'$  may be equated to  $\varphi_w \bar{k}_i$  where  $\varphi_w$  is the volume fraction of water in the membrane. Equation (3.9.17), therefore, becomes

$$\bar{t}_+ = \bar{t}_{+(app)} + [\bar{t}_{-(app)} + \bar{s}] F \bar{X}_v \beta \quad (3.9.18)$$

where  $\bar{X}_v = \bar{X} / \varphi_w$ , equivalent of fixed groups per unit volume of interstitial water.

Since the method usually used to measure the transport number of water  $\bar{t}_w$  which is equal to (F6/18), depends on following volume changes in the anode and cathode chambers, the observed volume changes, which measures only solution flow, have to be corrected for both salt transport and electrode reactions to give values for water flow only. If reversible Ag-AgCl electrodes are used, the passage of a Faraday of current produces at the cathode, a mole of Ag and  $\bar{t}_+$  moles of MCl (M = univalent cation) and in the same time a mole of AgCl disappears. The actual increase in volume  $\Delta V_c$ , which is equal to the volume decrease at the anode, due to water transport, is given by

$$\Delta V_c = \Delta V_o + \bar{V}_{AgCl} - \bar{V}_{Ag} - \bar{t}_+ \bar{V}_{MCl} \quad (3.9.19)$$

where the  $\bar{V}$ 's are partial molar volumes and  $\Delta V_o$  is the observed volume change. As  $V_{AgCl} = 25,77$  and  $V_{Ag} = 10,28$ , eq. (3.9.19) becomes

$$\Delta V_c = \Delta V_o + 15,5 - \bar{t}_+ \bar{V}_{MCl}$$

$\bar{V}_{MCl}$  values can be evaluated using the usual equations<sup>(61)</sup> and  $\bar{t}_+$  values must be obtained by experiment using the appropriate concentration. Then

$$\bar{t}_w = \Delta V / \bar{V}_{H_2O} = \Delta V / 18 \quad (3.9.20)$$

$F\bar{X}_v\beta$  may be written as  $\bar{t}_w/\bar{W}_e$

where  $\bar{t}_w = F\beta/18$  and  $\bar{W}_e = 1/18\bar{X}_v$ ; i.e., moles of water per equivalent of ion-exchange site. Substitution of these values in eq. (3.9.18) gives

$$t_+ = \begin{cases} \bar{t}_{+(app)} + [\bar{t}_{-(app)} + \bar{s}](\bar{t}_w/\bar{W}_e) \\ \text{or} \\ (\bar{t}_w/\bar{W}_e)(1 + \bar{s}) + \bar{t}_{+(app)}(1 - (\bar{t}_w/\bar{W}_e)) \end{cases} \quad (3.9.21)$$

Oda and Yawataya computed  $\bar{t}_+$  values from eq. (3.9.18) by measuring  $\bar{t}_{+(app)}$ ,  $\bar{s}$ ,  $\bar{X}_v$  and  $\beta$ . Although these values were lower than the observed values of  $\bar{t}_+$ , they considered the agreement good since the divergence of the calculated values from the observed values was within the limits of experimental error.

### 3.10 Electro-Osmotic Pumping - The Stationary State - Brine Concentration and Volume Flow

#### 3.10.1 Ion Fluxes and Volume Flow

In the unit cell flow regime ED becomes a three-port system like reverse osmosis. The feed solution is introduced between the concentrating cells, passes between the cells and leaves the system. The permeate composition is completely determined by membrane performance under the conditions of the process. A schematic diagram of a unit cell showing ion and water fluxes in the system is shown in Figure 3.10.1<sup>(1)</sup>. For a uni-univalent salt-like sodium chloride, the current density through a cation-exchange membrane is related to the ion fluxes according to Garza<sup>(1)</sup> by:

$$I = F(z_1j_1^c + z_2j_2^c) \quad (3.10.1)$$

$$= F(j_1^c - j_2^c) \quad (3.10.2)$$

$$= F(|j_1^c| + |j_2^c|) \quad (3.10.3)$$

where  $z_1 = 1$  (cation)

and  $z_2 = -1$  (anion)

and  $j_1^c$  and  $j_2^c$  are the cation and anion fluxes through the cation-exchange membrane respectively.

Effective transport numbers are defined as follows<sup>(1, 2)</sup>:

$$\bar{t}_1^c = \frac{|j_1^c|}{(|j_1^c| + |j_2^c|)} = (1 + \Delta t^c)/2 \quad (3.10.4)$$

$$\bar{t}_2^c = \frac{|j_2^c|}{(|j_1^c| + |j_2^c|)} = (1 - \Delta t^c)/2 \quad (3.10.5)$$

$$\text{where } \Delta t^c = \bar{t}_1^c - \bar{t}_2^c \quad (3.10.6)$$

$$\text{and } \bar{t}_1^c + \bar{t}_2^c = 1 \quad (3.10.7)$$

$\Delta t^c$  = difference between counter- and co-ion transport number or membrane permselectivity.

$\bar{t}_1^c$  = cation transport number through cation membrane

$\bar{t}_2^c$  = anion transport number through cation membrane

and the bar refers to the membrane phase.

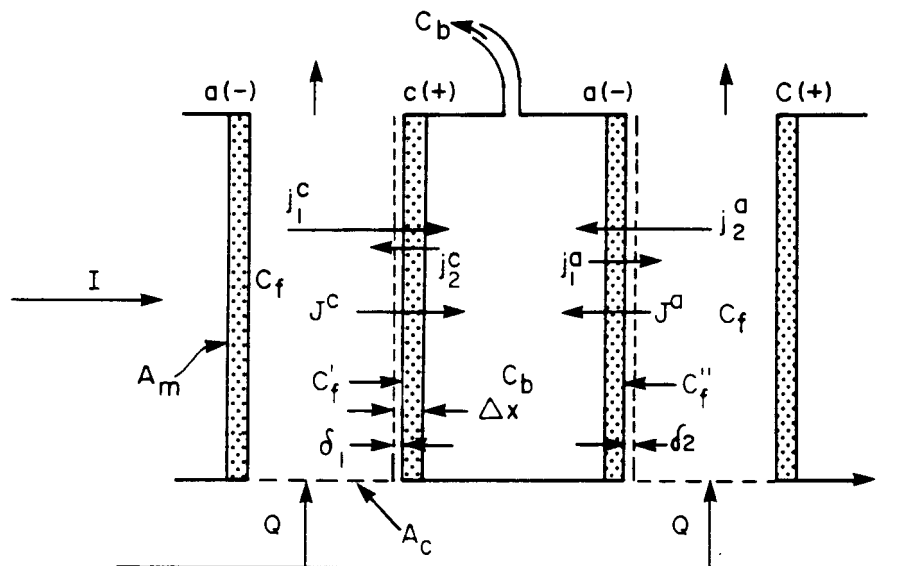


Figure 3.10.1: Representation of fluxes in the ED unit-cell system.

c and a indicate the cation- and anion-exchange membranes and subscripts 1 and 2 refer to the cations and anions, respectively (uni-univalent salts);  $\Delta x$ : membrane thickness;  $\delta$ 's: effective Nernst layers;  $c_f$ 's: feed concentration;  $c_b$ : brine concentration;  $J^c$  and  $J^a$ : water fluxes;  $j^c$  and  $j^a$  anion and cation currents.  $A_m$ : effective membrane area;  $A_c$ : transversal area of the dialysate compartment;  $Q$ : flow of dialysate. The arrows show the direction of the fluxes.

Further,

$$j_1^c = \bar{t}_1^c (|j_1^c| + |j_2^c|) = \bar{t}_1^c I/F = (1 + \Delta t^c) I/2F \quad (3.10.8)$$

$$j_2^c = \bar{t}_2^c (|j_1^c| + |j_2^c|) = \bar{t}_2^c I/F = (1 - \Delta t^c) I/2F \quad (3.10.9)$$

(Note: Effective transport numbers are to be distinguished from the usual transport numbers which refer to the above ratio's in the absence of concentration gradients).

The brine concentration,  $c_b$ , can be obtained from the following material balance (Figure 3.10.1):

$$c_b = \frac{|j_1^c| - |j_1^a|}{|J^c| + |J^a|} = \frac{|j_2^a| - |j_2^c|}{|J^c| + |J^a|} \quad (3.10.10)$$

where  $J^c$  and  $J^a$  are the water fluxes (flows) through the cation and anion membranes, respectively.

Consider,

$$c_b = \frac{|J^c| - |j_1^a|}{|J^c| + |J^a|} \quad (3.10.11)$$

Substitute eq. (3.10.8) into eq. (3.10.11)

$$\therefore c_b = \frac{(\bar{t}_1^c I/F) - (\bar{t}_1^a I/F)}{|J^c| + |J^a|} \quad (3.10.12)$$

$$= \frac{(1 + \Delta t^c) I/2F - (1 - \Delta t^a) I/2F}{|J^c| + |J^a|} \quad (3.10.13)$$

$$= \frac{I/2F [(1 + \Delta t^c) - (1 - \Delta t^a)]}{|J^c| + |J^a|} \quad (3.10.14)$$

$$= \frac{I (\Delta t^c + \Delta t^a)}{2F (|J^c| + |J^a|)} \quad (3.10.15)$$

$$c_b = \frac{I \Delta \bar{t}}{F (|J^c| + |J^a|)} \quad (3.10.16)$$

$$= \frac{I \Delta \bar{t}}{2FJ} \quad (3.10.17)$$

$$\Delta \bar{t} = \frac{\Delta t^c + \Delta t^a}{2} \quad (3.10.18)$$

$$\text{and } 2J = |J^c| + |J^a| \quad (3.10.19)$$

The volume flow through every membrane is equal to the sum of the electro-osmotic and osmotic contributions<sup>(2)</sup>.

$$\text{Therefore } J = J_{\text{elosm}} + J_{\text{osm}} \quad (3.10.20)$$

The electro-osmotic water flow for the cation and anion membrane is given by<sup>(2)</sup>:

$$J_{\text{elosm}}^c = (\beta_1^c t_1^c - \beta_2^c t_2^c) I \quad (3.10.21)$$

$$J_{\text{elosm}}^a = (\beta_2^a t_2^a - \beta_1^a t_1^a) I \quad (3.10.22)$$

The assumption here according to Garza & Kedem<sup>(2)</sup> is that the electro-osmotic water flow is governed by the drag exerted by the ions. The  $\beta$ 's are 'drag' coefficients. They represent the amount of water dragged along with every type of ion by electro-osmosis. For tight membranes, the value of the  $\beta$ 's should not be very different from the primary hydration water associated with the ions. For porous membranes, however, the value of the  $\beta$ 's may be several ten folds larger.

The osmotic contribution is given by<sup>(2)</sup>:

$$J_{\text{osm}} = 2RT \sigma L_p \Delta(g c_s) \quad (3.10.23)$$

where  $R$  is the universal gas constant,  $T$  the absolute temperature,  $g$  the osmotic coefficient,  $\sigma$  the reflection coefficient and  $L_p$  the hydraulic permeability.

Therefore,

$$J_{\text{osm}}^c + J_{\text{osm}}^a = 2RT(g_b c_b - g_f c_f) (\sigma^c L_p^c + \sigma^a L_p^a) \quad (3.10.24)$$

Introduction of equations (3.10.20); (3.10.21); (3.10.22) into equation (3.10.16) and neglecting the terms  $(\beta_1^c - \beta_2^c) \bar{t}_2^c$  and  $(\beta_2^a - \beta_1^a) \bar{t}_1^a$  in comparison with  $\beta_1^c \Delta t^c$  and  $\beta_2^a \Delta t^a$ , gives: (note: use was made of eq.(3.10.6)



$$c_b = \frac{l(\Delta t^c + \Delta t^a)2}{F(\beta_1^c \Delta t^c + \beta_2^a \Delta t^a) + 2RT(g_b c_b - g_f c_f) \sigma^c L_p^c + \sigma^a L_p^a} \quad (3.10.25)$$

$$= \frac{(\Delta t^c + \Delta t^a)/2}{F(\beta_1^c \Delta t^c + \beta_2^a \Delta t^a) + 2FRT(g_b c_b - g_f c_f) \sigma^c L_p^c + \sigma^a L_p^a / l} \quad (3.10.26)$$

Equation (3.10.26) is justified for very permselective membranes where  $t_2^c$  and  $t_1^a$  are small, or where  $\beta_1^c \approx \beta_2^a$  and  $\beta_2^c \approx \beta_1^a$ .

For high current densities, the second term (osmotic contribution) in the denominator of equation (3.10.26) may be neglected.

Therefore,

$$c_b^{\max} = \frac{(\Delta t^c + \Delta t^a)/2}{F(\beta_1^c \Delta t^c + \beta_2^a \Delta t^a)} \quad (3.10.27)$$

For  $\beta^c \approx \beta^a$  and  $\Delta t^c \approx \Delta t^a$  (symmetric membranes), equation (3.10.27) becomes

$$c_b^{\max} = \frac{1}{F(\beta_1^c + \beta_2^a)} = \frac{1}{2FB} \quad (3.10.28)$$

where  $2B = \beta_1^c + \beta_2^a$ .

$\beta_1^c$  and  $\beta_2^a$  are the drag coefficients associated with the counterions. These coefficients are identical with the electro-osmotic coefficient,  $\beta = (J/l)_{\Delta P = \Delta T = 0}$  measured at low concentration where co-ion exclusion is practically complete, i.e.

$$t_{\text{counter-ion}} \approx 1, t_{\text{co-ion}} \approx 0.$$

The cases for which equation (3.10.28) applies (i.e. for very permselective and/or for approximately symmetric membranes, at high current densities) are of considerable interest and importance according to Garza and Kedem<sup>(2)</sup> since the brine concentration depends only on the electro-osmotic coefficients,  $\beta_1^c$  and  $\beta_2^a$ .  $c_b^{\max}$  can also be determined from equations (3.10.26); (3.10.27) and (3.10.28)

$$c_b = \frac{l \Delta \bar{t}}{F(J_{\text{elosm}} + J_{\text{osm}})} \quad (3.10.29)$$

$$= \frac{l \Delta \bar{t}}{F J_{\text{elosm}} (1 + J_{\text{osm}} / J_{\text{elosm}})} \quad (3.10.30)$$

$$= \frac{C_b^{\max}}{1 + J_{\text{osm}}/J_{\text{elosm}}} \quad (3.10.31)$$

### 3.10.2 Symmetric cells

The theory of EOP in general leads to difficult computations which must be carried out numerically according to Garza<sup>(1)</sup>. However, there is one case in which results can be given in terms of simple closed formula. This case depends on the assumption of a symmetric cell<sup>(1)</sup>. In a symmetric cell the cation- and anion-exchange membranes have identical physical properties in all regards except for the sign of their fixed charges. Because of cell symmetry, the magnitudes of the counter-ion fluxes through both membranes are the same. When a symmetric salt is chosen like potassium chloride, the anion and cation have equal mobilities. In other words, the magnitude of the cation flux through the cation exchange membrane is the same as the magnitude of the anion flux through the anion-exchange membrane. Also the magnitudes of the co-ion fluxes through both membranes are the same, i.e., the magnitude of the anion flux through the cation-exchange membrane is the same as the magnitude of the cation flux through the anion-exchange membrane.

$$|j_1^c| = |j_2^a|; |j_1^a| = |j_2^c| \quad (3.10.32)$$

and thus

$$\bar{i}_1^c = \bar{i}_2^a; \bar{i}_1^a = \bar{i}_2^c; \Delta t^c = \Delta t^a = \Delta \bar{t} \quad (3.10.33)$$

Water flows also are of equal magnitude and opposite direction:

$$|J^c| = |J^a| = J \text{ or } J^c = -J^a = J \quad (3.10.34)$$

The amount of salt leaving through the brine outlet per unit time and membrane area,  $2J c_b$ , is related to the cation flows by (eqs. 3.10.10 and 3.10.19):

$$2Jc_b = |j_1^c| - |j_1^a| \quad (3.10.35)$$

and in the symmetric system is :

$$J = |\Delta \bar{t}| / 2c_b F \quad (3.10.36)$$

### 3.10.2.1 Current Efficiency

The amount of salt transferred per Faraday of current passed through a symmetric unit cell is given from equation 3.10.36 by

$$\varepsilon_p = \frac{2Jc_b}{I/F} = \Delta \bar{t} \quad (3.10.37)$$

The overall efficiency,  $\varepsilon$ , is, however, somewhat smaller than  $\varepsilon_p$ , since water is also lost with the salt. The effective current density, i.e. the purification of the product achieved, is given by<sup>(1)</sup>:

$$I_{\text{eff}} = F \left( \frac{Q}{A_m} - 2J \right) (c_f - c_p) = F \left( \frac{Q}{A_m} - 2J \right) (\Delta c_f) \quad (3.10.38)$$

where  $Q$  is the amount of feed solution entering a channel per unit time,  $A_m$  the effective membrane area (Figure 3.10.1),  $\Delta$  the degree of mineralization given by:

$$\Delta = \frac{c_f - c_p}{c_f} \quad (3.10.39)$$

where

$c_f$  is the concentration of the feed solution entering the stack, and  $c_p$  the concentration of the product leaving it.

The mass balance for the salt is:

$$\frac{Qc_f}{A_m} = \left( \frac{Q}{A_m} - 2J \right) c_p + 2Jc_b \quad (3.10.40)$$

Therefore

$$I_{\text{eff}}/F = \left( \frac{Q}{A_m} - 2J \right) (c_f - c_p) = 2J(c_b - c_f) \quad (3.10.41)$$

and

$$\varepsilon = \frac{I_{\text{eff}}}{I} = \Delta t \left( 1 - \frac{c_f}{c_b} \right) = \varepsilon_p \times \varepsilon_w \quad (3.10.42)$$

where

$$\varepsilon_{\omega} = 1 - c_i/c_o \quad (3.10.43)$$

As is customary in ED, the overall efficiency is presented as the product of two terms, one due to the lack of ideal permselectivity in the membranes,  $\varepsilon_p$ , the other reflecting the loss of water to the brine,  $\varepsilon_w$ .

### 3.10.2.2 Electro-Osmotic Flow

Electro-osmotic flow is measured under the restrictions<sup>(1)</sup>:

$$\Delta c = 0, \quad du_w/dx = 0$$

Under these conditions are :

$$J_{\text{elosm}} = (j_1 \beta_1 + j_2 \beta_2)F \quad (3.10.44)$$

Equation 3.10.44 can also be written as :

$$J_{\text{elosm}} = (\beta_1 t_1 - \beta_2 t_2)I \quad (3.10.45)$$

$$= [\beta_1(t_1 - t_2) + (\beta_1 - \beta_2) t_2]I \quad (3.10.46)$$

$$= [\beta_1 \Delta t + (\beta_1 - \beta_2) t_2]I \quad (3.10.47)$$

For small values of  $t_2$ , or for  $\beta_1 = \beta_2 = \beta$  equation (3.10.47) becomes :

$$J_{\text{elosm}} = \beta^{\circ} \Delta t I \quad (3.10.48)$$

where  $\beta^{\circ}$  is the customary electro-osmotic coefficient measured at low ionic strength where co-ion exclusion is high and  $\Delta t \approx 1$ , i.e.:

$$\beta^{\circ} = (J/I)_{\Delta C = \Delta P = \Delta T = 0, \Delta t = 1} = (J_{\text{elosm}}/I)_{\Delta t = 1}$$

### 3.10.2.3 Osmotic Flow at High Co-Ion Exclusion

Osmotic flow is measured under the restrictions<sup>(1)</sup>:

$$I = \Delta p = 0, \quad j_1 = j_2 = 0.$$

(absence of electric current, hydrostatic pressure and impermeable solutes). In this case is<sup>(1)</sup>:

$$J_{osm} = L_p \sigma \Delta \pi \quad (3.10.49)$$

### 3.10.2.4 Volume Flow in Electro-Osmotic Pumping

The volume flow into the membrane concentrating cells in EOP is the sum of the electro-osmotic and osmotic water flows and is given by<sup>(1)</sup>:

Therefore,

$$J = -L_p \sigma \Delta \Pi + \beta^\circ \Delta t I \quad (3.10.50)$$

### 3.10.3 Non-Symmetric Cell

#### 3.10.3.1 Porous membranes

In the previous section a simplified theory of the electro-osmotic pumping process was given where only the symmetric cell case was treated. By 'symmetric cell' is meant that the cation- and anion-exchange membranes are assumed to have the same values for the physical properties of interest in the process, namely, absolute effective charge density, electro-osmotic coefficient, and hydraulic permeability. If this were not the case, the calculations would become much more complicated since  $\Delta t$  (difference between the effective transport numbers of counter- and co-ions) may have different values for the two types of membranes, and the expression for the brine concentration,  $c_b$ , will not be as simple as for the symmetric case<sup>(1)</sup>.  $c_b$  may be found in the general case from material balance considerations to be equal to :-

$$c_b = \frac{|j_1^c| - |j_1^a|}{|J^c| + |J^a|} \quad (3.10.11)$$

From the definition of 'effective' transport numbers given before (eqs. 3.10.4 and 3.10.5), it can be written :

$$\begin{aligned} |j_1^c| - |j_1^a| &= |j_2^a| - |j_2^c| \\ &= (1 + \Delta t^c)I/2F - (1 - \Delta t^a)I/2F \end{aligned}$$

$$= (\Delta t^c + \Delta t^a)l/2F \quad (3.10.51)$$

The volume flow is given by the sums of electro-osmotic and osmotic terms, namely:

$$\begin{aligned} J &= J_{\text{elosm}} + J_{\text{osm}} \\ &= (\beta_1 t_1 - \beta_2 t_2)l + 2RT \sigma L_p \Delta(\phi_s c_s) \end{aligned} \quad (3.10.52)$$

Therefore,

$$\begin{aligned} &|J^c| + |J^a| \\ &= l(\beta_1^c t_1^c - \beta_2^c t_2^c + \beta_2^a t_2^a - \beta_1^a t_1^a) + 2RT (\phi_b c_b - \phi_f c_f) \times (\sigma^c L_p^c + \sigma^a L_p^a) \\ &= l[\beta_1^c (t_1^c - t_2^c) + (\beta_1^c - \beta_2^c) t_2^c + \beta_2^a (t_2^a - t_1^a) + (\beta_2^a - \beta_1^a) t_1^a] + \dots + 2RT (\phi_b c_b - \phi_f c_f) \\ &\times (\sigma^c L_p^c + \sigma^a L_p^a) \end{aligned} \quad (3.10.53)$$

for small values of  $t_2^c$  and  $t_1^a$ , or for  $\beta_1^c = \beta_2^a = \beta_c^o$ , and  $\beta_2^c = \beta_1^a = \beta_a^o$ ; equation (3.10.53) becomes:

$$|J^c| + |J^a| = l(\beta_1^c \Delta t^c + \beta_2^a \Delta t^a) + 2RT (\phi_b c_b - \phi_f c_f) \times (\sigma^c L_p^c + \sigma^a L_p^a) \quad (3.10.54)$$

Substituting equations (3.10.51) and (3.10.54) into (3.10.11), gives:

$$c_b = \frac{(\Delta t^c + \Delta t^a)/2}{F(\beta_1^c \Delta t^c + \beta_2^a \Delta t^a) + 2RT(\phi_b c_b - \phi_f c_f)(\sigma^c L_p^c + \sigma^a L_p^a)l/F} \quad (3.10.55)$$

In the case of high current density, the second term in the denominator of equation (3.10.55) can be neglected. Therefore,

$$c_b^{\text{max}} = \frac{(\Delta t_{\text{max}}^c + \Delta t_{\text{max}}^a)/2}{F(\beta_1^c \Delta t_{\text{max}}^c + \beta_2^a \Delta t_{\text{max}}^a)} \quad (3.10.56)$$

Plots of  $\Delta t$  versus current density for every membrane are expected to have the same kind of behaviour as for the symmetric cell case, as no new elements have been added. The value of  $c_b$ , however, depends now on the properties of both membranes, and not on those of only one of them. Therefore, for high current densities the values of  $\Delta t$  become independent on  $l$ , and can be calculated<sup>(1)</sup>. Since the values of  $\Delta t$  depends on  $c_b$ , which in its turn depends on  $\Delta t^c$  and  $\Delta t^a$ , trial and error calculations are necessary according to Garza.

In conclusion, for the non-symmetric-cell case (as for the symmetric cell) the following is expected<sup>(1)</sup>:

- The Coulomb efficiency of the concentrating cell will reach a maximum (plateau) value at high current densities (below the limiting value of the current)

$$\begin{aligned}\varepsilon &= \Delta t = t_1^c - t_1^a = (1 + \Delta t^c)/2 - (1 - \Delta t^a)/2 \\ &= (\Delta t^c + \Delta t^a)/2\end{aligned}\quad (3.10.57)$$

- The brine concentration,  $c_b$ , to reach a maximum value (also at high current densities below the limiting value) independent of  $I$  and of the feed concentration;
- The volume flow (3.10.54) versus  $I\Delta t$  plots will become straight lines at high current densities since the osmotic contribution becomes almost independent of current density when the latter is sufficiently high (because  $c_b$  becomes constant and  $c'$  - the concentration at the feed interface (Fig. 3.10.1) may be kept within certain limits by controlling concentration polarization); and the electro-osmotic contribution is directly proportional to  $I\Delta \bar{t}$  ( $\Delta \bar{t} = (\Delta \bar{t}^c + \Delta \bar{t}^a)/2$ , when either  $\Delta t^c = \Delta t^a$  or  $\beta_1^c = \beta_2^a$ ).

### 3.11 Flux Equations, Membrane Potentials and Current Efficiency

Flux equations, membrane potentials and current efficiency relevant to EOP-ED have been described by Kedem and Bar-On<sup>(5)</sup>. The total ED process comprises three independent flows and forces; electric current and potential; volume flow and pressure/osmotic pressure; salt flow and concentration difference. For small flows and gradients linear equations can be written for each of the flows, including the influence of all gradients<sup>(14)</sup>.

In practical ED, especially in EOP, flows and forces are large and one can not expect linear equations to hold, even if the usually defined membrane transport coefficients are constant, according to Kedem and Bar-on. In fact, transport coefficients may vary considerably in the concentration range between feed and brine. For an adequate discussion of flows under these conditions, Kedem and Bar-On have followed the analysis given previously for reverse osmosis<sup>(82)</sup>.

In the schematic presentation shown in Figure 3.11.1, the membrane is broken down into differential elements, separated by uniform solution segments which are in equilibrium with the two contiguous membrane faces. All fluxes going from left to right are counted positive. The gradient of a scalar  $y$ ,  $dy/dx$ , is taken as the value of the scalar on the right (double prime) minus the value on the left (single prime), divided by the distance. On the other hand, the operator  $\Delta$  is defined with the opposite sign, in order to bring the notation used by Kedem and Bar-On in line with that of previous publications<sup>(6)</sup>:

$$\Delta c = c' - c'' \text{ and}$$

$$y = \int dy$$

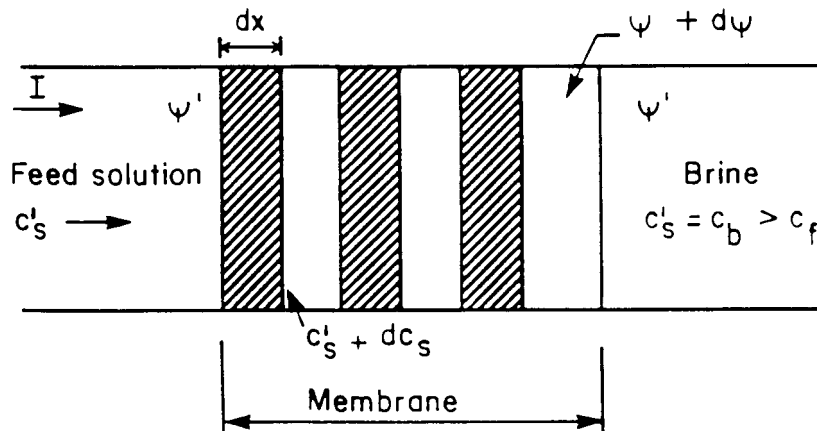


**Figure 3.11.1: Schematic representation of cation-exchange membrane.**

Salt flow across a differential layer of cation-exchange membrane can be written as a function of electric current, volume flow and concentration gradient according to Kedem and Katchalsky<sup>(14)</sup>:

$$S^c = \frac{J_1^c + J_2^c}{2} = c_s (1 - \sigma^c) J_v^c + \bar{P} \Delta c + \frac{\Delta t}{2} \frac{I}{F} \quad (3.11.1)$$

where

$$\Delta t^c = t_1^c - t_2^c = 2t_1^c - 1 \quad (3.11.2)$$



Equation (3.11.1) can be derived as follows according to Kedem and Bar-On<sup>(5)</sup>:

In a discontinuous system containing water and one uni-valent salt in the absence of hydrostatic pressure, the rate of free energy dissipation is :

$$\phi = j_1 \Delta \tilde{\mu}_1 + j_2 \Delta \tilde{\mu}_2 + j_w \Delta \mu_w \quad (\text{A1})$$

where the  $\mu_i$ 's are the electro-chemical potentials of ions 1 and 2.

$$\Delta \tilde{\mu}_1 + \Delta \tilde{\mu}_2 = \Delta \mu_s \quad (\text{A2})$$

$$\Delta \tilde{\mu}_1 + \Delta \tilde{\mu}_2 = 2F\Delta\Psi (\Delta p = 0) \quad (\text{A3})$$

$$I = F(J_1 - J_2) \quad (\text{A4})$$

$$\Delta \mu_w = -\bar{V}_w \Delta \Pi_s \quad (\text{A5})$$

$$J_v = \bar{V}_w J_w \quad (\text{A6})$$

Equation (A1) can be transformed to :

$$\phi = \frac{(J_1^c + J_2^c)}{2} \Delta \mu_s + I \Delta \Psi - J_v \Delta \pi_s \quad (\text{A7})$$

because

$$\begin{aligned} & \frac{J_1 + J_2}{2} (\Delta \tilde{\mu}_1 + \Delta \tilde{\mu}_2) + (J_1 - J_2) \frac{(\Delta \tilde{\mu}_1 - \Delta \tilde{\mu}_2)}{2} - J_v \Delta \pi_s \\ &= \frac{J_1}{2} \Delta \tilde{\mu}_1 + \frac{J_2}{2} \Delta \tilde{\mu}_1 + \frac{J_1}{2} \Delta \tilde{\mu}_2 + \frac{J_2}{2} \Delta \tilde{\mu}_2 + \frac{J_1}{2} \Delta \tilde{\mu}_1 - \frac{J_2}{2} \Delta \tilde{\mu}_1 - \frac{J_1}{2} \Delta \tilde{\mu}_2 + \frac{J_2}{2} \Delta \tilde{\mu}_2 - J_v \Delta \pi_s \\ &= J_1 \Delta \tilde{\mu}_1 + J_2 \Delta \tilde{\mu}_2 + J_w \Delta \mu_w \end{aligned}$$

The salt flow was identified with  $J_1$  (uni-valent cation). Therefore

$$J_2 = J_1 - I/F \quad (3.11.3)$$

The expressions for the ion fluxes in terms of the practical coefficients are<sup>(14)</sup>:

$$J_1 = \omega \Delta \Pi_s + c_s (1 - \sigma) J_v + t_1 I/F \quad (3.11.4)$$

and

$$J_2 = \omega \Delta \Pi_s + c_s (1 - \sigma) J_v - (1 - t_1) I/F \quad (3.11.5)$$

Therefore, the salt flow

$$\frac{J_1 + J_2}{2} = c_s(1-\sigma)J_v + \omega \Delta \pi_s + \frac{\Delta t}{2}I/F \quad (3.11.6)$$

where  $\omega$  = solute permeability

and  $\Delta \pi_s$  = difference in osmotic pressure of permeable solute

Equation (3.11.1) is identical with equation (3.11.6).

$\bar{P}$  in equation (3.11.1) is the specific salt permeability,  $\Delta c$  the concentration difference and  $\sigma$  the reflection coefficient. In an ideally permselective cation-exchange membrane will  $\Delta t^c \rightarrow 1$ ,  $P \rightarrow 0$ ,  $\sigma \rightarrow 1$ , so that  $S^c = 1/2F$ . Similarly, in an ideal anion-exchange membrane will  $\Delta t^a \rightarrow 0$ ,  $P \rightarrow 0$ ,  $\sigma \rightarrow 1$ , and  $-S^a = 1/2F$  and  $\eta_c = 1$ .

Consider now a cation-exchange membrane in which salt exclusion is not complete with co-ions carrying a significant fraction of the current<sup>(5)</sup>. In this case  $\Delta t$  will be smaller than 1 and will decrease with increasing  $c_s$  (salt concentration) as salt invasion becomes pronounced. Salt permeability will increase when  $c_s$  increases. If the influence of volume flow is negligible, a constant stationary value of  $S^c$  is possible only if the concentration profile is concave, i.e.  $dc/dx$  decreases from the feed to the brine surface<sup>(5)</sup>. A region of constant  $c_s$  may then develop near the brine surface at high current density. The upper limit of the partial current efficiency  $\eta_c^c$  is then determined by  $\Delta t^c$  characterizing the membrane equilibrated with the brine solution. The same argument holds for the anion-exchange membrane. Therefore, according to Kedem and Bar-on, without the influence of volume flow

$$\eta_c < \frac{\Delta t^c(c_b) + \Delta t^a(c_b)}{2} \quad (3.11.7)$$

when back diffusion is overcome by high current density.

The conventional method for determination of transport numbers is the measurement of membrane potential, i.e.  $\Delta \Psi$  between two solutions separated by the examined membrane without electric current. The potential across a differential layer is given by the expression<sup>(5)</sup>:

$$-F \frac{d\Psi}{dx} = \Delta t \frac{1}{2} \frac{d\mu_s}{dx} - F \frac{\beta}{L_p^R} J_v \quad (3.11.8)$$

where  $\beta$  is the electro-osmotic coefficient and  $L_p$  is the hydraulic permeability. The last

term represents a streaming potential. If this can be neglected, the potential between feed and brine solution is given by :

$$\Delta \Psi_m = \frac{RT}{F} \int_{c_i}^{c_b} \Delta t \left( 1 + \frac{d \ln \gamma^\pm}{d \ln c_s} \right) d \ln c_s \quad (3.11.9)$$

for an ideal membrane is  $\Delta t = 1$

$$\Delta \Psi_i = \frac{RT}{F} \ln \frac{(c_s \gamma^\pm)_b}{(c_s \gamma^\pm)_i} \quad (3.11.10)$$

where  $\gamma^\pm$  is an activity coefficient and the average transport number is

$$\bar{\Delta t} = \frac{\Delta \Psi_m}{\Delta \Psi_i} \quad (3.11.11)$$

This average transport number, according to Kedem and Bar-on, is closer to the value for  $c_i$  than for  $c_b$ . The conclusion from equations (3.11.7), (3.11.9) and (3.11.11) is that for concentration dependent transport numbers, the actual current efficiency is expected to be less than predicted from membrane potentials, i.e.

$$\eta < \frac{\Delta \Psi_m^c + |\Delta \Psi_m^a|}{|2\Delta \Psi_i|} \quad (3.11.12)$$

The correlation given by equation (3.11.12) is valid only if the influence of volume flow is negligible.

The potential per cell pair,  $V_{cp}$  (in volt), at a given current density ( $i = l/cm^2$ , mA/cm<sup>2</sup>), is the sum of several terms<sup>(4)</sup>:

$$V_{cp} = V_n + i (R_m + R_p + R_d + R_b) \quad (3.11.13)$$

where  $V_n$  is the concentration potential, a counter driving force built up by the concentration process. Its magnitude depends on the concentration ratio between the brine and dialysate and the permselectivity of the membrane at the given conditions.  $V_n$  is measured during interruption of the current for a few seconds - long enough to disperse concentration gradients near the membranes, short enough to avoid changes of bulk concentration.

$\frac{V_{cp} - V_n}{i}$  is the resistance of the cell pair;  $R_m$  membrane resistance;

$R_b$ , brine compartment resistance;  $R_d$ , dialysate compartment resistance; and  $R_p$ , the ohmic resistance and additional counter potential due to polarization layers adjacent to the membrane surface facing the dialysate. In this system,  $R_b$  is negligible, since the brine is always more concentrated than the dialysate. For the simplest characterization of the system, it can be written<sup>(4)</sup>:

$$R_{cp} = \frac{V_{cp} - V_n}{i} = R_m + \rho d_{eff} \quad (3.11.14)$$

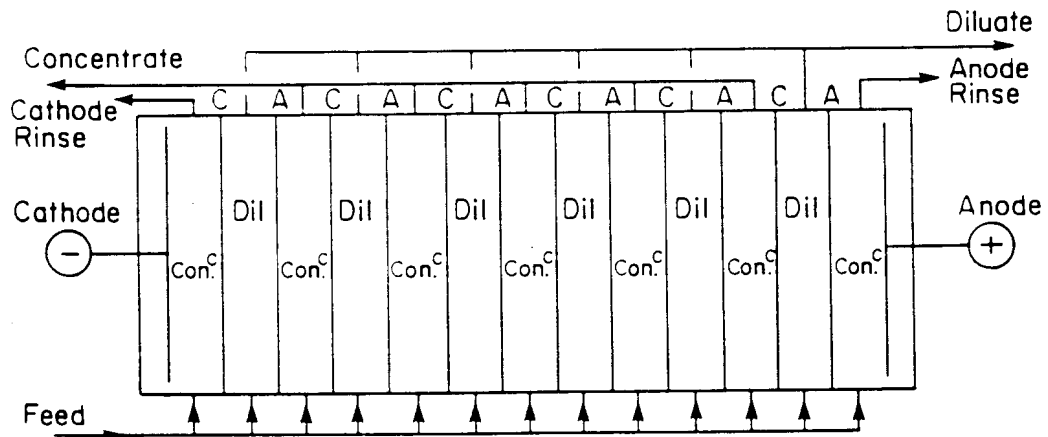
where  $\rho$  is the specific resistance of the dialysate solution, and  $d_{eff}$  is the effective thickness of the dialysate compartment. In this simple representation the shadow effect of the spacer, polarization layers and any other possible disturbances are lumped into  $d_{eff}$ .

The measurement of voltage and current during desalination at a given circulating flow velocity gives the stack resistance as a function of concentration. If desalination is carried out at constant voltage, straight lines are obtained for a plot of cell pair resistance ( $R_{cp}$ ) as a function of specific resistance of the bulk dialysate solution ( $\rho$ ) in a wide range of currents and concentrations ( $c$ ). This is due to nearly constant  $i/c$ , which determines, at given bulk flow, the polarization. Straight lines show not only that  $R_d$ , but also that the contribution of polarization, is an approximately linear function of bulk dialysate resistance.

### 3.12 Electro dialysis Theory

#### 3.12.1 Basic Principles

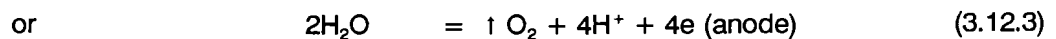
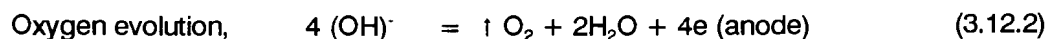
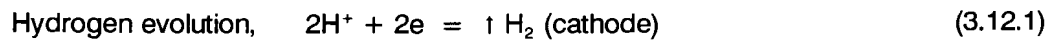
An ED cell is shown in Figure 3.12.1. It comprises of a driven electrochemical cell containing electrodes at each end and a series of compartments or channels of typically 1 mm width, separated by membranes<sup>(6)</sup>. Alternate membranes are "anion permeable" ("A" in Fig. 3.12.1) and "cation-permeable" ("C" in Fig. 3.12.1). The membranes are thin sheets of polymer which have been treated with cationic and anionic groups to impart selective permeability. Under the influence of an applied potential between the electrodes, current flows within the ED cell, being carried by cations - which tend to migrate towards the negatively charged electrode (cathode) - and anions - which tend to move in the direction of the positively charged electrode (anode).



**Figure 3.12.1: General layout of an ED stack. Dil = diluting compartments; Con.<sup>c</sup> = concentrating compartments.**

To see how water purification can occur in such a cell, consider the smaller set-up shown in Figure 3.12.2 and, in particular, the events in the compartment marked D<sub>2</sub>. The various cations present in the water (say Na<sup>+</sup>, Ca<sup>2+</sup>, etc.) can pass freely through the cation-permeable membrane at one end of the compartment and the anions can pass through the anion-permeable membrane at the opposite end. However, neither the cations nor the anions can move out of the adjacent compartments F because the membranes towards which they move (under the influence of the applied potential) are of the wrong type (electrical charge) to allow passage of the ions. Ions, however, can escape from compartments D<sub>2</sub>. The result of all this, in a multi-compartment cell, is that water is diluted and concentrated in alternate compartments (as noted in Fig. 3.12.1) - thus enabling the collection of the purer water from the so-called diluate channels.

During ED of a natural water, several electrode reactions are possible, but the most generally observed ones are<sup>(63)</sup>:



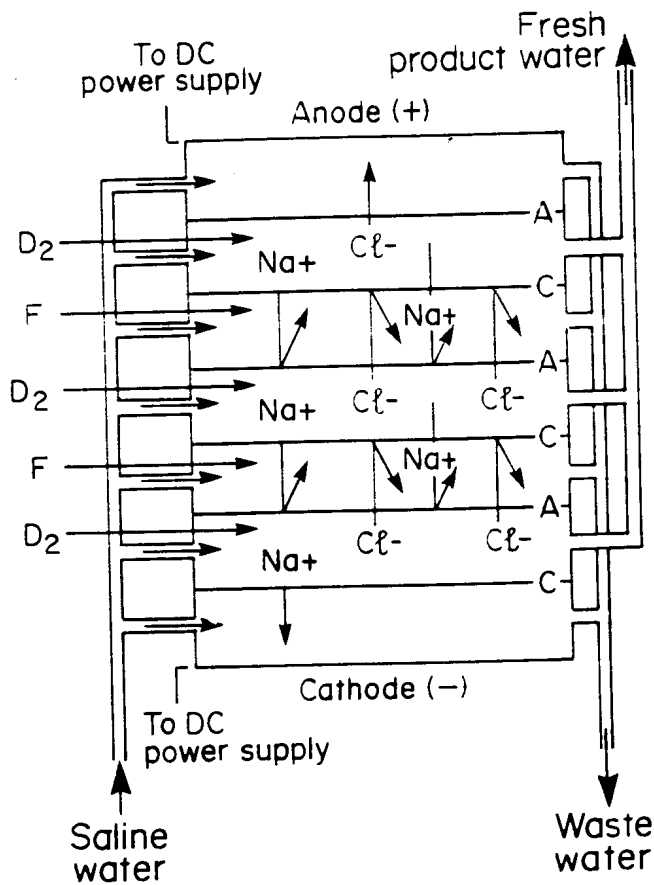


**Figure 3.12.2: Ion movement during ED.**

### 3.12.2 Desalting Rate

An important factor in any desalination process is the rate at which desalination occurs. In order to determine the factors which control the desalination rate in an ED unit, it is necessary to examine in some detail the ion-transport processes occurring in the cell<sup>(10)</sup> (and particularly within and around the membranes). This is done by considering the ion-transport numbers (i.e. the fraction of the current carried by the different kinds of ions in the cell), in particular, it is necessary to compare the transport numbers in the bulk solution and in the membranes. Consider, therefore, desalination of a solution of sodium chloride. In the bulk solution, away from the membranes, the current is carried by the opposite drift of Na<sup>+</sup> and Cl<sup>-</sup> ions, in fact, 60% of the current is carried by the Cl<sup>-</sup> ions and 40% by Na<sup>+</sup> ions, i.e. the transport numbers in the bulk solution are  $t_1 = 0,4$  and  $t_2 = 0,6$ . In perfect membranes, however, only one type of ion can pass through a membrane and the total current is carried by that ion. The characteristics of perfect and practical ion-exchange membranes are shown in Table 3.12.1.

**Table 3.12.1: Characteristics of perfect and practical ion-exchange membranes.**

Membrane Type	Cation-permeable membrane (CPM)	Anion-permeable membrane (APM)
Perfect membrane	$\bar{t}_1^c = 1,0; \bar{t}_2^c = 0$	$\bar{t}_1^a = 0; \bar{t}_2^a = 1,0$
"Practical" membrane	$\bar{t}_1^c \approx 1,0; \bar{t}_2^c \ll 1$	$\bar{t}_1^a \ll 1; \bar{t}_2^a \approx 1,0$

where  $\bar{t}_1^c$  = transport number of cations ( $\text{Na}^+$ ) in CPM  
 $\bar{t}_2^c$  = transport number of anions ( $\text{Cl}^-$ ) in CPM  
 $\bar{t}_1^a$  = transport number of cations in APM  
 $\bar{t}_2^a$  = transport number of anions in APM

The efficiency with which a membrane excludes a particular ion is expressed by the permselectivity of the membrane with respect to that ion. The permselectivity is defined as follows<sup>(7)</sup>:

For cation permeable membranes:

$$P^c = \frac{t_2 - \bar{t}_2}{t_2} = \frac{\bar{t}_1 - t_1}{1 - t_1} \quad (3.12.4)$$

For anion permeable membranes:

$$P^a = \frac{t_1 - \bar{t}_1}{t_1} = \frac{\bar{t}_2 - t_2}{1 - t_2} \quad (3.12.5)$$

Consider now the ion transport processes occurring within an ED unit and it is useful to begin with a simple cell containing sodium chloride solution with just one perfect membrane (a CPM) inserted (Fig. 3.12.3). In the situation depicted in Figure 3.12.3, chloride ions are drifting to the right and sodium ions to the left. At the membrane the sodium ion flux is proportional to the current  $I$ . Thus, as indicated in the magnified sketch of the membrane region (Fig. 3.12.3a),

$$\bar{t}_{\text{Na}^+} = 1,0; \bar{t}_{\text{Cl}^-} = 0,0$$

i.e. the  $\text{Na}^+$  migration rate is  $I/F$  equiv/s where  $I$  is the current and  $F$  is Faraday's constant. In the bulk solution on either side of, but away from, the membrane,

$$t_{\text{Na}^+} = 0,4 \text{ and } t_{\text{Cl}^-} = 0,6$$

i.e. migration rates in equiv/s are  $0,4 I/F$  of  $\text{Na}^+$  and  $0,6 I/F$  of  $\text{Cl}^-$ .

Consider now the two boundary-layer regions on either side of the membrane. The

ion flow due to the electrical current will produce the following mass balance for the passage of each Faraday of current.

**R.H.S. Sodium**

Inflow from solution	Outflow through membrane
0,4	1,0
Sodium depletion	= 0,6 (equiv)

**Chloride**

Inflow from membrane	Outflow to solution
0,0	0,6
Chloride depletion	= 0,6 (equiv)

Consequently, it appears that there is a deficiency in the salt mass balance on the R.H.S. of the membrane, when account is taken only of the electrical flow of ions. However, the nett efflux of salt from this region will reduce the concentration at the membrane surface and this will trigger an additional migration process, namely a diffusive flux of salt from the bulk solution into the depleted boundary region. In the steady state, the mass flux due to diffusion must be equivalent to sodium and chloride depletion rates of 0,6 (caused by the electrical flux) in order to maintain the salt concentrations in the boundary region.

**L.H.S. Sodium**

Inflow from membrane	Outflow to solution	Accumulation Rate
1,0	0,4	0,6 (equiv)

**Chloride**

Inflow from solution	Outflow to membrane	Accumulation Rate
0,6	0,0	0,6 (equiv)



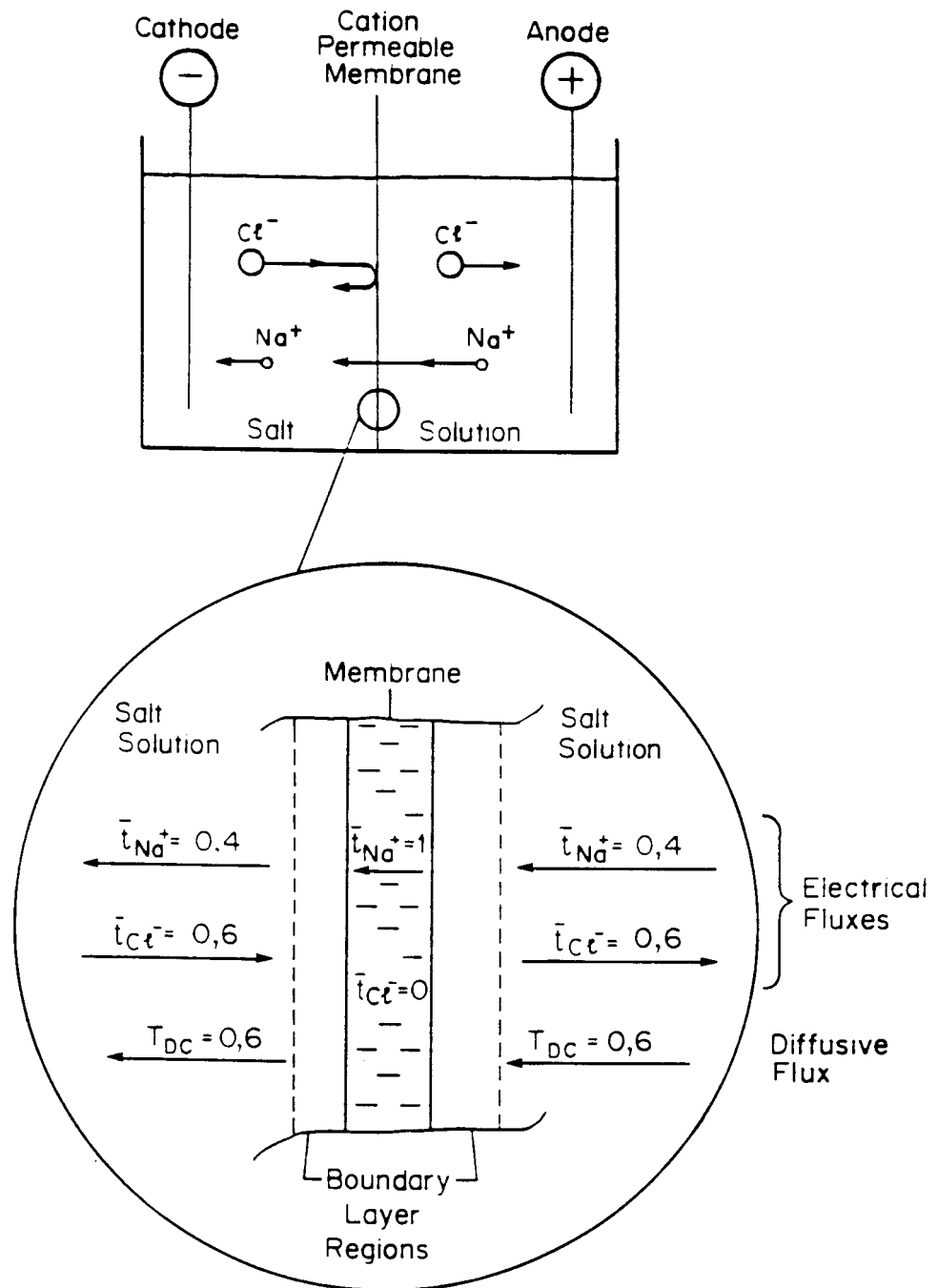


**Figure 3.12.3 (Upper) and Figure 3.12.3(a) (Lower).**

**Processes occurring within and around a cation-permeable membrane in an electrochemical cell containing NaCl solution.**

In a similar manner to the salt deficiency on the R.H.S. of the membrane as a result of Coulombic migration, there appears to be an accumulation of salt on the L.H.S. of the membrane equivalent to a transport number of 0,6. This imbalance of mass flow is again in the steady state, counted by a diffusive flow of salt. This time the salt concentration is increased at the membrane surface by the electrical migration and the salt therefore diffuses away into the bulk of the solution. Comparing this situation with

the straightforward electrolysis process without the membrane, the nett effect of inserting the membrane is to produce an apparent diffusion of salt from right to left across the membrane. The rate (in equivs per Faraday) of this apparent diffusion transport number,  $T_{DC}$  may be expressed in terms of the transport numbers. For the present case, it is clear that  $T_{DC} = 0,6$  equiv/Faraday, i.e.  $T_{DC} = t_2$ . However, in the general case for imperfect membranes, a similar analysis as that above leads to:

$$T_{DC} = t_2 - \bar{t}_2^c$$

A similar analysis and argument may be set up for an anion-permeable membrane. In this case, if the membrane was perfect (i.e.  $\bar{t}_1^a = 0$  and  $\bar{t}_2^a = 1,0$ ), there would appear to be a salt depletion on the L.H.S. To balance these there would have to be an apparent diffusion of salt from left to right across the membrane. In this case for an imperfect membrane,  $T_{DA} = t_1 - \bar{t}_1^a$  which reduces to  $T_{DA} = 0,4$  for the case of a perfect APM in a NaCl solution.

Consider now what will happen if an anion-permeable membrane is inserted on the right hand side of the cation permeable membrane in Figure 3.12.3. Such a set up is depicted in Figure 3.12.4. Passage of current through this system will produce an apparent effect of salt diffusion out of the space between the two membranes. For the simple example of perfect membranes in NaCl solution, the rates of these apparent diffusions will be

$$\text{To the left across the C.P.M., } T_{DC} = 0,6$$

$$\text{To the right across the A.P.M., } T_{DA} = 0,4$$

But, for the general case with imperfect membranes  $T_{DC} = t_2 - \bar{t}_2^c$  and  $T_{DA} = t_1 - \bar{t}_1^a$ .

Therefore, the total apparent diffusive flux out of the central compartment of a set-up like Figure 3.12.4 is:

$$T_D = T_{DC} + T_{DA} = t_2 - \bar{t}_2^c + t_1 - \bar{t}_1^a \quad (3.12.6)$$

$$= 1 - \bar{t}_2^c - \bar{t}_1^a \text{ equiv per Faraday} \quad (3.12.7)$$

$$= 1 \text{ for perfect membranes.} \quad (3.12.8)$$

$T_D$ , the salt flux out of the central compartment, is clearly a measure of the desalting rate, i.e. for a current flow of  $I$  amp,

$$\text{Desalting rate} = I/F (T_{DC} + T_{DA}) \text{ equiv/s} \quad (3.12.9)$$

$$= I/F \text{ equiv/s (for perfect membranes).} \quad (3.12.10)$$

Hence, for a system with perfect membranes, the salt removal from the space between the membranes is exactly equivalent to the charge that is passed through the system. This is exactly equivalent to the decrease in salt concentration in sodium chloride in a simple electrolytic cell in which the electrode reactions involved sodium deposition (cathodic) and chlorine evolution (anodic). (Note: If the membranes been the other way round in Figure 3.12.4, the APM on the left and the CPM on the right, then the effect would be to concentrate rather than dilute the solution between the membranes).

Thus, the desalting rate increases with cell current. Another important factor is the number of membranes. As mentioned earlier, the above expressions apply to a simple ED cell containing just one pair of membranes. The system can be greatly improved by inserting many pairs of membranes because each pair produces an equivalent amount of desalination. Thus, the total desalination achieved per unit charge flow is

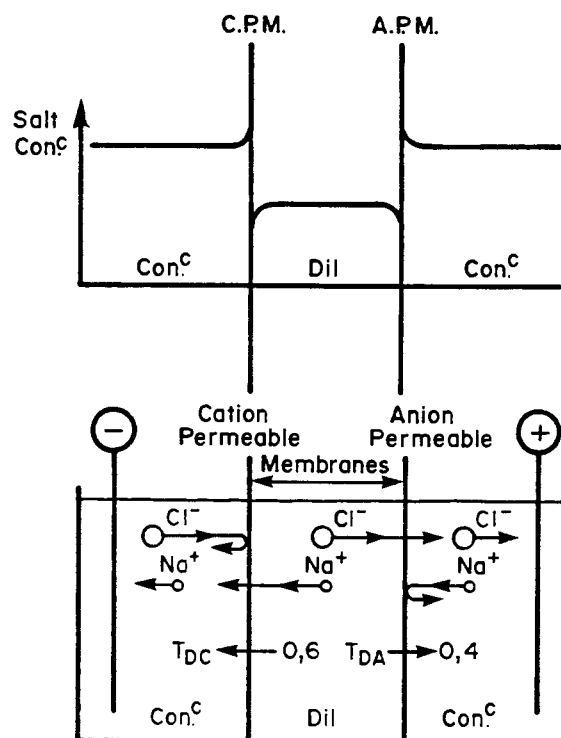


Figure 3.12.4: Cell containing a pair of membranes.

N times that in a one-pair set-up, where N is the number of membrane pairs, i.e.

$$\text{Desalting rate} = \frac{NI}{F} (T_{DC} + T_{DA}) \quad (3.12.11)$$

Note that, in Figure 3.12.2, there are 6 membrane pairs giving a desalting rate of  $6I/F$  equiv/s for perfect membranes.

### 3.12.3 Energy Requirements for Electrodialysis

In order to estimate the energy requirements for ED all the potential differences (or IR drops) in the cell must be investigated. The required applied voltage for ED comprises several elements<sup>(16)</sup>:

- i) a voltage necessary to drive the electrode reactions;
- ii) a voltage required to overcome the aqueous solution resistances in the ED cell;
- iii) a voltage necessary to overcome the membrane potentials;

The first of these is determined from the electrode potentials for the particular electrode reaction and increases with cell current due to polarisation of the electrode reactions. However, in commercial units, this component of the required applied voltage is usually small in comparison to those arising from (ii) and (iii). Therefore, the latter factors will be considered in more detail.

#### 3.12.3.1 Solution Resistances

The resistivity of an aqueous electrolyte decreases with increasing ionic concentration. Therefore, IR drops through the diluate channels are considerably greater than those through the concentrate channels. A further complication, with consequences for ED energy requirements, is concerned with concentration changes which occur in the regions immediately adjacent to the membranes. These are summarized in Figure 3.12.5 which illustrates that salt depletion occurring in the boundary regions adjacent to the membranes in the diluate channels and enrichment occurring in the boundary layers on the concentrate side of the membranes. For a cation-permeable membrane,

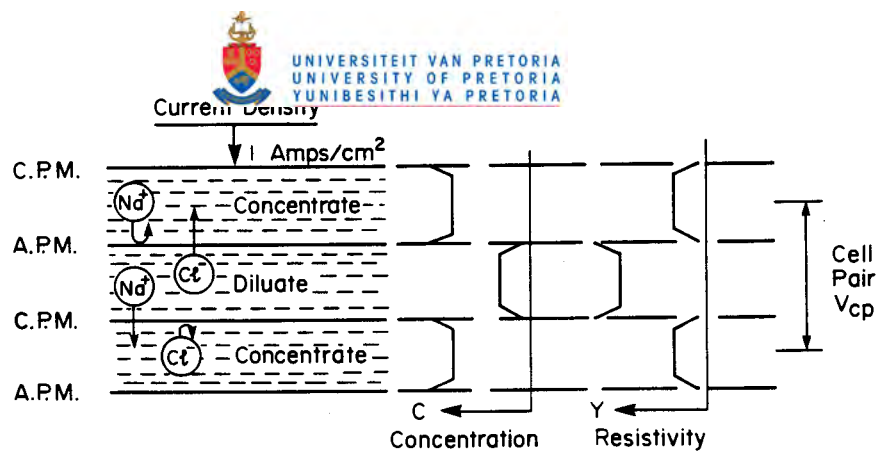


**Figure 3.12.5: The cell pair showing salt depletion occurring in the boundary regions adjacent to the membranes in the diluate channels and salt enrichment occurring in the boundary layers on the concentrate side of the membrane.**

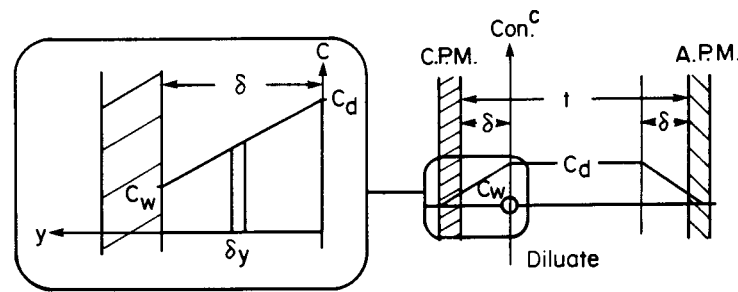


**Figure 3.12.6: Concentration changes in boundary layers around membranes.**

the concentration of salt in the "diluate boundary layer" is lower than the concentration of salt in the "main diluate stream", but the salt concentration is relatively enriched in the "concentrate boundary layer". Both these effects are clear on the concentration profiles shown in Figure 3.12.5. This phenomenon is very similar to concentration polarization processes which can occur around electrodes in electrochemical cells except that, in the present context, there is an unbalanced Faradaic transport in and around membranes which promotes additional diffusion fluxes to establish the steady-state concentration profile. Thus, these concentration-polarization phenomena around membranes in ED cells are a natural and inevitable result of the desalting mechanism i.e. of the change in electrical transport numbers at the membrane interface upon which the ED desalination process relies.

One important practical consequence of concentration polarization around membranes in ED units, indicated in Figure 3.12.5, is that the resistance of the diluate boundary layers is significantly greater than in the bulk diluate stream. Therefore, the occurrence

of concentration polarization increases the energy requirements for ED.

### 3.12.3.2 Membrane Potentials

When an ion-selective membrane separates two solutions of a salt at different concentrations, a potential difference is set-up across the membrane. This happens because, in the absence of any applied potentials, Na<sup>+</sup> ions will tend to migrate across the cation-exchange membrane from the concentrated solution to the diluate solution. This will lead to a charge imbalance across the membrane with the diluate side becoming positively charged relative to the concentrated side. Eventually this potential difference across the membrane will build up to such a level that further ion transfer is discouraged and the value of the potential difference at this equilibrium condition is known as the membrane potential. For a salt consisting of single-charged ions, and assuming that activities can be equated to concentrations, the magnitude of the membrane potential is given by

$$E_m = - (\bar{t}_1 - \bar{t}_2) \frac{RT}{F} \ln \left( \frac{C_{w1}}{C_{w2}} \right) \quad (3.12.12)$$

where  $C_{w1}$  and  $C_{w2}$  are the concentrations of the salt in the concentrated and dilute solutions respectively.

The important point about the above is that natural flow across a membrane is from concentrate to diluate (i.e. the opposite to that required in desalination) and, to reverse this natural flow direction requires the application of a potential of magnitude greater than  $E_m$ , i.e. the membrane potential represents a potential drop which has to be overcome by the external applied voltage in order for desalination to occur. However, this is not the whole story. The magnitude of the membrane potential indicated by the above equation only applies to the equilibrium (i.e. infinitely-low current) state. As previously discussed, an inevitable consequence of desalination at finite currents is the occurrence of concentration polarization. The consequent concentrate enrichment and diluate depletions at the membrane/solution interface means that  $C_{w1}$  will be greater than the bulk concentrate composition and  $C_{w2}$  will be less than the bulk diluate concentrations. Therefore, another important effect of concentration polarization is to increase the membrane potential and hence the energy requirements for desalination.

### 3.12.3.3 The Cell-Pair Potential

The major part of the energy requirements for ED comprises the voltage necessary to overcome the solution resistances and membrane potentials. Estimation of the voltage is conveniently done by considering one cell pair which, as shown in Figure 3.12.5, encompasses a pair of membranes. The cell pair potential  $V_{cp}$ , is the sum of all the potential drops across the membranes and solutions comprising one cell pair.

Consider the basic conflict between attempts to maximise desalting rate and to minimize energy requirements. The flux of salts from the diluate channel is given by

$$T_D = 1 - \bar{t}_2^c - \bar{t}_1^a \quad (3.12.13)$$

and that the desalting rate,  $d$ , is given by:

$$d = \frac{IT_D}{F} \text{ equiv cm}^{-2} \text{ s}^{-1} \quad (3.12.14)$$

(using current density,  $i$ , instead of current  $I$ ). The power required to drive a cell pair is:

$$P = V_{cp} i \text{ watts cm}^{-2} \quad (3.12.15)$$

Therefore, increases in  $i$ , whilst raising the desalting rate, also lead to higher energy consumption - not only directly but also by increasing  $V_{cp}$  due to higher IR drops and concentration-polarization effects.

### 3.12.3.4 Resistances

The major contributor to  $V_{cp}$  is the resistance of the diluate stream. It is normal practice to keep the concentration of the concentrate high enough for its resistance to be negligible in comparison to that of the diluate. Modern membranes have, however, negligible small resistances. As a first approximation, it can be considered that the diluate stream is providing all the resistance. To calculate the resistance, the main stream and the boundary layers must be considered separately.

Considering the total thickness (including boundary layers) of the diluate stream to be ' $t$ ' cm (typically 0,1 cm) (see Fig. 3.12.6). Let the thickness of the boundary layers (adjacent to the membranes) be  $\delta$  (determined by hydrodynamic conditions and typically 0,01 cm).

### 3.12.3.5 Main stream of diluate

The resistance of 1 cm<sup>2</sup> cross section, d, is given by:

$$R_d = \frac{t - 2\delta}{\kappa} \text{ ohm} \quad (3.12.16)$$

with the conductivity,  $\kappa$ , expressed in units of (ohm/cm)<sup>-1</sup>.

But the conductivity,  $\kappa$ , depends on the concentration  $C_d$  (equiv/cm<sup>3</sup>) of the diluate stream via  $\kappa = \Lambda C_d$  (3.12.17)

where  $\Lambda$  = equivalent conductivity in cm<sup>2</sup>/ohm equiv.

$$\therefore R_d = \frac{t - 2\delta}{\Lambda C_d} \quad (3.12.18)$$

### 3.12.3.6 Boundary layers of diluate

Faradaic transport (i.e. under the influence of the applied electric field) of ions, across the membranes out of the diluate compartment, leads to a depletion of salt in the boundary layers which, in turn, causes a diffusion flux from the bulk diluate. The concentration gradient across the boundary layer stabilises (i.e. steady-state conditions are established) when the two fluxes are equal.

Consider the CPM boundary layer (left diagram on Fig. 3.12.6).

$$\text{Faradaic Flux} = i/F (t_2 - \bar{t}_2^0) \approx (it_2/F) \quad (3.12.19)$$

$$\text{Diffusion flux} = -D \frac{dc}{dy} \quad (3.12.20)$$

Therefore, at steady state,

$$-D \frac{dc}{dy} = t_2 i/F \quad (3.12.21)$$

Conductivity (and hence resistance) is concentration dependent. Therefore, to find the



boundary-layer resistance,  $R_{BC}$ , integration must be carried out across the layer.

$$\text{Resistance of element } \delta y = \frac{\delta y}{\kappa} = \frac{\delta y}{\Delta C} \quad (3.12.22)$$

(see Fig. 3.12.6)

Therefore, resistance of boundary layer,

$$R_{BC} = \int_0^\delta \frac{dy}{\Delta C} \quad (3.12.23)$$

Concentration gradient (assumed linear - see Figure 3.12.6) is:-

$$\frac{dc}{dy} = \frac{C_w - C_d}{\delta} \quad (3.12.24)$$

Changing the integration variable limits:-

$$R_{BC} = \int_{C_d}^{C_w} \frac{\delta}{\left(\frac{C_w - C_d}{\Delta C}\right)} dc = \frac{\delta}{(C_w - C_d)\Delta} \ln \left(\frac{C_w}{C_d}\right) \quad (3.12.25)$$

$$R_{BC} = \frac{\delta}{(C_d - C_w)\Delta} \ln \left(\frac{C_d}{C_w}\right) \quad (3.12.26)$$

(since  $C_d - C_w = -(C_w - C_d)$  and  $\ln x = -\ln 1/x$ )

An alternative expression for  $R_{BC}$  can be produced by using the previously formulated steady-state relation.

$$-D \frac{dc}{dy} = t_2 \frac{i}{F} = -D \frac{(C_w - C_d)}{\delta} = \frac{D(C_d - C_w)}{\delta} \quad (3.12.27)$$

$$\therefore C_d - C_w = \frac{t_2 \delta i}{FD} \quad (3.12.28) \text{ (A)}$$

$$\therefore R_{BC} = \frac{\delta FD}{t_2 \delta i \Delta} \ln \left[ \frac{C_d}{\frac{C_d - \left(\frac{t_2 \delta i}{FD}\right)}{1}} \right] \quad (3.12.29)$$

$$= - \frac{FD}{t_2 i \Delta} \ln \left( 1 - \frac{t_2 \delta i}{FDC_d} \right) \quad (3.12.30)$$

A similar analysis can be carried out to obtain an expression for the resistance,  $R_{BA}$ , of the diluate boundary layer at the APM (right hand side of Figure 3.12.6). This leads to the following expression:-

$$R_{BA} = -\frac{FD}{t_1 i \Lambda} \ln \left( 1 - \frac{t_1 \delta i}{FDC_d} \right) \quad (3.12.31)$$

The depletion of solute in the boundary layers arises from the rapid flux of solute species through the membranes - this flux being directly proportional to the current flowing in the cell. In other words, as  $i$  increases from zero, the concentration gradient in the boundary layer increases ( $C_w$  decreases as  $i$  increases). It follows, therefore, that there are limits to the current that can be carried by the solute ions in an ED system - this limit being reached when  $C_w$  approaches zero.

As  $C_w$  approaches 0, equation (A) becomes:

$$C_d = \frac{t_2 \delta i_{max}}{FD} \quad (3.12.32)$$

and

$$i_{max} = \frac{C_d FD}{t_2 \delta} \quad (3.12.33) \quad (B)$$

which in turn, defines, for any given ED unit, a definite limit to the desalting rate -

$$\frac{Ni_{max}}{F}$$

Another aspect of this "limiting current density phenomenon concerns the transport of  $H^+$  and  $OH^-$  ions across CPM and APM membranes, respectively. At low current densities, the current is carried almost exclusively by solute ions rather than by  $H^+$  and  $OH^-$ . This is because of the very low concentrations of  $H^+$  and  $OH^-$  in neutral solution ( $10^{-7}$  mol/l) - and is despite the approximately ten times higher mobilities of  $H^+$  and  $OH^-$  compared with solute ions. But, as  $i$  increases, the flux of  $H^+$  and  $OH^-$  across the membranes increases until, as  $i_{max}$  is approached, the flux of  $H^+$  at the CPM and of  $OH^-$  at the APM becomes a substantial fraction of the total current. In rather more precise

terms, because of their tenfold higher mobilities, an appreciable fraction of the current will be carried by H<sup>+</sup> and OH<sup>-</sup>, present at concentrations of 10<sup>-7</sup> mol/l, when the solute concentration at the membrane/diluate interface C<sub>w</sub>, falls towards a value of about 5 x 10<sup>-6</sup> mol/l. Such a situation not only results in an obvious decreased efficiency of desalination but also in highly undesirable pH changes in the solutions. One consequence of such pH changes is that they can lead to an increased tendency towards scale precipitation if the pH increases significantly in any local region.

### 3.12.3.7 Membrane Potentials

The contribution of membrane potentials to the cell-pair potential is most conveniently predicted by considering ED of a solution of a single salt comprising of univalent ions. As was noted earlier, for this case the membrane potential was given by:

$$E_m = - (\bar{t}_1 - \bar{t}_2) \frac{RT}{F} \ln \frac{C_{w1}}{C_{w2}} \quad (3.12.34)$$

where C<sub>w1</sub> and C<sub>w2</sub> now represent the bulk concentrations of the salt in the compartments on either side of the membrane. Note, though, that the membrane potential is determined by the salt concentrations at the membrane/salt interface. It was noted earlier that finite cell-current flow resulted in salt depletions and enrichments within the boundary region beside the membrane. In such circumstances, E<sub>m</sub> will no longer be determined by the bulk-salt concentrations (C<sub>w1</sub> and C<sub>w2</sub>) but by the concentration-polarised membrane/boundary layer interfacial values (C<sub>wbc</sub> and C<sub>wdc</sub>, in the C.P.M. in Figure 3.12.7). Therefore, in order to obtain an expression for E<sub>m</sub> in these practically-relevant conditions, it is necessary to estimate the concentrations C<sub>wbc</sub> and C<sub>wdc</sub> for C.P.M. and C<sub>wda</sub> and C<sub>wba</sub> for the A.P.M.. This exercise is considerably simplified if it is assumed (see Figure 3.12.7) that the four boundary layers have identical effective thickness, δ. If we assume a perfect cation permeable membrane (C.P.M.) and use the notation of Figure 3.12.7, the polarised C.P.M. membrane potential is given by:-

$$E_{mc} = -(1-0) \frac{RT}{F} \ln \frac{C_{wbc}}{C_{wdc}} \quad (3.12.35)$$

$$\text{Now } C_d - C_{wdc} = \frac{t_2 \cdot \delta \cdot i}{FD} \quad (\text{see A}) \quad (3.12.36)$$

$$\therefore C_{wdc} = C_d - \frac{t_2 \cdot \delta \cdot i}{FD} \quad (3.12.37)$$

$$\text{Similarly } C_{wbc} = C_c + \frac{t_2 \cdot \delta \cdot i}{FD} \quad (3.12.38)$$

$$\text{hence } E_{mc} = \frac{RT}{F} \ln \left[ \frac{C_c + \frac{t_2 \cdot \delta \cdot i}{FD}}{C_d - \frac{t_2 \cdot \delta \cdot i}{FD}} \right] \quad (3.12.39)$$

Similarly for the AMP.

$$E_{ma} = \frac{RT}{F} \ln \left[ \frac{C_c + \frac{t_1 \cdot \delta \cdot i}{FD}}{C_d - \frac{t_1 \cdot \delta \cdot i}{FD}} \right] \quad (3.12.40)$$

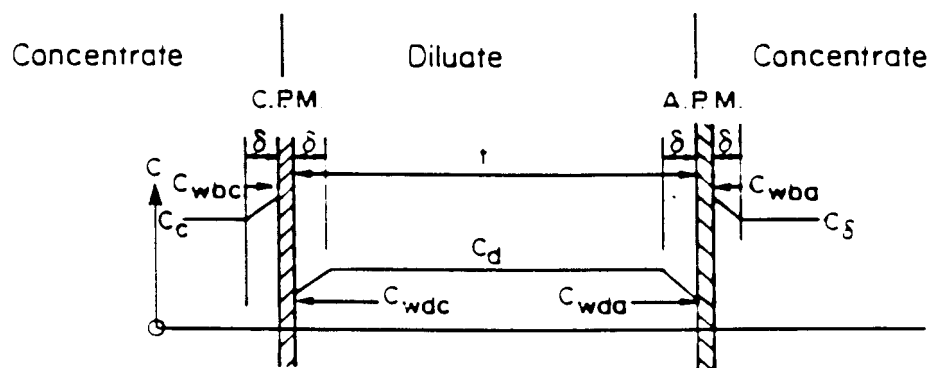


**Figure 3.12.7: Concentration polarisation effects on membrane potential.**

If the concentrate stream is several or more times as concentrated as the diluate stream, then

$$\frac{C_c}{C_d} > \frac{t_2 \delta i}{FDC_d} \quad (3.12.41)$$

$$\text{because } \frac{1}{i_{\max}} = \frac{t_2 \delta}{FDC_d} \quad (\text{see equation B}) \quad (3.12.42)$$

and  $\frac{i}{i_{\max}}$  has a maximum value of 1

All the relevant terms have now been covered, which, to a first approximation, contribute to the cell pair potential  $V_{cp}$ .

Cell pair potential  $V_{cp}$  is given by:

$$\text{i.e. } V_{cp} = i (R_d + R_{BC} + R_{BA}) + E_{mc} + E_{ma} \quad (3.12.43)$$

$$\begin{aligned} \therefore V_{cp} &= \frac{i(t-2\delta)}{\Delta C_d} - \frac{FD}{t_2 \Lambda} \ln \left( 1 - \frac{t_2 \delta i}{FDC_d} \right) - \frac{FD}{t_1 \Lambda} \ln \left( 1 - \frac{t_1 \delta i}{FDC_d} \right) \\ &+ \frac{RT}{F} \ln \left( \frac{C_c}{C_d} + \frac{t_2 \delta i}{FDC_d} \right) - \frac{RT}{F} \ln \left( 1 - \frac{t_2 \delta i}{FDC_d} \right) \\ &+ \frac{RT}{F} \ln \left( \frac{C_c}{C_d} + \frac{t_1 \delta i}{FDC_d} \right) - \frac{RT}{F} \ln \left( 1 - \frac{t_1 \delta i}{FDC_d} \right) \end{aligned} \quad (3.12.44)$$

Rearranging:-

$$\begin{aligned} V_{cp} &= \frac{i(t-2\delta)}{\Delta C_d} - \left( \frac{FD}{t_2 \Lambda} + \frac{RT}{F} \right) \ln \left( 1 - \frac{t_2 \delta i}{FDC_d} \right) \\ &- \left( \frac{FD}{t_1 \Lambda} + \frac{RT}{F} \right) \ln \left( 1 - \frac{t_1 \delta i}{FDC_d} \right) \\ &+ \frac{RT}{F} \left[ \ln \left( \frac{C_c}{C_d} + \frac{t_1 \delta i}{FDC_d} \right) + \ln \left( \frac{C_c}{C_d} + \frac{t_2 \delta i}{FDC_d} \right) \right] \end{aligned} \quad (3.12.45)$$

Further simplification of the bottom line of the above expression it is necessary to recall that:-

$$\frac{C_c}{C_d} \gg \frac{t_2 \delta i}{FDC_d} \quad \left( \text{and similarly } \gg \frac{t_1 \delta i}{FDC_d} \right)$$

$$V_{cp} = \frac{i(t - 2\delta)}{\Delta C_d} - \left( \frac{FD}{t_2 \Lambda} + \frac{RT}{F} \right) \ln \left( 1 - \frac{t_2 \delta i}{FDC_d} \right) - \left( \frac{FD}{t_1 \Lambda} + \frac{RT}{F} \right) \ln \left( 1 - \frac{t_1 \delta i}{FDC_d} \right) +$$

$$\frac{2RT}{F} \ln \frac{C_c}{C_d} \quad (3.12.46) \text{ (C)}$$

The order of magnitudes of some of the terms in the above relation is as follows by considering the desalination of sodium chloride:-

$$F = 96\,500 \text{ Coulomb/equiv}, t_2 = 0,6, R = 8,3 \text{ joule}^\circ\text{K}$$

$$D \text{ (diffusion coefficient)} = 1,5 \times 10^5 \text{ cm}^2/\text{s}, t_1 = 0,4$$

$$\Lambda = 108,9 \text{ cm}^2 \text{ ohm}^{-1} \text{ equiv}^{-1}.$$

From which we can estimate the following terms:-

$$\frac{FD}{t_2 \Lambda} = \frac{96\,500 \times 1,5 \times 10^5}{0,6 \times 108,9} \left| \frac{\text{coulomb cm}^2 \text{ ohm equiv}}{\text{equiv s cm}^2} = \text{volts} \right|$$

$$= 0,02215 \text{ volt}$$

$$\frac{RT}{F} = \frac{8,3 \times 300}{96\,500} = 0,0258 \text{ volt}$$

In short  $\frac{FD}{t_2 \Lambda}$  and  $\frac{RT}{F}$  are of the same order

$$\text{Also } \frac{FD}{t_1 \Lambda} = 0,03323 \text{ volt}$$

Remember also that  $\frac{t_2 \delta i}{FDC_d}$  and  $\frac{t_1 \delta i}{FDC_d}$  have maximum values of 1.

Of the remaining terms in equation (C)  $t, \delta$  and  $C_c$  may be considered as design parameters which may be chosen and fixed. Therefore, in estimating the energy requirement for  $V_{cp}$ , it remains to find the most suitable combination of variables in  $V_{cp}$ ,  $i$  and  $C_d$ . A convenient way of doing this is too recast equation (C) in a non-dimensional form. This operation can be done in several steps:-

- (i) Multiply both sides of (C) by  $F/RT$ .

This makes the L.H.S of (C)  $\frac{V_{cp}F}{RT}$  which is a (voltage) non-dimensional term,

which we call  $V$ .

- (ii) The first term on the RHS of (C) now becomes

$$\frac{i(t-2\delta) F}{C_d \Delta RT}$$

If we multiply this term by  $\frac{i_{max}}{i_{max}} = \frac{C_d F D}{t_2 \delta} \times \frac{1}{i_{max}}$  (3.12.47)

we get  $\frac{i}{i_{max}} \frac{t-2\delta}{\delta} \frac{F^2 D}{\Delta t_2 RT} = \beta \lambda I$  (3.12.48)

when it is separated into three non-dimensional terms

$$I = \frac{i}{i_{max}} \quad (3.12.49)$$

$$\lambda = \left( \frac{t-2\delta}{\delta} \right) \quad (3.12.50)$$

$$\beta = \frac{F^2 D}{\Delta t_2 RT} \quad (3.12.51)$$

- (iii) Replace  $C_o/C_d$  by  $C$ -another non-dimensional ("concentration ratio") term.

The substitution of the above non-dimensional terms into (C), together with some manipulation, gives the following non-dimensional equation:

Simple Resistance	Polarization	Useful
$V = \beta \lambda I$	$-(1 + \beta) \ln \left( 1 - \frac{t_2}{t_1} \beta \right)$	$\ln \left( 1 - \frac{t_1}{t_2} I \right) + 2 \ln C$ (3.12.52) (D)

Possible ranges of values for  $\lambda$ ,  $I$ , and  $C$

	Typical plant values
$0 < \lambda < \text{large}$	9
$0 < I < 1$	0,95
$10 < C < 200$	15 - 70

Equation (D) is divided into terms coming from simple resistive losses (since the  $\beta\Delta I$  term is derived from the first term on the RHS of equation (C) which represents the bulk dilute resistance), and the work done against the membrane potentials (said to be "useful" because it represents the minimum energy without polarization effects), and the polarization-losses (all these terms being derived from all the terms in (C) except the first and the last (simple membrane potential). These contributions to the cell pair potential may be plotted separately as they are in Figure 3.12.8. The "useful" potential is only a function of C and the two "loss" potentials are both functions of I, the resistive loss being a function of  $\lambda$  as well. This graph then covers the total likely range of conditions to be found in practical ED stacks. Thus, the various curves for different values of  $\lambda$  are plots of the contributions of the resistance loss ( $\beta\lambda I$ ) to the V term for different values of  $\lambda$  (the cell to boundary layer thickness ratio). Note that, as  $\lambda$  increases (i.e. as the cell size increases) the energy requirements increase. Note also, that, for the calculations of the value of  $\beta$  (used in the  $\lambda$ -plots and also in the polarization plot) that a temperature of 300 °K has been used.

#### 3.12.4 Estimation of Effects of Flow of Solution through Stack on Desalting Process

No account of the effects of flow of solution through the compartments of the ED stack have been taken up to now. This matter can be estimated by investigating how conditions vary as the diluate passes along its channel<sup>(16)</sup>. This procedure can be started by carrying out a salt mass balance on an element, dx, in which the concentration changes from  $C_d$  by a small amount  $dC_d$  (See Figure 3.12.9).

Area of element =  $1 \times t = t \text{ cm}^2$

Therefore, rate of salt flow into element is  $C_d U_d t \text{ equiv s}^{-1}$ .

Salt flux out of element along diluate channel is  $(C_d + dC_d) t U_d \text{ equiv s}^{-1}$ .

Flux of salt through membranes (= desalting rate)

$$= \frac{i}{F} \text{ equiv/cm}^2 \text{ s}$$

$$= \frac{i}{F} dx \text{ equiv/s (out of element dx of membrane area dx cm}^2\text{)}$$

∴ Mass balance on salt gives:-

$$C_d t U_d = (C_d + dC_d) t U_d + i dx / F \quad (3.12.52)$$

$$\text{or, } -dC_d t U_d = i dx / F \quad (3.12.53)$$

$$-dC_d = \frac{i}{t} \frac{dx}{F U_d} \quad (3.12.54)$$



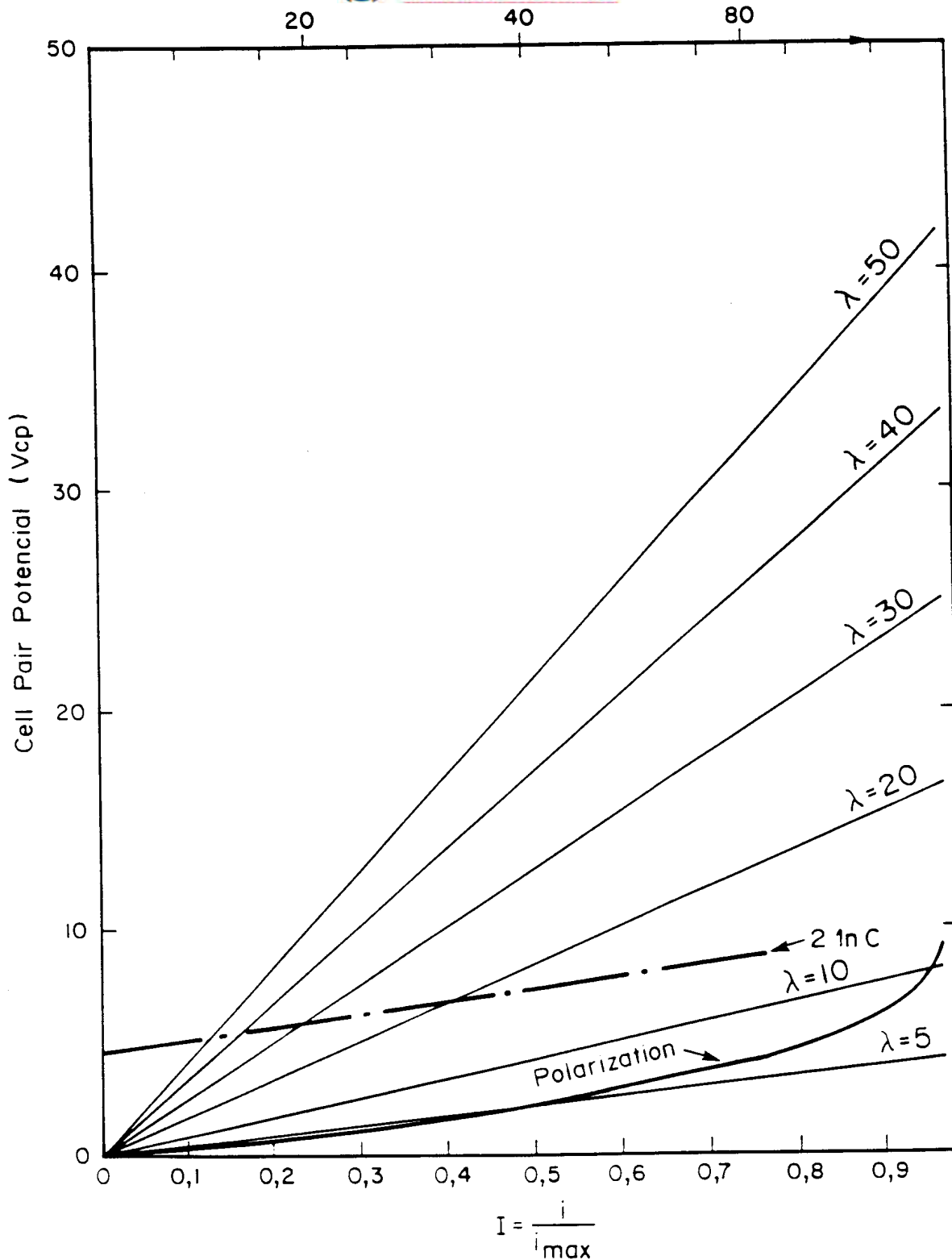


**Figure 3.12.8:** Effect of  $I$  on  $V_{cp}$  ( $V_{cp} = \beta \lambda I$ ) at different cell to boundary layer thickness ratio's ( $\lambda$ ) (simple resistive losses); effect of  $I$  on  $V_{cp}$  ( $V_{cp} = -(1 + \beta) \ln(1 - I) - (1 + \frac{t_2}{t_1} \beta) \ln(1 - \frac{t_1}{t_2} I)$ ) (polarisation losses); effect of  $C$  ( $C_d/C_d$ ) on  $V_{cp}$  ( $V_{cp} = 2 \ln C$ ) (useful potential).

If  $i$  in the above equation is replaced by the dimensionless current term  $I = i/i_{\max}$

$$\text{or } I = \frac{i t_2 \delta}{C_d F D} \quad (3.12.55)$$

i.e. using the expression (derived earlier) for  $i_{\max}$ :-

$$i_{\max} = \frac{C_d F D}{t_2 \delta} \quad (3.12.56)$$

one obtain:

$$-dC_d = \frac{I C_d D}{t_2 \delta} \times \frac{dx}{t U_d} \quad (3.12.57)$$

or:

$$dx = -\frac{t_2 \delta t U_d}{D I} \times \frac{dC_d}{C_d} \quad (3.12.58)$$

$$\int_0^x dx = -\frac{t_2 \delta t U_d}{D I} \int_{C_d(x=0)}^x \frac{dC_d}{C_d} \quad (3.12.59)$$

$$\therefore x = -\frac{t_2 \delta t U_d}{D I} [\ln C_d(x) - \ln C_d(x=0)] \quad (3.12.60)$$

$$= -\frac{t_2 \delta t U_d}{D I} \ln \frac{C_d(x)}{C_d(x=0)} \quad (3.12.61)$$

$$\text{and } C_d(x) = C_d(0) e^{-\left(\frac{D I}{t_2 \delta t U_d}\right) x} \quad (3.12.62)$$

$$= C_f e^{-\left(\frac{D I}{t_2 \delta t U_d}\right) x} \quad (3.12.63)$$

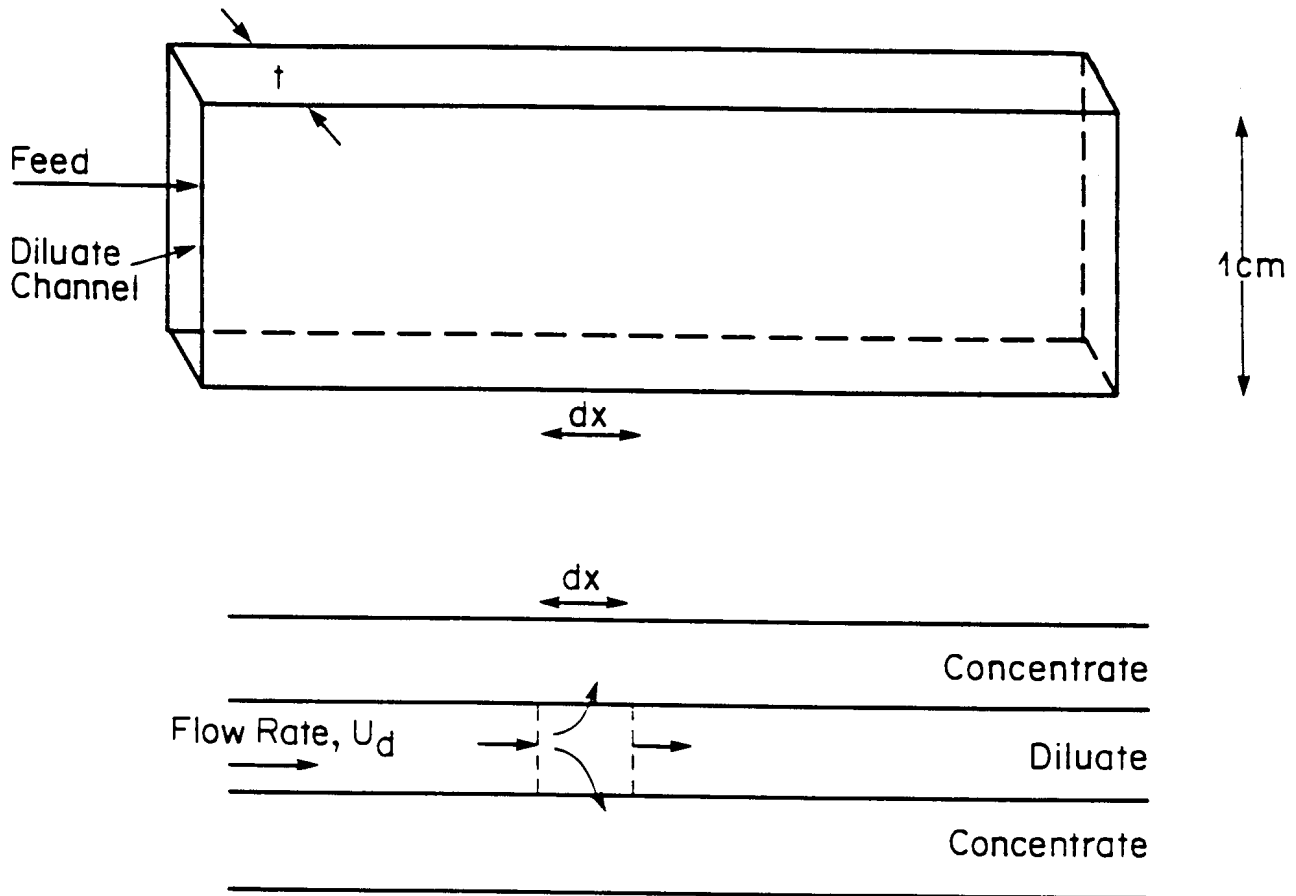


**Figure 3.12.9: Flow through a diluate channel.**

Now  $V_{cp}$  will be constant along the cell, but  $C_d$  and  $I$  will vary with  $x$ . Polarisation will be worse (i.e. highest value of  $I$ ) at the stack entrance. Hence, if there is a "design" limit on polarisation it must be applied here (at  $x = 0$ ). Hence, at this location  $C_d = C_f$  (feed concentration) and  $I = I_{max}$ . It can therefore be worked out what the cell pair voltage will be at this point and this will be the value for the whole stack. Having settled on a value for  $V_{cp}$ , it can be examined how  $C_d$  and  $i$  (or  $I$ ) vary with  $x$ . A typical result of such an analysis is shown in Figure 3.12.10.

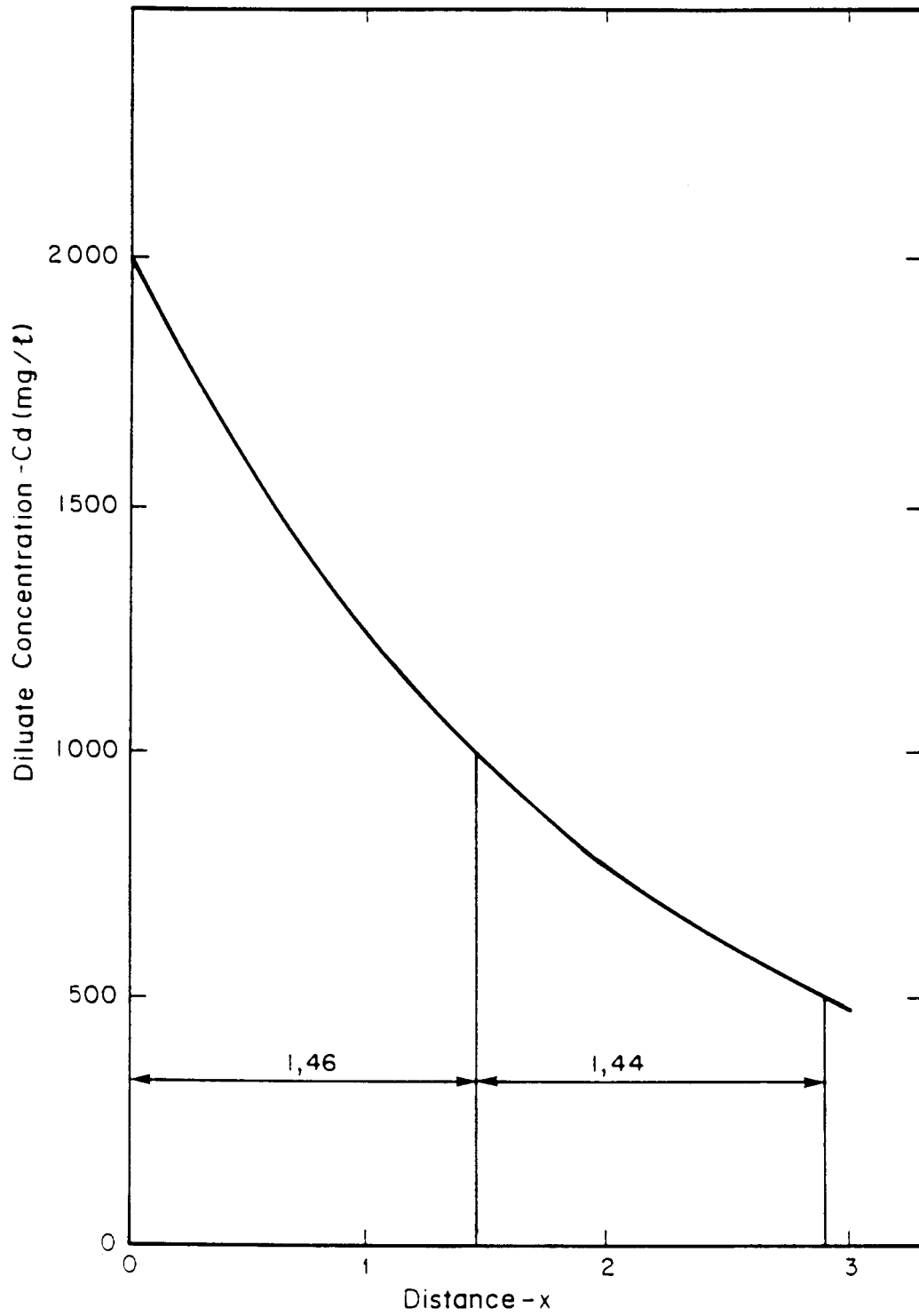


Figure 3.12.10: Variation of diluate concentration along cell pair.